THESIS
Z
(1995)

This is to certify that the

dissertation entitled

HARMONIC RESPONSE AND PASSIVE VIBRATION ISOLATION OF RIGID BODIES

presented by

R. Matthew Brach

has been accepted towards fulfillment
of the requirements for

Ph.D. degree in Mechanical Engineering

Alan G. Haddow
Major professor

Date 10/9/95

MSU is an Affirmative Action/Equal Opportunity Institution

O-12771

LIBRARY
Michigan State
University

PLACE IN RETURN BOX to remove this checkout from your record.
TO AVOID FINES return on or before date due.

DATE DUE	DATE DUE	DATE DUE

MSU is An Affirmative Action/Equal Opportunity Institution
c:\circ\datedue.pm3-p.1

HARMONIC RESPONSE AND PASSIVE VIBRATION ISOLATION OF RIGID BODIES

By

R. Matthew Brach

A DISSERTATION

Submitted to
Michigan State University
in partial fulfillment of the requirements
for the degree of

DOCTOR OF PHILOSOPHY

Department of Mechanical Engineering

1995

ABSTRACT

HARMONIC RESPONSE AND PASSIVE VIBRATION ISOLATION OF RIGID BODIES

By

R. Matthew Brach

Passive vibration isolation is important in the automotive industry where the undesirable effects of powerplant vibrational excitation need to be isolated from the occupants and the automobile interior. Recently, hydraulic engine mounts have proven to be effective in this capacity and have replaced traditional elastomeric mounts in many automobiles. While the characteristics of the mount itself are well-established, no systematic investigations have been conducted that consider the nonlinear response of the *total* system consisting of an engine on mounts.

Therefore, to better understand this type of vibration system, the harmonic response and vibration isolation performance of a planar, three degree of freedom rigid body on resilient linear supports is investigated. The nonlinear differential equations of motion for the system are derived using Lagrange's equations. Approximate solutions of these equations for four different forcing cases are formulated using the method of multiple scales. The frequency response of each degree of freedom for these four cases is obtained from these approximate solutions. Specifically, the response for this system where 1:1 and 2:1 internal resonances exist between the system linear natural frequencies is found. The analysis identifies regions where multiple steady-state solutions exist, and other regions where no constant amplitude steady-state solutions exist. The

efficient transfer of energy from one mode to another is also investigated and related to a novel type of vibration isolator.

This thesis also includes a review of the four common metrics used to assess the performance of isolation systems. These metrics are: transmissibility, effectiveness, transmitted power, and the forces transmitted to the support structure. The assumptions made in the formulation of these metrics are presented, and the measure of the transmitted forces is modified and applied to the planar problem presented in the thesis.

Copyright by

R. MATTHEW BRACH

1995

DEDICATION

To my wife, Paula

ACKNOWLEDGEMENTS

This research was possible with the help of several individuals, most notably my thesis advisor, Dr. Alan Haddow. Without his help, encouragement, and patience, this work would not have been completed. Thanks also goes to the members of my dissertation committee: Drs. Clark Radcliffe, Philip FitzSimons and Charles MacCluer. Thanks also to the Amoco Foundation for their financial support of my research efforts through a fellowship from 1990 to 1993 and to my present employer, the Ford Motor Company, which supported my efforts while I completed my research.

I would also like to acknowledge Scott Emery for the many conversations, engineering and otherwise, Paul Ferraiuolo for his understanding of my commitment to this task, and my father for our conversations about my research.

Special thanks to my wife Paula. Her patience through the six years of this pursuit made it all possible. Without her encouragement I would have never returned to school. Thank you.

And last but not at all in the least, thank you to my three children Elizabeth, Olivia, and Daniel for their patience with their daddy while he "did his homework".

TABLE OF CONTENTS

LIST OF TABLES

LIST OF FIGURES

NOMENCLATURE

A	Half width of the rigid body (m)
B	Half height of the rigid body (m)
c_j	Coefficient of viscous damping
D_j	Time derivative with respect to time T_i
E_v	Velocity effectiveness (dimensionless)
E_f	Force effectiveness (dimensionless)
$\bar{F}$	Force transmitted to the foundation
$\hat{f}_i$	Nondimensionalized form of F_i
F_i	Forcing amplitude (N)
F_T	Transmitted force (N)
$\hat{F}$	Applied impulse (kg-m/s)
I_G	Mass moment of inertia (m^2-kg)
I_{ij}	Moments and products of inertia (m^2-kg)
k_G	Radius of gyration about an axis through G
k_i	Spring constant (N/m)
ℓ	Length (m)
L	Lagrangian (N-m)
L_i	Spring length (m)
m	Mass (kg)
Q_j	Generalized forces

r	Radius (m)
R_N	Remainder of a Taylor series expansion
T	Kinetic energy (N-m)
T_n	Time scale
T_v	Velocity transmissibility
V	Potential energy (N-m)
X_1, X_2, X_3	Coordinate variables x, α, and y respectively
α	Angular displacement (radians)
$\hat{\alpha}_i$	Nondimensionalized form of β_i
β_j	Coefficient produced by a Taylor series expansion
γ_j	Phase parameter
ϵ	Small parameter used in multiple scales analysis
μ_j	Dimensionless damping coefficient
ν	Ratio $\frac{B}{A}$
σ_j	Detuning parameter
ω	Angular velocity (rad/s)
ω_x, ω_y, ω_z	Natural frequency (rad/s)
Ω_j	Forcing frequency (rad/s)

INTRODUCTION

This thesis documents an analytical investigation into the harmonic response and vibration isolation of a rigid body mounted on resilient supports. The rigid body system, with two translational and one rotational degrees of freedom, is a planar analog of an automotive engine on mounts.

In the automotive industry, emphasis is being placed on producing automobiles with a ride that is smooth and quiet. This has increased the importance of the isolation of engine vibrations from the rest of the automobile. The analytical methods currently used in the automotive industry to determine the position and orientation of engine mounts, i.e. elastic axes theory, torque axis theory, and natural frequency placement, have shortcomings which prevent them from establishing an accurate prediction of the harmonic response of the system. Consequently, the placement and orientation of the engine mounts predicted by these methods will be less than optimum, and experimental tuning of the system will be required prior to production. The most salient of these shortcomings is the fact that linear system theory is used in the formulation of these methods. The work in this thesis demonstrates that the response of this system will often be nonlinear.

The equations of motion for this system are derived using Lagrange's equations. It is desirable that these equations contain no simplifications

such that the general nonlinear response of the system can be investigated. However, due to the complexity of the resulting equations, the potential energy of the system is written using a Taylor series. This simplifies the nonlinear terms in the equations of motion to polynomial form enhancing the application of a perturbation solution.

The method of multiple scales is used to effect a solution of these equations of motion. This technique ultimately leads to six nonlinear algebraic equations, the solutions of which are the steady state response amplitudes of the system. The response from these equations is pursued for parameter values appropriate for an in-line four cylinder engine. The response of this system is found for four different forcing conditions. The stability of the solutions is established through examination of the of the eigenvalues of the Jacobian matrix of these algebraic equations. This system response is then used to analyze the isolation performance of the system.

The contents of this thesis are divided into six chapters. The first chapter presents a review of the literature pertinent to the major topics addressed in the thesis: vibration isolation and harmonic response of rigid bodies.

Since this investigation was motivated partially from interest in the vibrational response of an automotive engine on mounts, the second chapter begins with a review of existing automotive engine mounting strategies. After this review, the problem geometry and system parameters for a three degree of freedom rigid body on resilient supports are presented. This system represents the planar equivalent of an engine supported on mounts. The equations of motion of the system are derived using the Lagrange formulation. Details of the assumptions and

approximations made in arriving at the governing equations of motion are given. The resulting equations of motion for this system are nonlinear, second order, ordinary differential equations. The approximate solution to these equations is pursued using a perturbation technique. The chapter ends with a presentation of the general scope of the analysis and details the three cases to be investigated.

The third chapter presents the perturbation analysis of the equations of motion using the method of multiple scales. This method is applied to each of the three cases resulting in six nonlinear ordinary differential equations for each case. These equations describe the slowly varying amplitudes and phases of the system.

The fourth chapter presents the numerical values of the system parameters used in the balance of the thesis to obtain the system response. The second part of the chapter utilizes these parameter values to demonstrate verification of the use of a Taylor series approximation of the potential energy used in the derivation of the equations of motion.

The fifth chapter presents the system response plots for each of the three cases. These response plots are obtained by repeatedly solving nonlinear algebraic equations for the steady-state amplitudes as a function of the forcing frequency. The final section of the chapter considers the vibration isolation aspect of the system. It begins with the study of the various approaches for the quantification of vibration isolation of rigid bodies presented in the literature. A modified version of one of the measures is used to assess the isolation performance of the planar rigid body problem considered herein.

The sixth chapter presents a summary of this thesis, the conclusions of the investigation and recommendations for future work.

CHAPTER 1 LITERATURE REVIEW

The majority of the information about the topics of harmonic response and passive vibration isolation of rigid bodies has been generated by the automotive industry. Therefore, the majority of the papers reviewed deal with the simulation, harmonic response and vibration isolation of multi-cylinder engines.

One of the earliest detailed works addressing vibration isolation of rigid bodies is *Vibration and Shock Isolation*, (Crede, 1951). In this book, vibration isolation is viewed from two perspectives. The first is that of reducing the forces transmitted to the supporting structure and, the second is the isolation of rigid body displacements. Crede (1951) addresses these two problems utilizing the same approach, that of tuning the system natural frequencies to be substantially lower than the forcing frequency of the input. Crede (1951) considers one, two and three degree of freedom linear, planar rigid body systems with various degrees of symmetry. Since his approach is to place the natural frequencies of the system far from the exciting frequency, much attention is placed on obtaining expressions for the natural frequencies of the systems considered.

Another book that addresses the topic of vibration isolation of rigid bodies is *Vibration Engineering* (Wilson, 1959). This book examines primarily the vibrational response of reciprocating engines and rotating machinery. This work considers the vibrational characteristics of multi-cylinder engines in detail. The equations of motion for a six degree of freedom rigid body system are derived using the Newtonian formulation. The

assumption is made that a displacement along any one of the three coordinate axes produces no force in the springs along the other two coordinate axes. This assumption reduces the number of terms that appear in the equations of motion. The displacements of the systems are assumed to be small. Therefore, the restoring forces and couples are written as linear expressions of the displacement variables. This results in equations of motion with only linear coupling terms.

As with the book by Crede (1951), considerable attention is paid to obtaining expressions for the natural frequencies of the various systems considered. The vibration isolation aspect of the text focuses on the prediction and management of the forces transmitted to the support structure (which throughout the majority of the text is considered rigid). Various other topics are also considered such as vibration of multi-cylinder engines, elastic characteristics of the foundation, systems with various degrees of symmetry, and information about rubber isolation mounts.

An extensive review article about vibration isolation (Snowdon, 1979), looks at simple mounting systems, primarily single degree of freedom systems. This article presents information and theory which address vibration isolation systems for which a single degree of freedom system is too simple to adequately describe system response. In addition, the article presents information regarding the static and dynamic properties of rubber and rubber-like materials, and some experimental aspects of isolation measurement. The article contains a lengthy bibliography of vibration isolation materials.

Since the time these three references were written, numerous papers have been written that specifically address the harmonic response of

multi-cylinder engines. Various approaches have been taken to simulate this rigid body system. These include Radcliffe, et. al., (1983); Butsuen, et. al., (1986); Matsuda, (1987); Furubayashi, (1991); Shiomi and Mizuguchi, (1991); Xuefeng, (1991); and Hata, (1992). These papers focus primarily on the modeling and simulation of the engine as a rigid body system. In these papers, linear system theory is used to investigate the response of an engine on a mount system.

Correspondingly, a number of articles have investigated the harmonic response of the engine mount. These include John and Straneva, (1966); Schmitt and Leingang, (1976); Sakamoto, et. al., (1981); Gennesseoux, (1993). These articles look specifically at the function, characteristics, and performance of the engine mount itself.

Of particular relevance to the topic of this thesis are those papers which deal with the performance of vibration isolation systems utilizing nonlinear characteristics in the suspension system. Eight papers were found which explore this particular topic (Tobias, 1959; Henry and Tobias, 1959; Grootenhuis and Ewins, 1965; Efstathiades and Williams, 1967; Shoup, 1971 and 1972; Shoup and Simmonds, 1977; Metwalli, 1986). The papers by Shoup (1971 and 1972) and Shoup and Simmonds (1977) investigate single degree of freedom systems possessing nonlinear force-displacement characteristics. Metwalli (1986) considers a two degree of freedom system representing a vehicle suspension model. In addition to nonlinear stiffness in the springs, nonlinear damping is also included in the system model.

The article by Grootenhuis and Ewins (1965) investigates the unforced response of a rigid body on resilient supports. The Lagrange's equations are used to obtain the equations of motion for the six degree of

freedom rigid body system. The equations of motion are computed with the assumption that the rigid body displacements are small. Hence the expression for the potential energy is simplified and only linear terms appear in the equations of motion. These equations are then used to find the natural frequencies of the system. Specifically, the change in these natural frequencies as a function of the location of the center of gravity is demonstrated.

In the paper by Efstathiades and Williams (1967), the coupled response of two of the six degrees of freedom of a rigid body system with supports at four corners is investigated. The corner supports possess symmetric cubic force-displacement characteristics. Internal resonances of the system are investigated using the method of harmonic balance. In contrast, the resiliently supported rigid body system investigated in this thesis demonstrates that supports with nonlinear force-displacement characteristics are not required for a rigid body system to produce nonlinear response. Nonlinear response is demonstrated analytically with supports having linear symmetric force-displacement characteristics.

Two articles were found which looked at the effects of nonlinear damping on the performance of isolation systems (Ruzika and Derby, 1971; ElMadany and ElTamini, 1990). Nonlinear damping is not considered in this thesis.

The response of a three dimensional rigid body system requires that the equations of motion of the rigid body on resilient supports be written considering six degrees of freedom. The two approaches to this problem are the Newtonian formulation and Lagrange formulation. The former is considered by Himelblau and Rubin (1961). In this paper, it is assumed that the supports have independent linear force-displacement

characteristics along each of the three mutually perpendicular coordinate axes. Only small translations and rotations are considered, which reduces the complexity of the derivation by neglecting certain components of the restoring force. The six resulting differential equations of motion contain only linear terms.

The Lagrange approach to the derivation of the equations of motion is presented by Andrews (1960). No assumptions are made in this paper regarding symmetry of the body or the location or orientation of the resilient supports. The supports are assumed to have independent linear force-displacement and linear viscous damping characteristics along each of the three mutually perpendicular coordinate axes. The assumption of small rotations of the rigid body is made, eliminating the need for Euler angles to represent the rotational motion of the rigid body. Therefore, the three angular velocities can then be written as the time derivative of its corresponding angular displacement. This enables the equations to be written in a simpler form. The resulting differential equations of motion are nonlinear.

The use of Lagrange's equations for the derivation of the equations of motion is the method used later in this thesis to obtain the general equations of motion for the resiliently supported rigid body system considered herein. This system is a planar three degree of freedom equivalent of the system considered in the above derivations by Andrews (1960) and Himelblau and Rubin (1961). For this particular case, the small angular displacement assumption is not needed to write the angular velocity as a time derivative of an angular displacement. Hence, the resulting equations of motion for this planar system are completely general.

With the pertinent literature related to the topics of this thesis identified, the analysis of the harmonic response of a rigid body on resilient supports can be pursued. The following chapter initiates this process by looking first at the methods used in the automotive industry to isolate engines. The geometry of the system to be investigated in this thesis is then presented, and the derivation of the equations of motion of the system is presented.

CHAPTER 2 SYSTEM BACKGROUND AND DEFINITION

Since the inception of the automotive industry, vibration of the engine has been an identified problem. Various isolation schemes have been devised to deal with this problem. Four methods have been identified in the literature that are used in the automotive industry to address this problem. They are: center of percussion mounting, natural frequency placement, torque axis mounting, and elastic axes mounting. A review of the literature indicates that the latter three techniques are more widely used and investigated. All four techniques are described here to establish a comprehensive background about engine mounting strategies that consider the motion of the engine as a rigid body only. The short review of each method contains the pertinent references that present the development and theory behind each method. In each case, discussion regarding the assumptions made in the development of the method is presented and the limitations of each method are also discussed. Vibration isolation methods which consider the flexural motion of the automotive engine and drivetrain are outside the scope of this thesis (Bolton-Knight, 1971).

Subsequent to this review, a simple problem of a planar rigid body on resilient supports is introduced. This problem is the planar equivalent to the grounded engine on mounts problem (the support structure is considered rigid) restricted to three degrees of freedom. The general equations of motion are derived in this chapter, with the perturbation analysis and the system response following in later chapters. The bearing of the results of the investigation of the response of this planar system

on the four existing engine isolation schemes is delineated in the sixth chapter.

2.1 REVIEW OF AUTOMOTIVE ENGINE ISOLATION STRATEGIES

2.1.1 Center of Percussion Mounting

This technique utilizes the fundamental mechanical phenomenon known as the center of percussion. One property of the center of percussion is that for a compound pendulum acted on by an impulse applied through the center of percussion and perpendicular to the line defined by the center of mass and the fixed point, no reactive impulse results at the fixed point. (A detailed presentation of the definition of the center of percussion and the properties associated with this point is given in Appendix A.) The application to engine mounting is direct. If the front and rear engine mounts are arranged such that their locations are reciprocal centers of percussion (see Appendix A), then an impulse to one mount from a road disturbance results in little or no reaction at the other mount (Wilson, 1959; Timpner, 1965; Bolton-Knight, 1971). This improves the overall isolation performance of the mounting system with respect to impulsive inputs. Although the application of this isolation scheme to actual mounting problems is typically not as simple as this example would indicate, placement of the engine mounts consistent with this theory will enhance their overall isolation effectiveness.

2.1.2 Natural Frequency Placement

Algorithms based on optimization routines have been developed which aim to move the rigid body linear natural frequencies of the engine away

from the frequencies of the input sources, thereby changing the mode shapes and reducing the transmitted forces. Numerous papers have been written about this topic, including Johnson and Subhedar, (1979); Bernard and Starkey, (1983); Geck and Patton, (1984); Spiekerman, Radcliffe, and Goodman, (1985); Staat, (1986); and Saitoh and Igarashi, (1989).

In these studies the engine is modelled as a rigid body with six degrees of freedom mounted on resilient supports attached to ground. The design parameters include the mount stiffnesses, mount locations and orientations. These methods depend largely on the ability to predict or determine the natural frequencies of the engine. This task can be difficult, and the results of this isolation method are only effective near the identified frequency. As such, this technique is used primarily to address vibrational problems which are due to the engine idle frequency or one of its associated orders being close to a natural frequency. Of course the trivial solution of the optimization process, that of a natural frequency being equal to zero, must be avoided. This is accomplished by incorporating a function which penalizes large parameter changes. A modification of this approach has been implemented which determines the mount stiffnesses by directly minimizing the forces transmitted through the mounts to the vehicle structure at idle (Oh, Lim and Lee, 1991; Swanson, Wu, and Ashrafiuon, 1993).

More recently, optimization methods have been used to analyze a rigid body mounted on resilient mounts attached to a flexible support (Ashrafiuon, 1993; Lee, Yim, and Kim, 1995).

2.1.3 Torque Axis Mounting

The torque axis, also referred to as the torque roll axis, is defined as the resulting fixed axis of rotation of an unconstrained three dimensional rigid body (i.e. either free or elastically supported on very soft springs) when a torque is applied along an axis not coincident with any of the principal axes (Timpner, 1965; Fullerton, 1984). For the case of an automotive engine, the axis about which torque is applied is the crankshaft axis. This axis is rarely coincident with a principal axis of the engine. It is hypothesized (Timpner, 1966) that the disturbances transferred to the vehicle can be reduced by positioning the engine mounts such that the engine oscillates predominantly about this torque axis. The two references above each give a method for determining the location of the torque axis of an engine.

In order to better understand the concept of torque axis and appreciate some of the shortcomings of this approach as used in the automotive industry, consider the equations of motion governing the rotational behavior of a rigid body in three dimensions acted on by the moment vector $\boldsymbol{M}$. These equations are given by (Greenwood, 1988):

$$\begin{aligned} M_x &= I_{xx}\dot{\omega}_x + I_{xy}(\dot{\omega}_y - \omega_x\omega_z) + I_{xz}(\dot{\omega}_z + \omega_x\omega_y) \\ &\quad + (I_{zz} - I_{yy})\omega_y\omega_z + I_{yz}(\omega_y^2 - \omega_z^2) \\ M_y &= I_{xy}(\dot{\omega}_x + \omega_y\omega_z) + I_{yy}\dot{\omega}_y + I_{yz}(\dot{\omega}_z + \omega_x\omega_y) \\ &\quad + (I_{xx} - I_{zz})\omega_x\omega_z + I_{xz}(\omega_z^2 - \omega_x^2) \\ M_z &= I_{xz}(\dot{\omega}_x - \omega_y\omega_z) + I_{yz}(\dot{\omega}_y + \omega_x\omega_z) + I_{zz}\dot{\omega}_z \\ &\quad + (I_{yy} - I_{xx})\omega_x\omega_y + I_{xy}(\omega_x^2 - \omega_x^2) \end{aligned} \tag{2.1}$$

For the case of an automotive engine, it is common to assume the engine can be assumed to be a rigid body on resilient supports which are attached to ground. It can be further assumed that the values of the moments, both the applied moments and the moments generated by the

reaction forces at the mounts, and inertia products are known or can be calculated. Then, for a given set of initial conditions, ω can theoretically be solved for as a function of time. In general, the magnitude and direction of the axis of rotation of the rigid body will also be a function of time. Thus, the torque axis as defined previously, does not exist.

It is further noted that equations (2.1) are derived under the assumption that the inertia properties of the engine are independent of time. This is not the case for an engine, because the motion of the pistons, cranks, connecting rods, and the crankshaft make the inertia properties periodic functions of time, independent of the coordinate system. This further influences the time dependent nature of ω in an actual engine. However, the time dependence of the inertia properties is typically neglected in practice (Bachrach, 1995).

2.1.4 Elastic Axes

Elastic axes for an elastically supported rigid body system are those axes for which application of a force or torque, along or about the axis produces only a corresponding translation or rotation, respectively. In the coordinate system defined by the elastic axes, the system response consists of decoupled translational and rotational modes.

The elastic axes of a rigid body on flexible supports are determined using the flexibility matrix A. Analytical modal decoupling of the flexibility matrix does not yield the elastic axes system because the eigenvectors do not typically span a physical space. Hence, the transformation to the elastic axes must be a physical coordinate transformation.

Since a physical coordinate transformation is required, a 2-dimensional system with three degrees of freedom can be decoupled since the six off-diagonal terms of the symmetric 3X3 flexibility matrix can be eliminated by two independent translations and one rotation. Full decoupling of the symmetric 6X6 flexibility matrix for a 3-dimensional rigid body system with six degrees of freedom cannot be accomplished since 30 off-diagonal terms exist and only three independent coordinate translations and three independent coordinate rotations can be defined (Kim, 1991). Due to this limitation, effort has been spent in the area of "partial" decoupling of the modes of vibration (Derby, 1973; Ford, 1985).

These four methods of automotive engine vibration isolation represent those documented in the literature. A common assumption in the implementation of these mounting strategies is that the response of the system is linear. This assumption is made to simplify the analysis of the system.

Recently, hydraulic engine mounts have proven to be effective vibration isolators and have replaced traditional elastomeric mounts in many automobiles. The experimental and analytical response characteristics of this class of engine mounts have been investigated and are inherently nonlinear (Kim, Singh, and Ravindra, 1992; Brach and Haddow, 1993; Kim and Singh, 1993). These nonlinear characteristics have been introduced intentionally to improve the isolation performance of the engine on mounts system. However, despite the apparent effectiveness of these mounts, no investigations have been found which establish the response of the complete system of an engine supported by such mounts. A clear understanding of the system response will improve the consideration of the isolation aspects of the system. Therefore, to better comprehend this

class of vibration system, the problem of determining the response and isolation performance of a rigid body on resilient supports is considered.

The most general approach to this problem is that of a three dimensional rigid body supported by arbitrarily located resilient supports. This problem has six degrees of freedom: three translational and three rotational. The problem considered presently is a two dimensional rigid body on resilient linear supports. Linear supports are used since it will be shown through this analysis that the geometry of the problem introduces nonlinear response. The same procedure used in the solution of this problem can be followed for supports with nonlinear characteristics. This planar problem has three degrees of freedom: two translational and one rotational. The problem was made planar to increase the tractability. The following section introduces the specific geometry of the problem investigated.

2.2 SYSTEM DEFINITION: PLANAR RIGID BODY ON RESILIENT SUPPORTS

2.2.1 Problem Geometry

The ensuing analysis is based on the geometry of a planar rigid body mounted on resilient linear supports as shown in Figure 2.1. Each of the mounts is characterized by two orthogonal stiffness values, one for the axial stiffness in the x-direction and one for the lateral stiffness in the y-direction. The dimensions shown in the drawing for the supports are exaggerated to emphasize the geometry used in the analysis. The dimensions utilized for the rigid body in the numerical analysis which follows were chosen to closely approximate an actual 4-cylinder automotive engine. The free lengths of the springs and the spring rates were chosen to be

representative of production elastomeric mounts. For this problem, the stiffness values were chosen such that $k_1 = k_4$ and $k_2 = k_3$ and the mounting geometry is symmetric. The numerical parameter values chosen for all problems will be given prior to the presentation of the response of the system. It should be noted that the procedure used to analyze this system with linear spring characteristics can also be used to analyze rigid body systems with nonlinear spring characteristics.

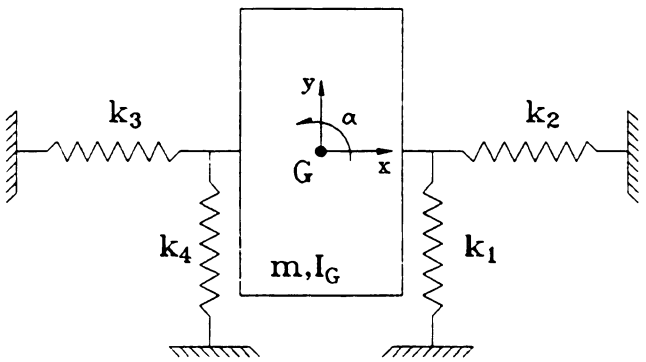

Figure 2.1 - Geometry of the rigid body system

Figure 2.1 depicts the rigid body in the static equilibrium position. The static equilibrium position is used in this instance as a more convenient point about which to write the equations of motion.

2.2.2 Equations of Motion

The equations of motion for this problem are derived using Lagrange's equations:

$$\frac{d}{dt}\left[\frac{\partial L}{\partial \dot{q}_j}\right] - \frac{\partial L}{\partial q_j} = Q_j \qquad (2.2)$$

where $L = T - V$, T is the kinetic energy, V is the potential energy, q_j are the generalized coordinates, and Q_j are the generalized forces applied to the system.

Using the notation given in Figure 2.1, the kinetic energy for the rigid body, T, can be written directly:

$$T = \frac{1}{2}m\dot{x}^2 + \frac{1}{2}m\dot{y}^2 + \frac{1}{2}I_G\dot{\alpha}^2 \tag{2.3}$$

The potential energy for the problem, V, is complicated. For this problem, the general equations of motion are desired, and therefore no simplifications of the potential energy are made. The potential energy of this system is the sum of the potential energies of the four springs. The potential energy of a given spring, $\frac{1}{2}k\delta^2$, where δ is the deflection in the spring and k is the linear spring constant, requires for this problem that the deflection δ be written in terms of the rigid body displacements x, y, and α. For this problem, δ for each spring is determined by writing the expression for the length of the spring in the deflected state and subtracting from this quantity the undeflected length of the spring, (i.e., the free length). The complexity of the expression for the potential energy for this geometry is simpler than for the general case of arbitrarily located springs. This is due to the fact that the attachment points of the springs are collinear with the center of mass of the rigid body and with each other. Appendix B presents more detail of the derivation of the potential energy for this system.

The next step is to take the partial derivatives of this expression with respect to x, y, and α. However,the resulting form of the equations of motion will be complicated, and not conducive to the solution technique of the method of multiple scales used later. It is more convenient to have the equations appear in polynomial form. Therefore a Taylor series expansion of the potential energy is performed prior to the implementation

of the partial derivatives required by the Lagrange formulation of the equations of motion[1]. The multi-variable version of the Taylor series is:

$$
\begin{aligned}
f(x,y,\alpha) &= f(x_0,y_0,\alpha_0) \\
&+ \left[\left[(x-x_0)\frac{\partial}{\partial x} + (y-y_0)\frac{\partial}{\partial y} + (\alpha-\alpha_0)\frac{\partial}{\partial \alpha}\right] f(x,y,\alpha)\right]\Big|_{(x_0,y_0,\alpha_0)} \\
&+ \frac{1}{2!}\left[\left[(x-x_0)\frac{\partial}{\partial x} + (y-y_0)\frac{\partial}{\partial y} + (\alpha-\alpha_0)\frac{\partial}{\partial \alpha}\right]^2 f(x,y,\alpha)\right]\Big|_{(x_0,y_0,\alpha_0)} \\
&+ \frac{1}{3!}\left[\left[(x-x_0)\frac{\partial}{\partial x} + (y-y_0)\frac{\partial}{\partial y} + (\alpha-\alpha_0)\frac{\partial}{\partial \alpha}\right]^3 f(x,y,\alpha)\right]\Big|_{(x_0,y_0,\alpha_0)} \\
&+ \sum_{n=4}^{N-1} \frac{1}{n!}\left[\left[(x-x_0)\frac{\partial}{\partial x} + (y-y_0)\frac{\partial}{\partial y} + (\alpha-\alpha_0)\frac{\partial}{\partial \alpha}\right]^n f(x,y,\alpha)\right]\Big|_{(x_0,y_0,\alpha_0)} \\
&+ R_N(x,y,\alpha)
\end{aligned}
\tag{2.4}
$$

where

$$
R_N(x,y,\alpha) = \frac{1}{N!}\left[(x-x_0)\frac{\partial}{\partial x} + (y-y_0)\frac{\partial}{\partial y} + (\alpha-\alpha_0)\frac{\partial}{\partial \alpha}\right]^N f(x,y,\alpha)\Big|_{(\xi,\eta,\zeta)} \tag{2.5}
$$

and (ξ,η,ζ) is a point somewhere on the straight line segment between (x_0,y_0,α_0) and (x,y,α).

The derivation of the Taylor series expansion in two variables (Hildebrand, 1976) was expanded to three variables to give the equations above. This treatment can be further generalized for expansions of variables of four or more variables. The Taylor series for the potential energy for this problem is taken about the static equilibrium position, $(x_0,y_0,\alpha_0) = (0,0,0)$. Hence, this is the point where the series is evaluated to establish the series coefficients. This position is chosen since the reference coordinate system is fixed in space at the location of the static equilibrium position as shown in Figure 2.1. Once the Taylor series expansion of the potential energy is determined, Lagrange's equations can be used to determine the equations of motion for the system.

---

[1]The order of the operation of the Taylor series and the partial differentiation is not important, i.e., these operations are commutative. Hence, the application of the Taylor series approximation could be performed on the appropriate terms after Lagrange's equations are obtained and the same equations of motion would result.

With the application of the Taylor series, questions of the convergence and accuracy of the series arise. The ratio test can be used to show that the Taylor series of a function $f(x,y,\alpha)$ about (x_0,y_0,α_0), is absolutely convergent for all real numbers if the function has derivatives of all orders on some interval containing the point (x_0,y_0,α_0). However, for application of the Taylor series to this problem, the series must be truncated to be useful, and the accuracy of this truncated series comes into question. The remainder of the series R_N shown above, gives an indication of the order of magnitude of the error of the truncated series.

The question of what constitutes an acceptable error then arises. Additionally, the exact means of computation also must be established. For the remainder R_N, the choice of (ξ,η,ζ) needs to be made, and only then can the numerical calculation of R_N be performed. Using any method, a norm could be established and the magnitude evaluated numerically, but the interpretation of the magnitude of the norm still presents difficulty. One alternative to this approach is to graphically compare the approximate potential energy to the actual potential energy to ascertain the accuracy of the truncated series over some appropriate range of system coordinates. Ultimately, it is only the applicability of the truncated series of the potential energy to represent the actual potential energy which is established.

The validity of the equations of motion derived using a Taylor series approximation of the potential energy was established through a comparison of the system response obtained by direct numerical integration of the equations of motion using a particular set of parameter values. The system response obtained from the equations of motion derived using the Taylor series approximation of the potential energy was compared to the

response given by the equations of motion derived with no approximation for the potential energy. This process is depicted in the flow chart shown in Figure 2.2.

Regardless of how closely the truncated series for the potential energy might approximate the actual potential energy, the response of the system using the equations obtained using the truncated series must closely match the response of the system using the equations obtained using the actual potential energy. If the response of the approximated system does not match the response of the actual system satisfactorily, terms must be added to the truncated series until the system responses match. If the comparison shows that similar steady state responses are obtained under identical forcing conditions, the truncated series was considered acceptable.

The equations which are given by the above analysis do not include damping. For this formulation, damping coefficients are introduced after the application of the Lagrange equations. Damping is required in this problem to bound the system response at resonance. Viscous damping included in the Lagrange formulation through the use of Rayleigh's dissipation function (Meirovitch, 1975) would introduce off-diagonal terms in the system damping matrix. To avoid these coupling terms, a single viscous damping term was added to each of the three equations. This approach reduces the algebraic complexity of the analysis of the equations of motion. Neglecting coupling damping terms in this analysis is reasonable as only light damping is considered and prior experience has shown that damping in these types of problems typically influences the amplitude of response, not the type of response and only then, close to resonant frequencies.

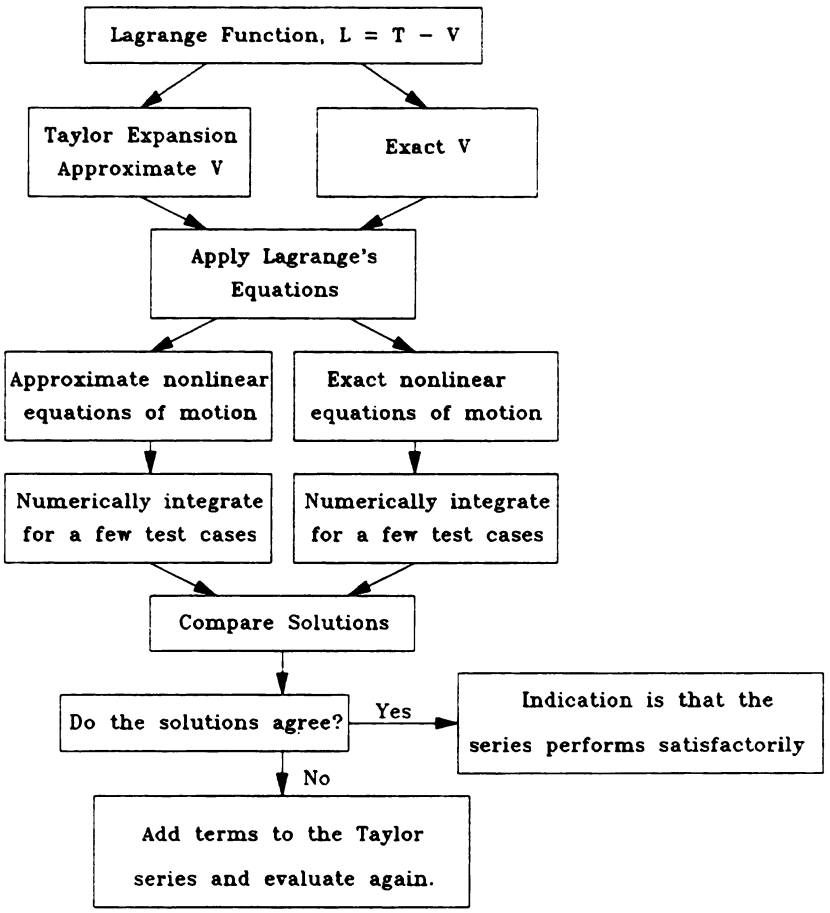

Figure 2.2 - Flow chart of the Taylor series evaluation process

The generalized forces, Q_j, associated with each of the system coordinates remain to be found. These forces are found using the principle of virtual work (Meirovitch, 1975). For this system, the generalized force associated with each coordinate is the force acting in that direction.

The equations of motion for the system can now be assembled. The equations can be put into a simpler format using the following coordinate reassignment: $x \rightarrow X_1$, $\alpha \rightarrow X_2$, and $y \rightarrow X_3$. The equations for the system are:

$$m\ddot{X}_1 + c_1\dot{X}_1 + (k_2+k_3)X_1 + \beta_1X_2X_3 + \beta_2X_1X_3 + \beta_3X_2^3 + \beta_4X_1X_2^2 + \beta_5X_1^3 + \beta_6X_1X_3^2 = F_1\cos\Omega_1 t \tag{2.6a}$$

$$I_G\ddot{X}_2 + c_2\dot{X}_2 + A^2(k_1+k_4)X_2 + \beta_7X_1X_3 + \beta_8X_2^3 + \beta_9X_1X_2^2 + \beta_{10}X_1^2X_2 + \beta_{11}X_2X_3^2 = F_2\cos\Omega_2 t \tag{2.6b}$$

$$m\ddot{X}_3 + c_3\dot{X}_3 + (k_1+k_4)X_3 + \beta_{12}X_1^2 + \beta_{13}X_1X_2 + \beta_{14}X_2^2X_3 + \beta_{15}X_1^2X_3 + \beta_{16}X_3^2 = F_3\cos\Omega_3 t \tag{2.6c}$$

where

$$I_G = \frac{1}{3}m(A^2+B^2) \tag{2.7}$$

The system parameters A and B are shown in Figure 2.3.

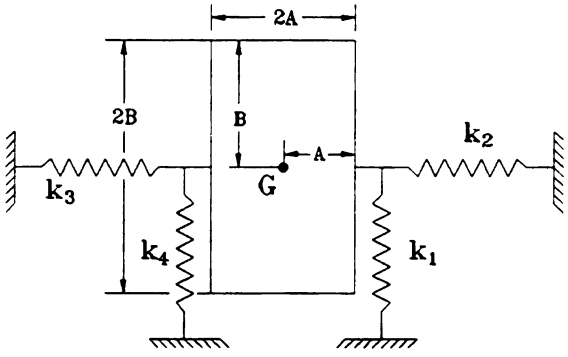

Figure 2.3 - Physical dimensions of the rigid body

The terms c_1, c_2, and c_3 in equations (2.6) represent the viscous damping associated with each of the degrees of freedom. The coefficients for the linear terms are given here in terms of system parameters. The coefficients for the nonlinear terms, represented in equations (2.6) by β_j's, are not given in terms of system parameters because this representation of these values is exceedingly lengthy. However, specific numerical values are assigned to the parameters of the problem in Chapter 4. In addition, Appendix C contains the Mathematica code used to derive

these equations of motion. It is noted that due to the symmetry of the problem, no linear coupling terms appear in the equations.

The equations of motion for the system can also be stated in a nondimensional form, given by equations (2.8). A detailed presentation of the procedure used to arrive at these equations is given in Appendix D.

$$\ddot{x}_1 + 2\hat{\mu}_1\dot{x}_1 + \omega_1^2 x_1 + \hat{\alpha}_1 x_2 x_3 + \hat{\alpha}_2 x_1 x_3 + \hat{\alpha}_3 x_2^3 + \hat{\alpha}_4 x_1 x_2^2 + \hat{\alpha}_5 x_1^3 + \hat{\alpha}_6 x_1 x_3^2 = \hat{f}_1 \cos\Omega_1 t \tag{2.8a}$$

$$\frac{1}{3}(1+\nu^2)\ddot{x}_2 + 2\hat{\mu}_2\dot{x}_2 + k' x_2 + \hat{\alpha}_7 x_1 x_3 + \hat{\alpha}_8 x_2^3 + \hat{\alpha}_9 x_1 x_2^2 + \hat{\alpha}_{10} x_1^2 x_2 + \hat{\alpha}_{11} x_2 x_3^2 = \hat{f}_2 \cos\Omega_2 t \tag{2.8b}$$

$$\ddot{x}_3 + 2\hat{\mu}_3\dot{x}_3 + \omega_3^2 x_3 + \hat{\alpha}_{12} x_1^2 + \hat{\alpha}_{13} x_1 x_2 + \hat{\alpha}_{14} x_2^2 x_3 + \hat{\alpha}_{15} x_1^2 x_3 + \hat{\alpha}_{16} x_3^3 = \hat{f}_3 \cos\Omega_3 t \tag{2.8c}$$

The parameter ν is the ratio $\frac{B}{A}$ where the dimensions A and B are shown in Figure 2.3.

For the purposes of this investigation, the nondimensionalized form of the equations are not used. No parameter studies are performed whereby use of the nondimensionalized equations would be advantageous. Hence, the physical parameters of the system are utilized throughout the analysis. This also makes direct comparison to the physical system simpler.

2.2.3 Scope of Analysis

The equations of motion for this system, given by equations (2.6), fall into the category of weakly nonlinear systems. A system is weakly nonlinear if, to the lowest order approximation, the system is always viewed as a simple harmonic oscillator; the nonlinearity enters as a

correction term (Kahn, 1990). For this system, this point can be seen by letting the $\beta_i = 0$ in equations (2.6). The resulting system is a set of three uncoupled, simple harmonic oscillators. However, as will be shown later, even if the amplitudes of the response are small, nonlinear response can still be realized through appropriate tuning of the natural frequencies.

Prior to presenting the perturbation analysis of the equations, it is useful to establish the scope of the investigation within the context of the perturbation analysis. For analysis of a nonlinear system, the relationships between the linear natural frequencies, referred to as internal resonance conditions, and the forcing frequencies are typically the defining attributes between problems. For this geometry, the possible relationships between the three linear natural frequencies (ω_1, ω_2, and ω_3), the forcing frequencies (Ω_1, Ω_2, and Ω_3), and the presence or absence of forcing (F_1, F_2, and F_3) is considered. Table 2.1 presents a subset of the many combinations. The number of possible entries in this table would increase significantly if the forcing (F_1, F_2, and F_3) were also included in generating the cases.

All of the cases listed in Table 2.1 lead to resonance-like conditions in which all modes are excited. There are many more possible combinations. Several different combinations, based on a physical system, are investigated.

Internal Resonance Relationships	External Resonance Relationships
$\omega_1 \approx \omega_2,\ \omega_1 \approx \omega_3$	$\Omega_1 \approx \omega_1,\ \Omega_2 \approx \omega_2,\ \Omega_3 \approx \omega_3$
$\omega_1 \approx \omega_2,\ \omega_1 \approx \omega_3$	$\Omega_1 \not\approx \omega_1,\ \Omega_2 \approx \omega_2,\ \Omega_3 \approx \omega_3$
$\omega_1 \approx \omega_2,\ \omega_1 \approx \omega_3$	$\Omega_1 \approx \omega_1,\ \Omega_2 \not\approx \omega_2,\ \Omega_3 \approx \omega_3$
$\omega_1 \approx \omega_2,\ \omega_1 \approx \omega_3$	$\Omega_1 \approx \omega_1,\ \Omega_2 \approx \omega_2,\ \Omega_3 \not\approx \omega_3$
$\omega_1 \approx \omega_2,\ \omega_1 \approx \omega_3$	$\Omega_1 \not\approx \omega_1,\ \Omega_2 \not\approx \omega_2,\ \Omega_3 \approx \omega_3$
$\omega_1 \approx \omega_2,\ \omega_1 \approx \omega_3$	$\Omega_1 \not\approx \omega_1,\ \Omega_2 \approx \omega_2,\ \Omega_3 \not\approx \omega_3$
$\omega_1 \approx \omega_2,\ \omega_1 \approx \omega_3$	$\Omega_1 \approx \omega_1,\ \Omega_2 \not\approx \omega_2,\ \Omega_3 \not\approx \omega_3$

Table 2.1 - A subset of possible natural frequency/forcing frequency combinations

In this physical system, the characteristics and parameters for the rigid body were chosen to represent an in-line four cylinder automotive (four-cycle) engine at hot idle. For this engine, all the first order forces[2] and moments are theoretically balanced while certain second order forces and moments are unbalanced (Den Hartog, 1984). Therefore, in the X_1 direction (horizontal) for first order, $F_1 = 0$. However, in actual engines, it has been found that the first order moments in the X_2 direction (torsional), actually do not completely balance (Whitekus, 1994) and so there is a component F_2 oscillating at the idle speed Ω_2. For the X_3 direction (vertical), unbalance appears at the second order, $\Omega_3 = 2\Omega_2$ = twice idle frequency. Table 2.2 depicts these results.

[2]First order refers to phenomena occurring at engine rotational speed and is also referred to as primary. Second order refers to phenomena occurring at twice the engine rotational speed and is also referred to as secondary.

	1st Order	2nd Order
Unbalanced Horizontal Force	Magnitude of this force at this order is equal to zero.	Magnitude of this force at this order is equal to zero.
Unbalanced Vertical Force	Magnitude of this force at this order is equal to zero.	Magnitude of this force at this order is not equal to zero.
Unbalanced Moment	Magnitude of this force at this order is not equal to zero.	Magnitude of this force at this order is not equal to zero.

Table 2.2 - Summary of forcing conditions

Typically, the six rigid body linear natural frequencies of an engine are between 5 Hz and 25 Hz. It is not unreasonable to expect that there could be nearly simple integer relationships between the system linear natural frequencies. Several papers that list the six linear natural frequencies for actual engines (Johnson and Subhedar, 1979; Geck and Patton, 1984; Spiekerman, et. al. 1985) indicate that such relationships do occur in actual systems. Guided by these works and the information in Table 2.2, the relationships between the linear natural frequencies chosen for this study are the following:

$$\omega_1 \approx \omega_2, \quad 2\omega_1 \approx \omega_3 \quad \text{and} \quad \Omega_2 \approx \omega_2, \quad \Omega_3 \approx \omega_3$$

with

$$F_1 = \epsilon \hat{f}_1 = 0, \quad F_2 = \epsilon \hat{f}_2 \neq 0, \quad \text{and} \quad F_3 = \epsilon \hat{f}_3 = 0 \quad \text{(first order)} \tag{15}$$

and

$$F_1 = \epsilon \hat{f}_1 = 0, \quad F_2 = \epsilon \hat{f}_2 = 0, \quad \text{and} \quad F_3 = \epsilon \hat{f}_3 \neq 0 \quad \text{(second order)} \tag{16}$$

The second order component of F_2 is neglected. This reduces the number of forcing terms, which correspondingly simplifies the multiple scales analysis. Inclusion of this forcing terms would create multiple-term, multiple-frequency excitation. Hence, excluding this term improves the understanding of the system response.

Therefore, the response of the system is analyzed in three cases of increasing complexity. This process of investigating the simpler of the three cases, cases 1 and 2, validates the methods required to analyze the problem and creates confidence in the results generated in the more complex case 3.

The first case, case 1, investigates the rigid body system with forcing in only the X_3-direction ($F_2 = 0$, $F_3 \neq 0$). The second case, case 2, investigates the system with forcing in only the X_2-direction ($F_2 \neq 0$, $F_3 = 0$). The third case, case 3, investigates combined vertical and torsional forcing ($F_2 \neq 0$, $F_3 \neq 0$). Table 2.3 gives a summary of these three cases.

	Natural Frequencies	Forcing Frequencies	Force Magnitudes
Case 1	$\omega_1 \approx \omega_2$, $2\omega_1 \approx \omega_3$	$\Omega_3 \approx \omega_3$	$F_1 = 0$, $F_2 = 0$, $F_3 \neq 0$
Case 2	$\omega_1 \approx \omega_2$, $2\omega_1 \approx \omega_3$	$\Omega_2 \approx \omega_2$	$F_1 = 0$, $F_2 \neq 0$, $F_3 = 0$
Case 3	$\omega_1 \approx \omega_2$, $2\omega_1 \approx \omega_3$	$\Omega_2 \approx \omega_2$, $\Omega_3 \approx \omega_3$	$F_1 = 0$, $F_2 \neq 0$, $F_3 \neq 0$

Table 2.3 - Summary of the cases investigated

Having derived the nonlinear differential equations of motion for the system, the solution for the three cases designated can be sought. A perturbation technique is used to find an approximate solution. Chapter 3 presents the perturbation analysis for each of the three cases. Chapters

4 and 5 present time and frequency response plots resulting from the approximate solution for each of the three cases.

CHAPTER 3 SOLUTION OF THE EQUATIONS OF MOTION

This chapter presents the perturbation analysis of the equations of motion presented in Chapter 2. The first part of the chapter presents the analysis germane to all three cases. The analysis is then completed through investigation of each individual case. For each case, a set of six nonlinear differential equations is obtained through which the frequency response of the system can be investigated. This aspect of the investigation is presented in Chapter 5. Prior to this, Chapter 4 presents verification of the approximation used for the potential energy of the system. Chapter 4 also presents the system parameter values used in the balance of the analysis.

3.1 PERTURBATION ANALYSIS

The modal interactions in this three degree of freedom planar rigid body system are examined through perturbation analysis. The method of multiple scales is used to effect a solution (Nayfeh and Mook, 1979). The nondimensionalized equations, as presented in equations (2.8), are not analyzed directly. The approach used is to perform the multiple scales analysis on equations (2.6) and (2.7) and then to assign numerical values to the constants such as the β_i's, A, and B, etc. The frequency response of the system can then be obtained. Two reasons motivated this approach.

The first reason is that as presented previously, a Taylor series expansion is used to simplify the expression for the potential energy. A general evaluation of the series approximation (treating all system constants as parameters) would yield unwieldy equations of motion and

reduce the effectiveness of the series to simplify the equations of motion and facilitate multiple scales analysis.

The second reason is that due to the complexity of the equations of motion, an analytical solution, although desirable, is precluded even though multiple scales analysis is used to simplify the equations describing the response of the system. Hence the solutions for all three cases are generated numerically using the results from the multiple scales analysis. Numerical values for the parameters are therefore required. Accordingly, the system parameters in equations (2.6) are assigned numerical values prior to the analysis. However, each equation is simplified by dividing through by the coefficient of its respective acceleration term. The equations then take a form similar to that of equations (2.8).

The method of multiple scales is used to obtain an approximation for X_1, X_2, and X_3. The basic assumption in this method is that the time t is viewed as being constructed from a succession of independent time scales. This is shown by the equation:

$$T_n = \epsilon^n t \quad \text{for} \quad 0 < \epsilon < 1 \quad \text{and} \quad n = 0, 1, 2, \ldots \tag{3.1}$$

The small parameter ϵ is introduced to distinguish responses with frequencies of close to ω_1, ω_2, and ω_3 occurring at the fast time scale $T_0 = t$, and response that occurs at the slower time scale $T_1 = \epsilon t$. The response at the slower time scale represents the modulations in the response at the faster time scale produced by the nonlinearities, the damping, and the excitation. Hence, these three terms must appear at the same order of ϵ. This is accomplished by ordering terms in equations (2.6) and (2.7) and letting:

$$\frac{c_i}{m} = 2\epsilon\mu_i \text{ for } i=1,3 \text{ and } \frac{c_i}{I_G} \text{ for } i=2$$
$$\frac{\beta_j}{m} = \epsilon\alpha_j \text{ for } j=1,..,6,12,..,16 \text{ and } \frac{\beta_j}{I_G} = \epsilon\alpha_j \text{ for } j=7,..,11 \quad (3.2)$$
$$\frac{F_k}{I_G} = \epsilon\hat{f}_k \text{ for } k=2 \text{ and } \frac{F_k}{m} = \epsilon\hat{f}_k \text{ for } k=3$$

Thus, equations (2.6) then take the form:

$$\ddot{X}_1 + 2\epsilon\mu_1\dot{X}_1 + \omega_1^2 X_1 + \epsilon\alpha_1 X_2 X_3 + \epsilon\alpha_2 X_1 X_3 + \epsilon\alpha_3 X_2^3 + \epsilon\alpha_4 X_1 X_2^2 + \epsilon\alpha_5 X_1^3 + \epsilon\alpha_6 X_1 X_3^2 = 0 \quad (3.3a)$$

$$\ddot{X}_2 + 2\epsilon\mu_2\dot{X}_2 + \omega_2^2 X_2 + \epsilon\alpha_7 X_1 X_3 + \epsilon\alpha_8 X_2^3 + \epsilon\alpha_9 X_1 X_2^2 + \epsilon\alpha_{10} X_1^2 X_2 + \epsilon\alpha_{11} X_2 X_3^2 = \epsilon\hat{f}_2 \cos\Omega_2 t \quad (3.3b)$$

$$\ddot{X}_3 + 2\epsilon\mu_3\dot{X}_3 + \omega_3^2 X_3 + \epsilon\alpha_{12} X_1^2 + \epsilon\alpha_{13} X_1 X_2 + \epsilon\alpha_{14} X_2^2 X_3 + \epsilon\alpha_{15} X_1^2 X_3 + \epsilon\alpha_{16} X_3^3 = \epsilon\hat{f}_3 \cos\Omega_3 t \quad (3.3c)$$

Following the practice of the method of multiple scales and neglecting terms of $O(\epsilon^2)$, the solutions to equations (3.3) are expressed in the form:

$$X_j(t;\epsilon) = x_{j0}(T_0, T_1) + \epsilon x_{j1}(T_0, T_1) \text{ where } T_0 = t \text{ and } T_1 = \epsilon t \quad (3.4)$$

The derivatives with respect to time must also account for the different time scales. Accordingly, they become:

$$\frac{d(X_j)}{dt} = (D_0 + \epsilon D_1)(X_j), \qquad \frac{d^2(X_j)}{dt^2} = (D_0^2 + 2\epsilon D_0 D_1)(X_j) \quad (3.5)$$

where

$$D_k(X_j) = \frac{\partial(X_j)}{\partial T_k} \quad \text{and} \quad D_k^2(X_j) = \frac{\partial^2(X_j)}{\partial T_k^2} \quad (3.6)$$

Substituting equations (3.4)-(3.6) into equation (3.3) and equating coefficients of like orders of ϵ gives:

$$
\begin{aligned}
D_0^2 x_{10} + \omega_1^2 x_{10} &= 0 \\
D_0^2 x_{20} + \omega_2^2 x_{20} &= 0 \\
D_0^2 x_{30} + \omega_3^2 x_{30} &= 0
\end{aligned}
\tag{3.7}
$$

$$
\begin{aligned}
D_0^2 x_{11} + \omega_1^2 x_{11} &= -2D_0 D_1 x_{10} - 2\mu_1 D_0 x_{10} - \alpha_1 x_{20} x_{30} - \alpha_2 x_{10} x_{30} - \alpha_3 x_{20}^3 \\
&\quad - \alpha_4 x_{10} x_{20}^2 - \alpha_5 x_{10}^3 - \alpha_6 x_{10} x_{30}^2 \\
D_0^2 x_{21} + \omega_2^2 x_{21} &= -2D_0 D_1 x_{20} - 2\mu_2 D_0 x_{20} - \alpha_7 x_{10} x_{30} - \alpha_8 x_{20}^3 - \alpha_9 x_{10} x_{20}^2 \\
&\quad - \alpha_{10} x_{10}^2 x_{20} - \alpha_{11} x_{20} x_{30}^2 + \hat{f}_2 \cos\Omega_2 T_0 \\
D_0^2 x_{31} + \omega_3^2 x_{31} &= -2D_0 D_1 x_{30} - 2\mu_3 D_0 x_{30} - \alpha_{12} x_{10}^2 - \alpha_{13} x_{10} x_{20} - \alpha_{14} x_{20}^2 x_{30} \\
&\quad - \alpha_{15} x_{10}^2 x_{30} - \alpha_{16} x_{30}^3 + \hat{f}_3 \cos\Omega_3 T_0
\end{aligned}
\tag{3.8}
$$

The solution to equations (3.7) can be written in the form:

$$
x_{j0} = A_j(T_1) e^{(i\omega_j T_0)} + cc \tag{3.9}
$$

for $j = 1,2$ and 3 and cc denotes the complex conjugate of the preceding term or terms. The A_j are complex functions of T_1 and are determined later in the analysis.

Substituting equations (3.9) into equations (3.8) leads to:

$$
\begin{aligned}
D_0^2 x_{11} + \omega_1^2 x_{11} &= -2A_1' i\omega_1 e^{i\omega_1 T_0} - 2\mu_1 A_1 i\omega_1 e^{i\omega_1 T_0} \\
&\quad - \alpha_1 (A_2 A_3 e^{(\omega_2+\omega_3)T_0} + \bar{A}_2 A_3 e^{(\omega_3-\omega_2)T_0}) \\
&\quad - \alpha_2 (A_1 A_3 e^{i(\omega_1+\omega_3)T_0} + \bar{A}_1 A_3 e^{i(\omega_3-\omega_1)T_0}) \\
&\quad - \alpha_3 (A_2^3 e^{3i\omega_2 T_0} + 3A_2^2 \bar{A}_2 e^{i\omega_2 T_0}) \\
&\quad - \alpha_4 (A_1 A_2^2 e^{i(\omega_1+2\omega_2)T_0} + 2A_1 A_2 \bar{A}_2 e^{i\omega_1 T_0} + \bar{A}_1 A_2^2 e^{i(-\omega_1+2\omega_2)T_0}) \\
&\quad - \alpha_5 (A_1^3 e^{3i\omega_1 T_0} + 3A_1^2 \bar{A}_1 e^{i\omega_1 T_0}) \\
&\quad - \alpha_6 (A_1 A_3^2 e^{i(\omega_1+2\omega_3)T_0} + 2A_1 A_3 \bar{A}_3 e^{i\omega_1 T_0} + \bar{A}_1 A_3^2 e^{i(-\omega_1+2\omega_3)T_0}) + cc
\end{aligned}
\tag{3.10}
$$

$$
\begin{aligned}
D_0^2 x_{21} + \omega_2^2 x_{21} = & -2A_2' i\omega_2 e^{i\omega_2 T_0} - 2\mu_2 A_2 i\omega_2 e^{i\omega_2 T_0} \\
& -\alpha_7 (A_1 A_3 e^{i(\omega_1+\omega_3)T_0} + \bar{A}_1 A_3 e^{i(\omega_3-\omega_1)T_0}) \\
& -\alpha_8 (A_2^3 e^{3i\omega_2 T_0} + 3A_2^2 \bar{A}_2 e^{i\omega_2 T_0}) \\
& -\alpha_9 (A_1 A_2^2 e^{i(\omega_1+2\omega_2)T_0} + 2A_1 A_2 \bar{A}_2 e^{i\omega_1 T_0} + \bar{A}_1 A_2^2 e^{i(-\omega_1+2\omega_2)T_0}) \\
& -\alpha_{10} (A_1^2 A_2 e^{i(2\omega_1+\omega_2)T_0} + 2A_1 \bar{A}_1 A_2 e^{i\omega_2 T_0} + A_1^2 \bar{A}_2 e^{i(2\omega_1-\omega_2)T_0}) \\
& -\alpha_{11} (A_2 A_3^2 e^{i(\omega_2+2\omega_3)T_0} + 2A_2 A_3 \bar{A}_3 e^{i\omega_2 T_0} + \bar{A}_2 A_3^2 e^{i(-\omega_2+2\omega_3)T_0}) \\
& + \frac{\hat{f}_2}{2} e^{i\Omega_2 T_0} + cc
\end{aligned}
\tag{3.11}
$$

$$
\begin{aligned}
D_0^2 x_{31} + \omega_3^2 x_{31} = & -2A_3' i\omega_3 e^{i\omega_3 T_0} - 2\mu_3 A_3 i\omega_3 e^{i\omega_3 T_0} - \alpha_{12} (A_1^2 e^{2i\omega_1 T_0} + A_1 \bar{A}_1) \\
& -\alpha_{13} (A_1 A_2 e^{i(\omega_1+\omega_2)T_0} + A_1 \bar{A}_2 e^{i(\omega_1-\omega_2)T_0}) \\
& -\alpha_{14} (A_2^2 A_3 e^{i(2\omega_2+\omega_3)T_0} + 2A_2 \bar{A}_2 A_3 e^{i\omega_3 T_0} + A_2^2 \bar{A}_3 e^{i(2\omega_2-\omega_3)T_0}) \\
& -\alpha_{15} (A_1^2 A_3 e^{i(2\omega_1+\omega_3)T_0} + 2A_1 \bar{A}_1 A_3 e^{i\omega_3 T_0} + A_1^2 \bar{A}_3 e^{(2\omega_1-\omega_3)T_0}) \\
& -\alpha_{16} (A_3^3 e^{3i\omega_3 T_0} + 3A_3^2 \bar{A}_3 e^{i\omega_3 T_0}) + \frac{\hat{f}_3}{2} e^{i\Omega_3 T_0} + cc
\end{aligned}
\tag{3.12}
$$

where the $\bar{A}_j$ denote the complex conjugate of the A_j. Since the expansions which are sought are uniformly valid in time[3], secular producing terms are identified and eliminated from the right hand side of equations (3.10), (3.11), and (3.12). In this way the expressions for the A_j are determined.

The balance of the perturbation analysis addresses each of the three cases separately since the secular terms for each case are distinct as they depend on the relationships between the linear natural frequencies and the forcing frequencies. The reduced equations for each of the three cases will be derived prior to presenting the numerical results.

---

[3]For the notation used here, the approximation for $X_i(t;\epsilon)$ of equation 3.4 should be such that small terms remain small for all time. That is, if x_{i0} is the principal term in the approximation and x_{i1} is the correction to it, we want $|\epsilon x_{i1}| < |x_{i0}|$ for all time. When this is accomplished, the resulting approximation is said to be uniformly valid in time (Kahn, 1990).

3.2 CASE 1 - (Vertical Forcing)

Consistent with the method of multiple scales, it is appropriate to introduce three detuning equations:

$$\Omega_3 = \omega_3 + \epsilon\sigma_1, \quad \omega_2 = \omega_1 - \epsilon\sigma_2, \quad \omega_3 = 2\omega_1 - \epsilon\sigma_3 \tag{3.13a,b,c}$$

where σ_1 is an external detuning parameter and σ_2 and σ_3 are internal detuning parameters. Using these relationships in equations (3.10)-(3.12), the secular terms are eliminated by letting:

$$\begin{aligned}(-2A_1' i\omega_1 - 2\mu_1 A_1 i\omega_1)e^{i\omega_1 T_0} &- \alpha_1(\bar{A}_2 A_3 e^{i(\omega_3-\omega_2)T_0}) \\ &- \alpha_2(\bar{A}_1 A_3 e^{i(\omega_3-\omega_1)T_0}) - \alpha_3(3A_2^2\bar{A}_2 e^{i\omega_2 T_0}) \\ &- \alpha_4(2A_1A_2\bar{A}_2 e^{i\omega_1 T_0} + \bar{A}_1 A_2^2 e^{i(2\omega_2-\omega_1)T_0}) \\ &- \alpha_5(3A_1^2\bar{A}_1 e^{i\omega_1 T_0}) - \alpha_6(2A_1A_3\bar{A}_3 e^{i\omega_1 T_0}) = 0\end{aligned} \tag{3.14}$$

$$\begin{aligned}(-2A_2' i\omega_2 - 2\mu_2 A_2 i\omega_2)e^{i\omega_2 T_0} &- \alpha_7(\bar{A}_1 A_3 e^{i(\omega_3-\omega_1)T_0}) \\ &- \alpha_8(3A_2^2\bar{A}_2 e^{i\omega_2 T_0}) - \alpha_9(2A_1A_2\bar{A}_2 e^{i\omega_1 T_0} + \bar{A}_1 A_2^2 e^{i(2\omega_2-\omega_1)T_0}) \\ &- \alpha_{10}(2A_1\bar{A}_1 A_2 e^{i\omega_2 T_0} + A_1^2\bar{A}_2 e^{i(2\omega_1-\omega_2)T_0}) \\ &- \alpha_{11}(2A_2A_3\bar{A}_3 e^{i\omega_2 T_0}) = 0\end{aligned} \tag{3.15}$$

$$\begin{aligned}(-2A_3' i\omega_3 - 2\mu_3 A_3 i\omega_3)e^{i\omega_3 T_0} &- \alpha_{12}A_1^2 e^{2i\omega_1 T_0} \\ &- \alpha_{13}(A_1A_2 e^{i(\omega_1+\omega_2)T_0}) - \alpha_{14}(2A_2\bar{A}_2A_3 e^{i\omega_3 T_0}) \\ &- \alpha_{15}(2A_1\bar{A}_1A_3 e^{i\omega_3 T_0}) - \alpha_{16}(3A_3^2\bar{A}_3 e^{i\omega_3 T_0}) + \frac{\hat{f}_3}{2}e^{i\Omega_3 T_0} = 0\end{aligned} \tag{3.16}$$

With further use of equations (3.13), equations (3.14)-(3.16) can be simplified to:

$$\begin{aligned}-2A_1' i\omega_1 - 2\mu_1 A_1 i\omega_1 &- \alpha_1\bar{A}_2A_3 e^{i(\sigma_2-\sigma_3)T_1} \\ &- \alpha_2\bar{A}_1A_3 e^{-i\sigma_3 T_1} - 3\alpha_3 A_2^2\bar{A}_2 e^{-i\sigma_2 T_1} \\ &- \alpha_4(2A_1A_2\bar{A}_2 + \bar{A}_1A_2^2 e^{-2i\sigma_2 T_1}) \\ &- 3\alpha_5 A_1^2\bar{A}_1 - 2\alpha_6 A_1A_3\bar{A}_3 = 0\end{aligned} \tag{3.17}$$

$$-2A_2' i\omega_2 - 2\mu_2 A_2 i\omega_2 - \alpha_7 \bar{A}_1 A_3 e^{i(\sigma_2-\sigma_3)T_1} - 3\alpha_8 A_2^2 \bar{A}_2$$
$$- \alpha_9 (2A_1 A_2 \bar{A}_2 e^{i\sigma_2 T_1} + \bar{A}_1 A_2^2 e^{-i\sigma_2 T_1}) \qquad (3.18)$$
$$- \alpha_{10} (2A_1 \bar{A}_1 A_2 + A_1^2 \bar{A}_2 e^{2i\sigma_2 T_1}) - 2\alpha_{11} A_2 A_3 \bar{A}_3 = 0$$

$$-2A_3' i\omega_3 - 2\mu_3 A_3 i\omega_3 - \alpha_{12} A_1^2 e^{i\sigma_3 T_1} - \alpha_{13} A_1 A_2 e^{i(\sigma_3-\sigma_2)T_1}$$
$$- 2\alpha_{14} A_2 \bar{A}_2 A_3 - 2\alpha_{15} A_1 \bar{A}_1 A_3 - 3\alpha_{16} A_3^2 \bar{A}_3 + \frac{\hat{f}_3}{2} e^{i\sigma_1 T_1} = 0 \qquad (3.19)$$

To facilitate the solution of equations (3.17)-(3.19), it is advantageous to put them into autonomous form. This can be done by letting:

$$A_k = \frac{B_k}{2} e^{i\phi_k T_1}$$

and solving for the ϕ_k such that all of the exponential terms have the same exponent. Utilizing the values of ϕ_k which result from this process, the A_k can be rewritten as follows:

$$A_1 = \frac{B_1}{2} e^{i\frac{\sigma_1-\sigma_3}{2}T_1}$$
$$A_2 = \frac{B_2}{2} e^{i\frac{\sigma_1+2\sigma_2-\sigma_3}{2}T_1} \qquad (3.20a,b,c)$$
$$A_3 = \frac{B_3}{2} e^{i\sigma_1 T_1}$$

These relationships can be substituted into equations (3.17)-(3.19) with $B_k = B_{kr} + iB_{kj}$ for $k = 1$, 2, and 3. Here the subscript r designates the real component of the term and the subscript j designates the imaginary component of the term. Taking the resulting equations, separating the real and imaginary terms gives the following six equations governing the behavior of the u_j's in time T_1:

$$u_1' = \frac{u_2}{2}(\sigma_1-\sigma_3) - \mu_1 u_1 - \frac{\alpha_1}{4\omega_1}(u_3u_6 - u_4u_5) - \frac{\alpha_2}{4\omega_1}(u_1u_6 - u_2u_5)$$
$$- \frac{3\alpha_3}{8\omega_1}(u_3^2u_4 + u_4^3) - \frac{\alpha_4}{8\omega_1}(u_2u_3^2 + 3u_2u_4^2 + 2u_1u_3u_4) \qquad (3.21a)$$
$$- \frac{3\alpha_5}{8\omega_1}(u_1^2u_2 + u_2^3) - \frac{\alpha_6}{4\omega_1}(u_2u_5^2 + u_2u_6^2)$$

$$u_2' = -\frac{u_1}{2}(\sigma_1-\sigma_3) - \mu_1 u_2 + \frac{\alpha_1}{4\omega_1}(u_3u_5 + u_4u_6) + \frac{\alpha_2}{4\omega_1}(u_1u_5 + u_2u_6)$$
$$+ \frac{3\alpha_3}{8\omega_1}(u_3^3 + u_3u_4^2) + \frac{\alpha_4}{8\omega_1}(3u_1u_3^2 + u_1u_4^2 + 2u_2u_3u_4) \qquad (3.21b)$$
$$+ \frac{3\alpha_5}{8\omega_1}(u_1^3 + u_1u_2^2) + \frac{\alpha_6}{4\omega_1}(u_1u_5^2 + u_1u_6^2)$$

$$u_3' = \frac{u_4}{2}(\sigma_1 + 2\sigma_2 - \sigma_3) - \mu_2 u_3 - \frac{\alpha_7}{4\omega_2}(u_1u_6 - u_2u_5) - \frac{3\alpha_8}{8\omega_2}(u_3^2u_4 + u_4^3)$$
$$- \frac{\alpha_9}{8\omega_2}(u_2u_3^2 + 3u_2u_4^2 + 2u_1u_3u_4)$$
$$- \frac{\alpha_{10}}{8\omega_2}(u_1^2u_4 + 3u_2^2u_4 + 2u_1u_2u_3) \qquad (3.21c)$$
$$- \frac{\alpha_{11}}{4\omega_2}(u_4u_5^2 + u_4u_6^2)$$

$$u_4' = -\frac{u_3}{2}(\sigma_1 + 2\sigma_2 - \sigma_3) - \mu_2 u_4 + \frac{\alpha_7}{4\omega_2}(u_1u_5 + u_2u_6) + \frac{3\alpha_8}{8\omega_2}(u_3^3 + u_3u_4^2)$$
$$+ \frac{\alpha_9}{8\omega_2}(3u_1u_3^2 + u_1u_4^2 + 2u_2u_3u_4)$$
$$+ \frac{\alpha_{10}}{8\omega_2}(3u_1^2u_3 + u_2^2u_3 + 2u_1u_2u_4) \qquad (3.21d)$$
$$- \frac{\alpha_{11}}{4\omega_2}(u_3u_5^2 + u_3u_6^2)$$

$$u_5' = u_6\sigma_1 - \mu_3 u_5 - \frac{\alpha_{12}}{2\omega_3}u_1u_2 - \frac{\alpha_{13}}{4\omega_3}(u_1u_4 + u_2u_3) - \frac{\alpha_{14}}{4\omega_3}(u_3^2u_6 + u_4^2u_6) \qquad (3.21e)$$
$$- \frac{\alpha_{15}}{4\omega_3}(u_1^2u_6 + u_2^2u_6) - \frac{3\alpha_{16}}{8\omega_3}(u_5^2u_6 + u_6^3)$$

$$u_6' = -u_5\sigma_1 - \mu_3 u_6 + \frac{\alpha_{12}}{4\omega_3}(u_1^2 - u_2^2) + \frac{\alpha_{13}}{4\omega_3}(u_1 u_3 - u_2 u_4)$$
$$+ \frac{\alpha_{14}}{4\omega_3}(u_3^2 u_5 + u_4^2 u_5) + \frac{\alpha_{15}}{4\omega_3}(u_1^2 u_5 + u_2^2 u_5) \qquad (3.21f)$$
$$+ \frac{3\alpha_{16}}{8\omega_3}(u_5^3 + u_5 u_6^2) - \frac{\hat{f}_3}{2\omega_3}$$

where the following variable reassignments were used:

$$B_{1r} \rightarrow u_1, \quad B_{1j} \rightarrow u_2, \quad B_{2r} \rightarrow u_3, \quad B_{2j} \rightarrow u_4, \quad B_{3r} \rightarrow u_5, \quad B_{3j} \rightarrow u_6 \qquad (3.22)$$

The relationship of the u_j coordinates to the physical system can be ascertained from equations (3.9), (3.20), and (3.22). Equation (3.9) establishes that the A_j are the time varying amplitudes (with time T_1) of the variables X_j. The A_j are complex quantities, having real and imaginary components, which account for the magnitude and the phase of the response variables X_j. Equations (3.20) give the relationships between the A_j and the B_j such that the secular equations (3.17), (3.18), and (3.19) are autonomous. The factor of ½ is introduced in the equations defining A_j in terms of the B_j to account for the amplitude differences which result from the use of complex notation. The B_j are complex quantities and have real and imaginary components. These components are reassigned to the variables u_j according to equation (3.22). The resultant magnitudes of the u_j are the envelopes of the response in time T_0. The relationship between the u_j and the X_j in equation form is:

$$X_1 \approx x_{10} = \sqrt{u_1^2 + u_2^2}\cos\left[\frac{\Omega_3}{2}t + \gamma_1\right] \quad \text{where} \quad \gamma_1 = \tan^{-1}\left[\frac{u_2}{u_1}\right] \qquad (3.23a)$$

$$X_2 \approx x_{20} = \sqrt{u_3^2 + u_4^2}\cos\left[\frac{\Omega_3}{2}t + \gamma_2\right] \quad \text{where} \quad \gamma_2 = \tan^{-1}\left[\frac{u_4}{u_3}\right] \qquad (3.23b)$$

$$X_3 \approx x_{30} = \sqrt{u_5^2 + u_6^2}\cos[\Omega_3 t + \gamma_3] \quad \text{where} \quad \gamma_3 = \tan^{-1}\left[\frac{u_6}{u_5}\right] \tag{3.23c}$$

3.3 CASE 2 - (Torsional Forcing)

As in case 1, it is appropriate to introduce three detuning equations:

$$\Omega_2 = \omega_2 + \epsilon\sigma_1, \quad \omega_2 = \omega_1 - \epsilon\sigma_2, \quad \omega_3 = 2\omega_1 - \epsilon\sigma_3 \tag{3.23}$$

where $\sigma 1$ now quantifies the nearness of the forcing frequency Ω_2 to ω_2. Using these relationships in equations (3.10)-(3.12), the secular terms are eliminated by letting:

$$\begin{aligned}(-2A_1' i\omega_1 - 2\mu_1 A_1 i\omega_1)e^{i\omega_1 T_0} &- \alpha_1(\bar{A}_2 A_3 e^{i(\omega_3-\omega_2)T_0}) \\ &- \alpha_2(\bar{A}_1 A_3 e^{i(\omega_3-\omega_1)T_0}) - \alpha_3(3A_2^2\bar{A}_2 e^{i\omega_2 T_0}) \\ &- \alpha_4(2A_1A_2\bar{A}_2 e^{i\omega_1 T_0} + \bar{A}_1 A_2^2 e^{i(2\omega_2-\omega_1)T_0}) \\ &- \alpha_5(3A_1^2\bar{A}_1 e^{i\omega_1 T_0}) - \alpha_6(2A_1A_3\bar{A}_3 e^{i\omega_1 T_0}) = 0\end{aligned} \tag{3.24}$$

$$\begin{aligned}(-2A_2' i\omega_2 - 2\mu_2 A_2 i\omega_2)e^{i\omega_2 T_0} &- \alpha_7(\bar{A}_1 A_3 e^{i(\omega_3-\omega_1)T_0}) \\ &- \alpha_8(3A_2^2\bar{A}_2 e^{i\omega_2 T_0}) - \alpha_9(2A_1A_2\bar{A}_2 e^{i\omega_1 T_0} + \bar{A}_1 A_2^2 e^{i(2\omega_2-\omega_1)T_0}) \\ &- \alpha_{10}(2A_1\bar{A}_1 A_2 e^{i\omega_2 T_0} + A_1^2\bar{A}_2 e^{i(2\omega_1-\omega_2)T_0}) \\ &- \alpha_{11}(2A_2A_3\bar{A}_3 e^{i\omega_2 T_0}) + \frac{\hat{f}_2}{2}e^{i\Omega_2 T_0} = 0\end{aligned} \tag{3.25}$$

$$\begin{aligned}(-2A_3' i\omega_3 - 2\mu_3 A_3 i\omega_3)e^{i\omega_3 T_0} &- \alpha_{12}A_1^2 e^{2i\omega_1 T_0} \\ &- \alpha_{13}(A_1A_2 e^{i(\omega_1+\omega_2)T_0}) - \alpha_{14}(2A_2\bar{A}_2A_3 e^{i\omega_3 T_0}) \\ &- \alpha_{15}(2A_1\bar{A}_1A_3 e^{i\omega_3 T_0}) - \alpha_{16}(3A_3^2\bar{A}_3 e^{i\omega_3 T_0}) = 0\end{aligned} \tag{3.26}$$

With further use of equations (3.23), equations (3.24)-(3.26) can be simplified to:

$$
\begin{aligned}
-2A_1' i\omega_1 - 2\mu_1 A_1 i\omega_1 &- \alpha_1 \bar{A}_2 A_3 e^{i(\sigma_2-\sigma_3)T_1} \\
&- \alpha_2 \bar{A}_1 A_3 e^{-i\sigma_3 T_1} - 3\alpha_3 A_2^2 \bar{A}_2 e^{-i\sigma_2 T_1} \\
&- \alpha_4 (2A_1 A_2 \bar{A}_2 + \bar{A}_1 A_2^2 e^{-2i\sigma_2 T_1}) \\
&- 3\alpha_5 A_1^2 \bar{A}_1 - 2\alpha_6 A_1 A_3 \bar{A}_3 = 0
\end{aligned} \tag{3.27}
$$

$$
\begin{aligned}
-2A_2' i\omega_2 - 2\mu_2 A_2 i\omega_2 &- \alpha_7 \bar{A}_1 A_3 e^{i(\sigma_2-\sigma_3)T_1} - 3\alpha_8 A_2^2 \bar{A}_2 \\
&- \alpha_9 (2A_1 A_2 \bar{A}_2 e^{i\sigma_2 T_1} + \bar{A}_1 A_2^2 e^{-i\sigma_2 T_1}) \\
&- \alpha_{10} (2A_1 \bar{A}_1 A_2 + A_1^2 \bar{A}_2 e^{2i\sigma_2 T_1}) - 2\alpha_{11} A_2 A_3 \bar{A}_3 + \frac{\hat{f}_2}{2} e^{i\sigma_1 T_1} = 0
\end{aligned} \tag{3.28}
$$

$$
\begin{aligned}
-2A_3' i\omega_3 - 2\mu_3 A_3 i\omega_3 &- \alpha_{12} A_1^2 e^{i\sigma_3 T_1} - \alpha_{13} A_1 A_2 e^{i(\sigma_3-\sigma_2)T_1} \\
&- 2\alpha_{14} A_2 \bar{A}_2 A_3 - 2\alpha_{15} A_1 \bar{A}_1 A_3 - 3\alpha_{16} A_3^2 \bar{A}_3 = 0
\end{aligned} \tag{3.29}
$$

Equations (3.27)-(3.29) can be put into autonomous form by letting

$$
A_k = \frac{B_k}{2} e^{i\phi_k T_1}
$$

and solving for the ϕ_k such that all of the exponential terms have the same exponent. Utilizing the values of ϕ_k which result from this process, the A_k can be rewritten as follows:

$$
\begin{aligned}
A_1 &= \frac{B_1}{2} e^{i(\sigma_1-\sigma_2)T_1} \\
A_2 &= \frac{B_2}{2} e^{i\sigma_1 T_1} \\
A_3 &= \frac{B_3}{2} e^{i(2\sigma_1-2\sigma_2+\sigma_3)T_1}
\end{aligned} \tag{3.30a,b,c}
$$

These relationships can be substituted into equations (3.27)-(3.29) with $B_k = B_{kr} + iB_{kj}$ for $k = 1$, 2, and 3. Here the subscript r designates the real component of the B_k term and the subscript j designates the imaginary component of the same term. Taking the resulting equations, separating the real and imaginary terms gives the following six equations governing the amplitude modulations in time T_1:

$$u_1' = u_2(\sigma_1-\sigma_2) - \mu_1 u_1 - \frac{\alpha_1}{4\omega_1}(u_3u_6 - u_4u_5) - \frac{\alpha_2}{4\omega_1}(u_1u_6 - u_2u_5)$$
$$- \frac{3\alpha_3}{8\omega_1}(u_3^2u_4 + u_4^3) - \frac{\alpha_4}{8\omega_1}(u_2u_3^2 + 3u_2u_4^2 + 2u_1u_3u_4) \quad (3.31a)$$
$$- \frac{3\alpha_5}{8\omega_1}(u_1^2u_2 + u_2^3) - \frac{\alpha_6}{4\omega_1}(u_2u_5^2 + u_2u_6^2)$$

$$u_2' = -u_1(\sigma_1-\sigma_2) - \mu_1 u_2 + \frac{\alpha_1}{4\omega_1}(u_3u_5 + u_4u_6) + \frac{\alpha_2}{4\omega_1}(u_1u_5 + u_2u_6)$$
$$+ \frac{3\alpha_3}{8\omega_1}(u_3^3 + u_3u_4^2) + \frac{\alpha_4}{8\omega_1}(3u_1u_3^2 + u_1u_4^2 + 2u_2u_3u_4) \quad (3.31b)$$
$$+ \frac{3\alpha_5}{8\omega_1}(u_1^3 + u_1u_2^2) + \frac{\alpha_6}{4\omega_1}(u_1u_5^2 + u_1u_6^2)$$

$$u_3' = u_4\sigma_1 - \mu_2 u_3 - \frac{\alpha_7}{4\omega_2}(u_1u_6 - u_2u_5) - \frac{3\alpha_8}{8\omega_2}(u_3^2u_4 + u_4^3)$$
$$- \frac{\alpha_9}{8\omega_2}(u_2u_3^2 + 3u_2u_4^2 + 2u_1u_3u_4) \quad (3.31c)$$
$$- \frac{\alpha_{10}}{8\omega_2}(u_1^2u_4 + 3u_2^2u_4 + 2u_1u_2u_3) - \frac{\alpha_{11}}{4\omega_2}(u_4u_5^2 + u_4u_6^2)$$

$$u_4' = -u_3\sigma_1 - \mu_2 u_4 + \frac{\alpha_7}{4\omega_2}(u_1u_5 + u_2u_6) + \frac{3\alpha_8}{8\omega_2}(u_3^3 + u_3u_4^2)$$
$$+ \frac{\alpha_9}{8\omega_2}(3u_1u_3^2 + 3u_1u_4^2 + 2u_2u_3u_4)$$
$$+ \frac{\alpha_{10}}{8\omega_2}(3u_1^2u_3 + u_2^2u_3 + 2u_1u_2u_4) \quad (3.31d)$$
$$- \frac{\alpha_{11}}{4\omega_2}(u_3u_5^2 + u_3u_6^2) - \frac{\hat{f}_2}{2\omega_2}$$

$$u_5' = u_6(2\sigma_1 - 2\sigma_2 + \sigma_3) - \mu_3 u_5 - \frac{\alpha_{12}}{2\omega_3}u_1u_2 - \frac{\alpha_{13}}{4\omega_3}(u_1u_4 + u_2u_3)$$
$$- \frac{\alpha_{14}}{4\omega_3}(u_3^2u_6 + u_4^2u_6) - \frac{\alpha_{15}}{4\omega_3}(u_1^2u_6 + u_2^2u_6) - \frac{3\alpha_{16}}{8\omega_3}(u_5^2u_6 + u_6^3) \quad (3.31e)$$

$$u_6' = -u_5(2\sigma_1 - 2\sigma_2 + \sigma_3) - \mu_3 u_6 + \frac{\alpha_{12}}{4\omega_3}(u_1^2 - u_2^2) + \frac{\alpha_{13}}{4\omega_3}(u_1u_3 - u_2u_4)$$
$$+ \frac{\alpha_{14}}{4\omega_3}(u_3^2u_5 + u_4^2u_5) + \frac{\alpha_{15}}{4\omega_3}(u_1^2u_5 + u_2^2u_5) + \frac{3\alpha_{16}}{8\omega_3}(u_5^3 + u_5u_6^2) \quad (3.31f)$$

where the following variable reassignments were used:

$$B_{1r} \rightarrow u_1, \quad B_{1j} \rightarrow u_2, \quad B_{2r} \rightarrow u_3, \quad B_{2j} \rightarrow u_4, \quad B_{3r} \rightarrow u_5, \quad B_{3j} \rightarrow u_6 \tag{3.32}$$

The relationship between these u_j and the X_j for this case can be written in equation form:

$$X_1 \approx x_{10} = \sqrt{u_1^2 + u_2^2}\cos[\Omega_2 t + \gamma_1] \quad \text{where} \quad \gamma_1 = \tan^{-1}\left[\frac{u_2}{u_1}\right] \tag{3.33a}$$

$$X_2 \approx x_{20} = \sqrt{u_3^2 + u_4^2}\cos[\Omega_2 t + \gamma_2] \quad \text{where} \quad \gamma_2 = \tan^{-1}\left[\frac{u_4}{u_3}\right] \tag{3.33b}$$

$$X_3 \approx x_{30} = \sqrt{u_5^2 + u_6^2}\cos[2\Omega_2 t + \gamma_3] \quad \text{where} \quad \gamma_3 = \tan^{-1}\left[\frac{u_6}{u_5}\right] \tag{3.33c}$$

3.4 CASE 3 - (Torsional and Vertical Forcing)

In this case, forcing in both the X_2 and X_3 coordinate directions is present. Hence, both of the forcing terms in equations (3.11) and (3.12) are nonzero. Rather than introduce an additional detuning relationship, the fact that $\Omega_3 = 2\Omega_2$ is used to keep the number of detuning relationships to three as in cases 1 and 2. Physically, this relationship represents the fact that the forcing frequency associated with X_3, Ω_3, is of second order and the forcing frequency associated with X_2, Ω_2, is of first order, and hence these two frequencies are always in the ratio of 2:1. Therefore the detuning equations for this case are:

$$\Omega_2 = \omega_2 + \epsilon\sigma_1, \quad \omega_2 = \omega_1 - \epsilon\sigma_2, \quad \omega_3 = 2\omega_1 - \epsilon\sigma_3, \tag{3.34a}$$

with the additional dependent detuning relationship

$$\Omega_3 = 2\omega_2 + 2\epsilon\sigma_1. \tag{3.34b}$$

Using these relationships in equations (3.10)-(3.12), the secular terms are eliminated by letting:

$$\begin{aligned}(-2A_1' i\omega_1 - 2\mu_1 A_1 i\omega_1) e^{i\omega_1 T_0} &- \alpha_1 (\bar{A}_2 A_3 e^{i(\omega_3-\omega_2)T_0}) \\ &- \alpha_2 (\bar{A}_1 A_3 e^{i(\omega_3-\omega_1)T_0}) - \alpha_3 (3A_2^2 \bar{A}_2 e^{i\omega_2 T_0}) \\ &- \alpha_4 (2A_1 A_2 \bar{A}_2 e^{i\omega_1 T_0} + \bar{A}_1 A_2^2 e^{i(2\omega_2-\omega_1)T_0}) \\ &- \alpha_5 (3A_1^2 \bar{A}_1 e^{i\omega_1 T_0}) - \alpha_6 (2A_1 A_3 \bar{A}_3 e^{i\omega_1 T_0}) = 0\end{aligned} \tag{3.35}$$

$$\begin{aligned}(-2A_2' i\omega_2 - 2\mu_2 A_2 i\omega_2) e^{i\omega_2 T_0} &- \alpha_7 (\bar{A}_1 A_3 e^{i(\omega_3-\omega_1)T_0}) - \alpha_8 (3A_2^2 \bar{A}_2 e^{i\omega_2 T_0}) \\ &- \alpha_9 (2A_1 A_2 \bar{A}_2 e^{i\omega_1 T_0} + \bar{A}_1 A_2^2 e^{i(2\omega_2-\omega_1)T_0}) \\ &- \alpha_{10} (2A_1 \bar{A}_1 A_2 e^{i\omega_2 T_0} + A_1^2 \bar{A}_2 e^{i(2\omega_1-\omega_2)T_0}) \\ &- \alpha_{11} (2A_2 A_3 \bar{A}_3 e^{i\omega_2 T_0}) + \frac{\hat{f}_2}{2} e^{i\Omega_2 T_0} = 0\end{aligned} \tag{3.36}$$

$$\begin{aligned}(-2A_3' i\omega_3 - 2\mu_3 A_3 i\omega_3) e^{i\omega_3 T_0} &- \alpha_{12} A_1^2 e^{2i\omega_1 T_0} - \alpha_{13} (A_1 A_2 e^{i(\omega_1+\omega_2)T_0}) \\ &- \alpha_{14} (2A_2 \bar{A}_2 A_3 e^{i\omega_3 T_0}) - \alpha_{15} (2A_1 \bar{A}_1 A_3 e^{i\omega_3 T_0}) \\ &- \alpha_{16} (3A_3^2 \bar{A}_3 e^{i\omega_3 T_0}) + \frac{\hat{f}_3}{2} e^{i\Omega_3 T_0} = 0\end{aligned} \tag{3.37}$$

With further use of equations (3.34), equations (3.35)-(3.37) can be simplified to:

$$\begin{aligned}-2A_1' i\omega_1 - 2\mu_1 A_1 i\omega_1 &- \alpha_1 \bar{A}_2 A_3 e^{i(\sigma_2-\sigma_3)T_1} - \alpha_2 \bar{A}_1 A_3 e^{-i\sigma_3 T_1} \\ &- 3\alpha_3 A_2^2 \bar{A}_2 e^{-i\sigma_2 T_1} - \alpha_4 (2A_1 A_2 \bar{A}_2 + \bar{A}_1 A_2^2 e^{-2i\sigma_2 T_1}) \\ &- 3\alpha_5 A_1^2 \bar{A}_1 - 2\alpha_6 A_1 A_3 \bar{A}_3 = 0\end{aligned} \tag{3.38}$$

$$\begin{aligned}-2A_2' i\omega_2 - 2\mu_2 A_2 i\omega_2 &- \alpha_7 \bar{A}_1 A_3 e^{i(\sigma_2-\sigma_3)T_1} - 3\alpha_8 A_2^2 \bar{A}_2 \\ &- \alpha_9 (2A_1 A_2 \bar{A}_2' e^{i\sigma_2 T_1} + \bar{A}_1 A_2^2 e^{-i\sigma_2 T_1}) \\ &- \alpha_{10} (2A_1 \bar{A}_1 A_2 + A_1^2 \bar{A}_2 e^{2i\sigma_2 T_1}) \\ &- 2\alpha_{11} A_2 A_3 \bar{A}_3 + \frac{\hat{f}_2}{2} e^{i\sigma_1 T_1} = 0\end{aligned} \tag{3.39}$$

$$-2A_3' i\omega_3 - 2\mu_3 A_3 i\omega_3 - \alpha_{12}A_1^2 e^{i\sigma_3 T_1} - \alpha_{13}A_1 A_2 e^{i(\sigma_3-\sigma_2)T_1}$$
$$- 2\alpha_{14}A_2\bar{A}_2 A_3 - 2\alpha_{15}A_1\bar{A}_1 A_3 \qquad (3.40)$$
$$- 3\alpha_{16}A_3^2\bar{A}_3 + \frac{\hat{f}_3}{2}e^{i(2\sigma_1-2\sigma_2+\sigma_3)T_1} = 0$$

Equations (3.38)-(3.40) can be put into autonomous form by letting

$$A_k = \frac{B_k}{2}e^{i\phi_k T_1}$$

and solving for the ϕ_k such that all of the exponential terms have the same exponent. Utilizing the values of ϕ_k which result from this process, the A_k can be rewritten as follows:

$$A_1 = \frac{B_1}{2}e^{i(\sigma_1-\sigma_2)T_1}$$
$$A_2 = \frac{B_2}{2}e^{i\sigma_1 T_1} \qquad (3.40a,b,c)$$
$$A_3 = \frac{B_3}{2}e^{i(2\sigma_1-2\sigma_2+\sigma_3)T_1}$$

These relationships can be substituted into equations (3.38)-(3.40) with $B_k = B_{kr} + iB_{kj}$ for $k = 1$, 2, and 3. Here the subscript r designates the real component of the B_k term and the subscript j designates the imaginary component of the same term. Taking the resulting equations and separating the real and imaginary terms gives the following six equations governing the amplitude modulations in time T_1:

$$u_1' = u_2(\sigma_1-\sigma_2) - \mu_1 u_1 - \frac{\alpha_1}{4\omega_1}(u_3u_6 - u_4u_5) - \frac{\alpha_2}{4\omega_1}(u_1u_6 - u_2u_5)$$
$$- \frac{3\alpha_3}{8\omega_1}(u_3^2u_4 + u_4^3) - \frac{\alpha_4}{8\omega_1}(u_2u_3^2 + 3u_2u_4^2 + 2u_1u_3u_4) \qquad (3.42a)$$
$$- \frac{3\alpha_5}{8\omega_1}(u_1^2u_2 + u_2^3) - \frac{\alpha_6}{4\omega_1}(u_2u_5^2 + u_2u_6^2)$$

$$u_2' = -u_1(\sigma_1 - \sigma_2) - \mu_1 u_2 + \frac{\alpha_1}{4\omega_1}(u_3 u_5 + u_4 u_6) + \frac{\alpha_2}{4\omega_1}(u_1 u_5 + u_2 u_6)$$
$$+ \frac{3\alpha_3}{8\omega_1}(u_3^3 + u_3 u_4^2) + \frac{\alpha_4}{8\omega_1}(3u_1 u_3^2 + u_1 u_4^2 + 2u_2 u_3 u_4) \qquad (3.42b)$$
$$+ \frac{3\alpha_5}{8\omega_1}(u_1^3 + u_1 u_2^2) + \frac{\alpha_6}{4\omega_1}(u_1 u_5^2 + u_1 u_6^2)$$

$$u_3' = u_4\sigma_1 - \mu_2 u_3 - \frac{\alpha_7}{4\omega_2}(u_1 u_6 - u_2 u_5) - \frac{3\alpha_8}{8\omega_2}(u_3^2 u_4 + u_4^3)$$
$$- \frac{\alpha_9}{8\omega_2}(u_2 u_3^2 + 3u_2 u_4^2 + 2u_1 u_3 u_4) \qquad (3.42c)$$
$$- \frac{\alpha_{10}}{8\omega_2}(u_1^2 u_4 + 3u_2^2 u_4 + 2u_1 u_2 u_3)$$
$$- \frac{\alpha_{11}}{4\omega_2}(u_4 u_5^2 + u_4 u_6^2)$$

$$u_4' = -u_3\sigma_1 - \mu_2 u_4 + \frac{\alpha_7}{4\omega_2}(u_1 u_5 + u_2 u_6) + \frac{3\alpha_8}{8\omega_2}(u_3^3 + u_3 u_4^2)$$
$$+ \frac{\alpha_9}{8\omega_2}(3u_1 u_3^2 + u_1 u_4^2 + 2u_2 u_3 u_4) \qquad (3.42d)$$
$$+ \frac{\alpha_{10}}{8\omega_2}(3u_1^2 u_3 + u_2^2 u_3 + 2u_1 u_2 u_4)$$
$$- \frac{\alpha_{11}}{4\omega_2}(u_3 u_5^2 + u_3 u_6^2) - \frac{\hat{f}_2}{2\omega_2}$$

$$u_5' = u_6(2\sigma_1 - 2\sigma_2 + \sigma_3) - \mu_3 u_5 - \frac{\alpha_{12}}{2\omega_3} u_1 u_2$$
$$- \frac{\alpha_{13}}{4\omega_3}(u_1 u_4 + u_2 u_3) - \frac{\alpha_{14}}{4\omega_3}(u_3^2 u_6 + u_4^2 u_6) \qquad (3.42e)$$
$$- \frac{\alpha_{15}}{4\omega_3}(u_1^2 u_6 + u_2^2 u_6) - \frac{3\alpha_{16}}{8\omega_3}(u_5^2 u_6 + u_6^3)$$

$$u_6' = -u_5(2\sigma_1 - 2\sigma_2 + \sigma_3) - \mu_3 u_6 + \frac{\alpha_{12}}{4\omega_3}(u_1^2 - u_2^2)$$
$$+ \frac{\alpha_{13}}{4\omega_3}(u_1 u_3 - u_2 u_4)' + \frac{\alpha_{14}}{4\omega_3}(u_3^2 u_5 + u_4^2 u_5) \qquad (3.42f)$$
$$+ \frac{\alpha_{15}}{4\omega_3}(u_1^2 u_5 + u_2^2 u_5) + \frac{3\alpha_{16}}{8\omega_3}(u_5^3 + u_5 u_6^2) - \frac{\hat{f}_3}{2\omega_3}$$

where the following variable reassignments were used:

$$B_{1r} \rightarrow u_1, \quad B_{1j} \rightarrow u_2, \quad B_{2r} \rightarrow u_3, \quad B_{2j} \rightarrow u_4, \quad B_{3r} \rightarrow u_5, \quad B_{3j} \rightarrow u_6 \qquad (3.43)$$

The relationship between these u_j and the X_j for this case can be written in equation form:

$$X_1 \approx x_{10} = \sqrt{u_1^2 + u_2^2}\cos[\Omega_2 t + \gamma_1] \quad \text{where} \quad \gamma_1 = \tan^{-1}\left[\frac{u_2}{u_1}\right] \tag{3.44a}$$

$$X_2 \approx x_{20} = \sqrt{u_3^2 + u_4^2}\cos[\Omega_2 t + \gamma_2] \quad \text{where} \quad \gamma_2 = \tan^{-1}\left[\frac{u_4}{u_3}\right] \tag{3.44b}$$

$$X_3 \approx x_{30} = \sqrt{u_5^2 + u_6^2}\cos[2\Omega_2 t + \gamma_3] \quad \text{where} \quad \gamma_3 = \tan^{-1}\left[\frac{u_6}{u_5}\right] \tag{3.44c}$$

3.5 REMARKS

The equations governing the response of the system in the slow time scale, T_1, for each of the three cases have been derived. These equations can now be used to investigate the system response for each of the three cases. This is done in Chapter 5. Prior to presenting this information, Chapter 4 presents the parameter values for the physical system to be investigated and gives information that validates the use of the Taylor series in the derivation of the equations of motion of the system.

CHAPTER 4 SYSTEM PARAMETERS AND TAYLOR SERIES VERIFICATION

4.1 SYSTEM PARAMETER VALUES

Prior to presenting the numerical results for each of the three cases, discussion of the parameter values to be used in the numerical analysis is needed. It is desirable that the parameter values for the numerical analysis be realistic. As such, the physical problem investigated here is an in-line four cylinder automotive engine. Certain aspects of the geometry were set to facilitate the tractability of the problem. The location of the center of mass at the geometric center of the rigid body and the symmetry of the support locations were set in this fashion. The physical dimensions of the rigid body are representative of the dimensions of an engine looking along the crankshaft axis. The geometry depicting these parameters are Figures 2.1 and 2.2. The values chosen for the physical problem are:

Mass m:	219.400 kg
Inertia I_G:	14.155 kg-m^2
Height $2B$:	0.842 m
Width $2A$:	0.254 m
k_1:	1,732,312.8 N/m
k_2:	433,078.2 N/m
k_3:	433,078.2 N/m
k_4:	1,732,312.8 N/m
Spring free length:	0.102 m

The values for I_G, k_1, k_2, k_3, and k_4 were chosen such that the tuning between the rigid body linear natural frequencies is: $2\omega_1 = 2\omega_2 = \omega_3$. These relationships between the linear natural frequencies need not be strict equalities. Indeed, the preceding analysis of Chapter 2 allows for

such inexact tuning through the parameters σ_2 and σ_3. However, we chose to set $\sigma_2 = \sigma_3 = 0$, realizing that only small changes in the main features of the response plots would occur for small changes in these relationships.

These parameter values are also used to obtain numerical coefficients of the terms of the Taylor series approximation of the potential energy about the static equilibrium point. These coefficients are then divided appropriately by either m or I_G producing the α_j's in equations (3.3). The resulting numerical values are:

$\alpha_1 =$ -4915.45
$\alpha_2 =$ 154,817.68
$\alpha_3 =$ -1248.52
$\alpha_4 =$ -30,601.07
$\alpha_5 =$ 758,908.77
$\alpha_6 =$ -1,897,270.97
$\alpha_7 =$ -76,188.63
$\alpha_8 =$ -144.52
$\alpha_9 =$ -58,055.75
$\alpha_{10} =$ -474,311.20
$\alpha_{11} =$ 180,387.67
$\alpha_{12} =$ 77,408.84
$\alpha_{13} =$ -4915.45
$\alpha_{14} =$ 11,638.05
$\alpha_{15} =$ -1,897,270.97
$\alpha_{16} =$ 189,727.10

The values of the viscous damping coefficients c_1, c_2, and c_3 were chosen such that the dimensionless viscous damping factors of the linearized system equal 0.01. This leads to the following dimensionless modal damping coefficients specified as μ_j in equations (3.2):

$\mu_1 = 0.63$
$\mu_2 = 0.63$
$\mu_3 = 1.26$

The magnitude of the forcing, F_2 and F_3, were chosen to be of the same order of magnitude of force found in production engines. Limited information was found regarding these values and the following values reflect the information available (Fullerton, 1984):

$F_2 = 150.0$ N-m
$F_3 = 1000.0$ N

The frequencies associated with the forcing terms F_2 and F_3, Ω_2 and Ω_3 respectively, were chosen to correspond to the first order and second order associated with a hot idle condition of an in-line four cylinder engine which is approximately 600 rpm. Thus the values of Ω_2 and Ω_3 are:

$$\Omega_2 = 20\pi$$
$$\Omega_3 = 40\pi$$

The parameter ϵ introduced in equations (3.3) must be specified to enable the numerical evaluation of the results of the multiple scales analysis of the rigid body system. For this problem, ϵ is not a naturally occurring parameter of the system. It was introduced as part of the multiple scales analysis as a means to distinguish between motions at the different time scales. The method of multiple scales as used here introduces corrections that are of $O(\epsilon)$ for the time interval $\frac{1}{\epsilon} > t > 0$ (Kahn, 1990). Hence for the value of ϵ chosen here, $\epsilon = 0.01$, this time interval is 100s. The time intervals associated with the transient response for the three cases investigated here are on the order of 10s and are well within this interval.

4.2 TAYLOR SERIES VERIFICATION

Prior to presenting the response curves of the three cases, verification is presented for the use of the Taylor series approximation of the potential energy used in the Lagrange formulation of the equations of motion for this system. Time response plots, obtained from numerical integration (4th-order Runge-Kutta) for a given set of parameter values, are shown for each of the three cases. The comparisons demonstrate good agreement between the response predicted by the numerical integration of

the reduced equations obtained from multiple scales analysis (hereafter referred to as "reduced equations") and the envelopes obtained from the numerical integration of the equations of motion obtained from the approximation of the potential energy using a Taylor series retaining up to quartic terms. These equations are hereafter referred to as "cubic equations" as it is cubic terms that appear in the equations of motion after the required partial derivatives of the quartic terms of the potential energy approximation are performed.

In addition, for case 2, further comparison is made with the envelopes obtained from the numerical integration of the equations of motion obtained from the approximation of the potential energy using a Taylor series retaining up to only cubic terms. These equations are hereafter referred to as "quadratic equations" as it is the quadratic terms that appear in the equations of motion after the required partial derivatives of the cubic terms of the potential energy approximation are performed. Comparison is also made with the envelopes obtained from the actual equations of motion with no approximation in for the potential energy, hereafter referred to as "actual equations".

It is shown clearly in this case that the time response obtained from the quadratic equations is different than the time response obtained from the actual equations. Hence, although not an exhaustive test, it is reasonable to assume that it is valid to neglect terms in the Taylor series higher than quartic. Hence all of the reduced equations are derived from multiple scales analysis of the cubic equations of motion.

4.2.1 Case 1 (Vertical Forcing)

Figure 4.1 shows the time response plots of the numerical integration of the cubic equations. This figure depicts the upper and lower envelopes of the time response for each of the three system coordinates. Figure 4.2 shows the time response of the numerical integration of the reduced equations, equations (2.28). Very close agreement is seen between these two response plots, particularly in the steady state amplitudes. However, small differences are seen between the transient aspects of the responses. These differences are due to the different initial conditions used to generate these two sets of responses. The initial conditions used to generate the responses in Figure 4.1 are specified in terms of the initial displacement and velocity of the system coordinates. The initial conditions used to generate Figure 4.2 are specified in terms of the real and imaginary parts of the complex response defining each of the system coordinates. Since the multiple scales analysis will be used to predict the steady state amplitudes of the systems, no effort was taken to show full agreement of the transient aspects of the time response.

Comparison of Figures 1 and 2 also show that the reduced equations fail to predict the bias in the steady-state response predicted in the cubic equations as shown in Figure 4.1. This is expected due to the approximation of the multiple scales analysis. The terms that govern this behavior are $O(\epsilon^2)$, and are not accounted for in the analysis performed here.

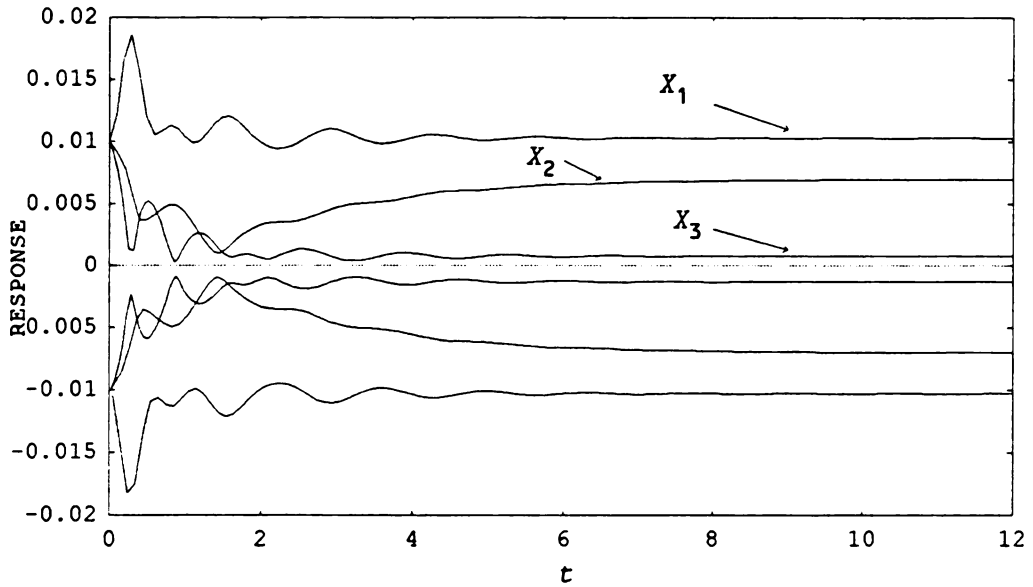

FIGURE 4.1 – Time response envelopes from the cubic equations Case 1 (Vertical forcing)

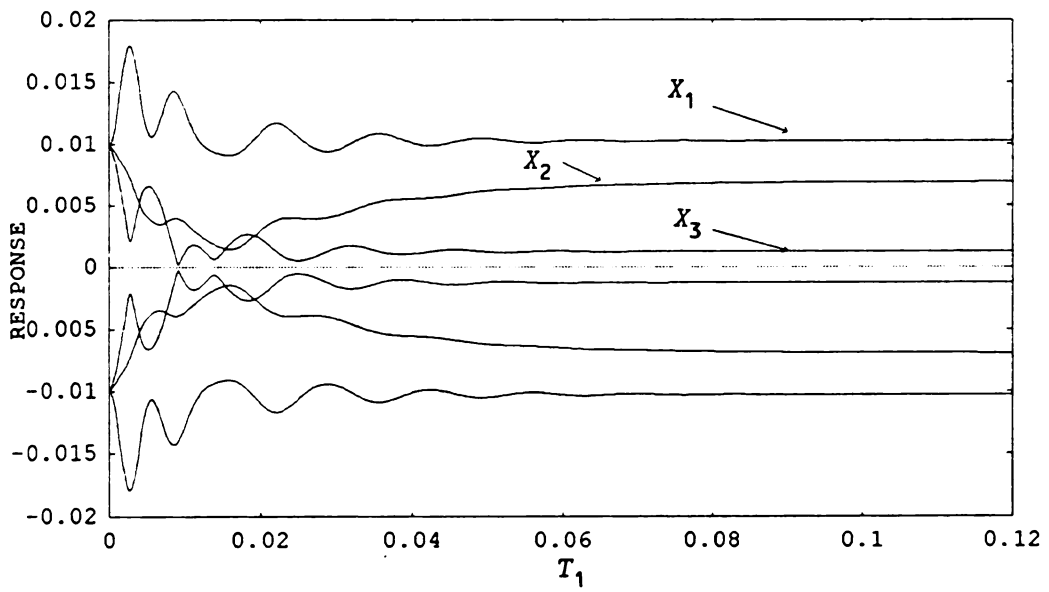

FIGURE 4.2 – Time response from the reduced equations Case 1 (Vertical forcing)

4.2.2 Case 2 (Torsional Forcing)

This case is used to present the correlation of the response predicted by the reduced equations and the actual equations. Figure 4.3 shows the envelope of the time response obtained from the actual equations

of motion. This response is contrasted with the time responses shown in Figures 4.4, 4.5 and 4.6.

Figure 4.4 is the time response for the system obtained from the quadratic equations. Comparison of this response with the response from the actual equations given in Figure 4.3 shows that retention of the cubic terms in the potential energy is not sufficient to predict the correct transient or steady state response of the system. However, the time response shown in Figure 4.5, obtained from the cubic equations, shows good agreement with the time response from the actual equations of motion shown in Figure 4.3. Here the comparison of the transient and the steady state aspects of the time response is valid as the initial conditions are identical between the two simulations. Good agreement is seen between these two simulations.

Figure 4.6 gives the time response of the reduced equations. This time response shows good agreement with the response of the actual equations of motion given in Figure 4.1 and with the time response of the cubic equations of motion shown in Figure 4.5.

The response for this particular set of parameter values clearly shows the importance of retaining the quartic terms in the Taylor series approximation of the system potential energy. This particular comparison illustrates the fact that it is not only differences in the transient or steady-state responses of the system which can be realized, but the qualitative nature of the response can be different. The time response obtained from the actual equations of motion, shown in Figure 4.3, shows that the steady state response of the system is time varying for this set of conditions. In contrast, the time response obtained from the quadratic equations, shown in Figure 4.4, incorrectly predicts that the system has

a fixed value steady state. The cubic equations do qualitatively and quantitatively predict the correct time response as shown in Figure 4.5.

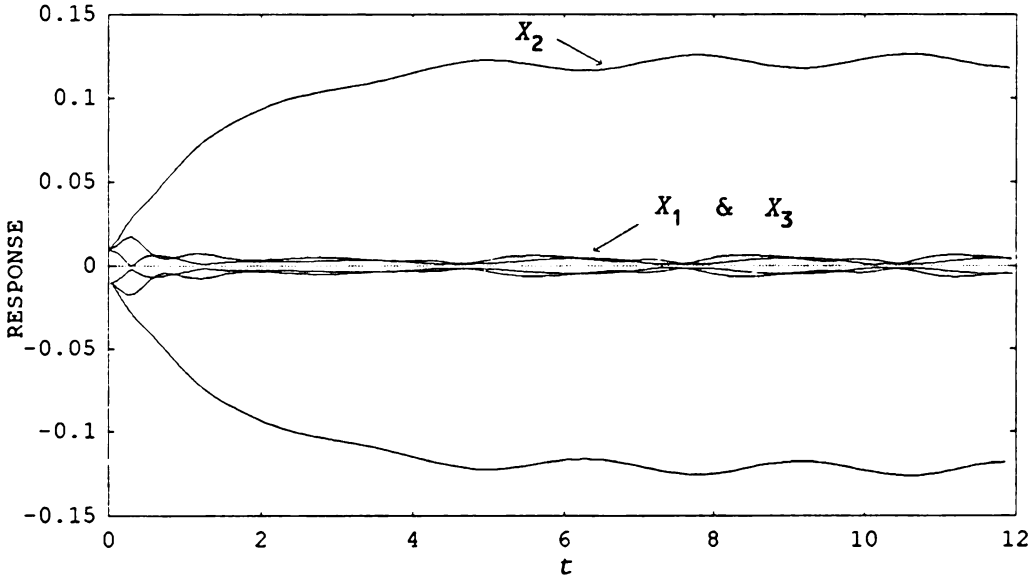

FIGURE 4.3 – Time response envelopes from the actual equations Case 2 (Torsional forcing)

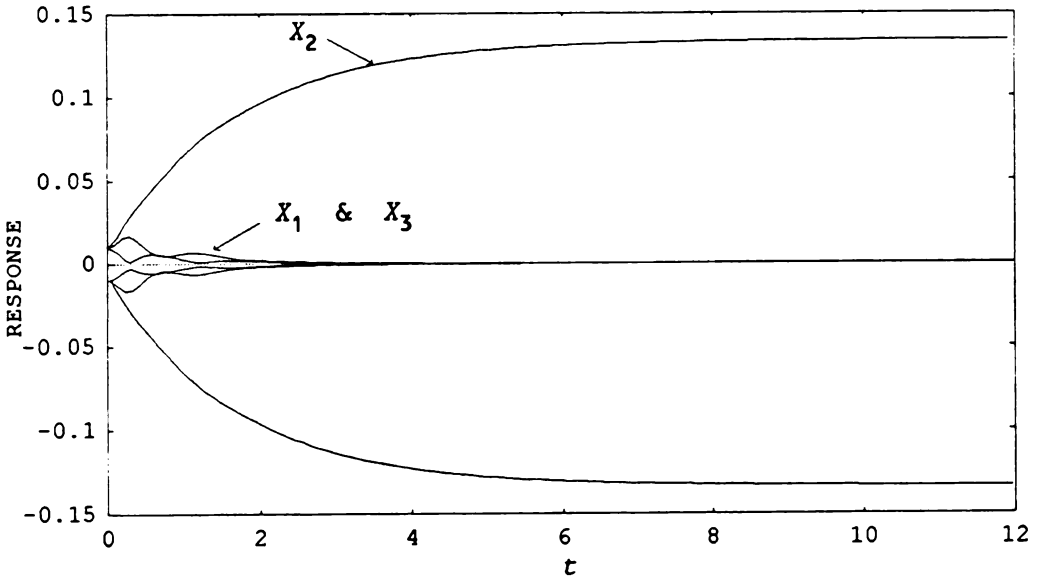

FIGURE 4.4 – Time response envelopes from the quadratic equations Case 2 (Torsional forcing)

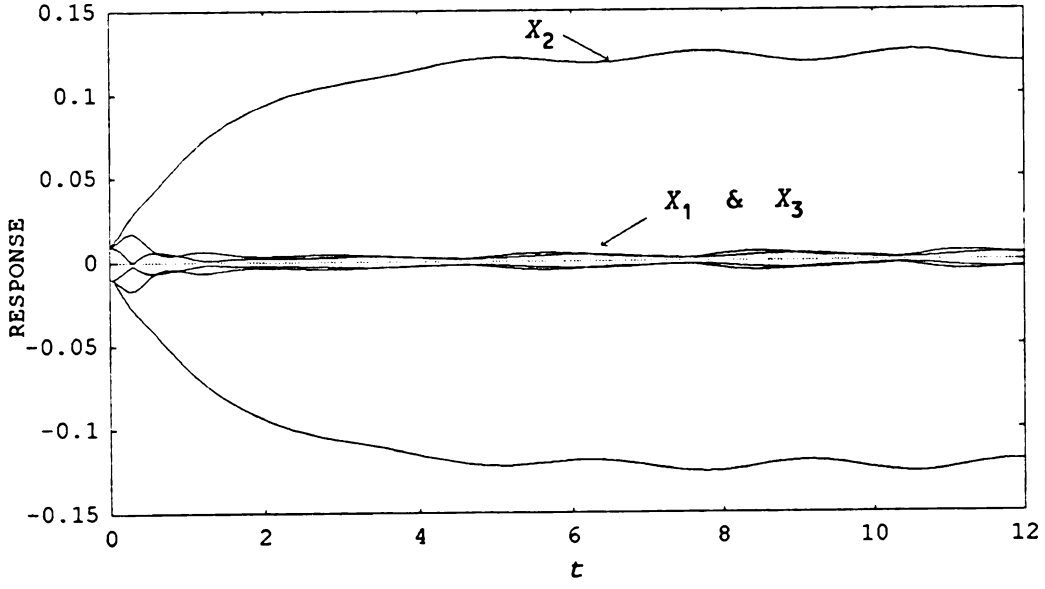

FIGURE 4.5 – Time response envelopes from the cubic equations
Case 2 (Torsional forcing)

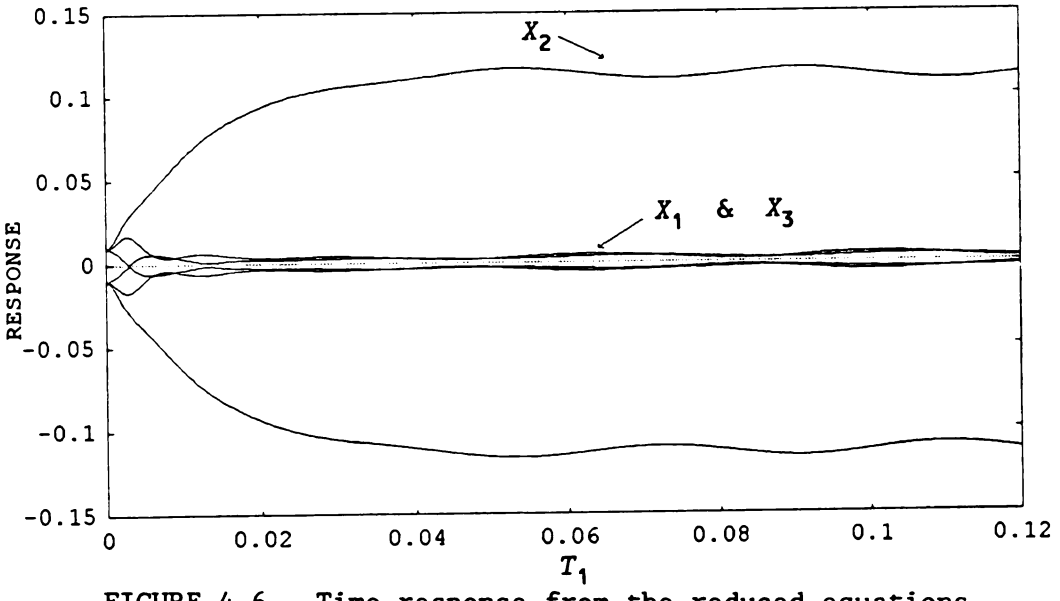

FIGURE 4.6 – Time response from the reduced equations
Case 2 (Torsional forcing)

4.2.3 Case 3 (Torsional and Vertical Forcing)

The results of the comparison of the time response of the cubic equations to the time response of the reduced equations are identical to the comparison performed in case 1. Figure 4.7 shows the envelopes of the time response obtained from the numerical integration of the cubic equations. Comparison of these with the time response obtained from the reduced equations, shown in Figure 4.8, shows good agreement for the steady-state response. Some differences are seen in the transient responses of the two sets of equations. This is again due to the different initial conditions used to generate the two response plots as explained above in case 1.

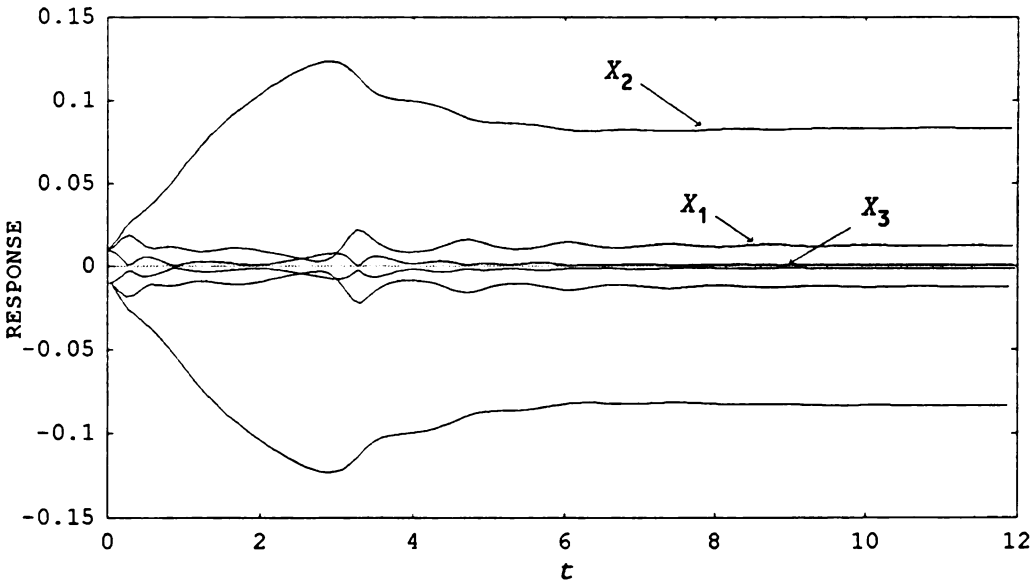

FIGURE 4.7 – Time response envelopes from the cubic equations Case 3 (Torsional and vertical forcing)

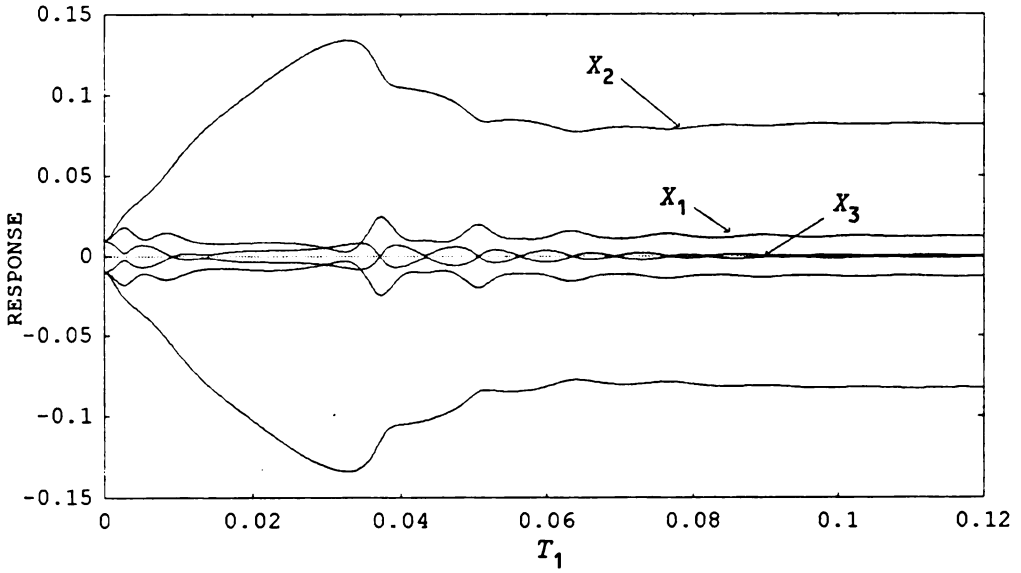

FIGURE 4.8 – Time response from the reduced equations
Case 3 (Torsional and Vertical forcing)

4.3 REMARKS

The results of this chapter are important in that they establish that use of the Taylor series for the potential energy expression in the derivation of the equations of motion leads to system response consistent with the actual equations of motion. Further, the reduced equations obtained from multiple scales yields system response consistent with both the actual equations of motion and the Taylor series equations retaining cubic terms. The reduced equations can now be used further to investigate the frequency response of the rigid body system for each of the three cases. This will be done by utilizing the reduced equations derived for each of the three cases and looking for the steady-state response of the system. This information is presented in the following chapter.

CHAPTER 5 SYSTEM FREQUENCY RESPONSE

Having completed the verification of the reduced equations, the next step in the investigation into the harmonic response of the rigid body system is to obtain the frequency response of the system. The frequency response can be obtained from the reduced equations produced by the multiple scales analysis. Steady state motions of the system are obtained by solving the reduced equations when the time derivatives of the system are set equal to zero. This can be done for each of the three cases and the frequency response plots obtained by plotting these solutions, and the associated stability information, for an appropriate range of the detuning the parameter, σ_1, i.e., the nearness of the forcing frequency to the associated natural frequencies. The stability of the solution is determined through examination of the eigenvalues of the Jacobian matrix for the system of reduced equations.

The detuning relationships for each case are given in Chapter 3. However, for all cases analyzed herein, σ_1 is the only detuning parameter varied in producing the response plots. In each case, this parameter represents the tuning of the forcing frequency relative to the natural frequency ω_j for $j = 2,3$ corresponding to the coordinate being forced. The detuning parameters σ_2 and σ_3 are both set to zero for all cases yielding perfect tuning of the internal resonances, $\omega_1 = \omega_2$, $2\omega_1 = \omega_3$. A fourth case, which is a variation of case 3 having reduced values for the magnitude of the forcing, will also be investigated.

Prior to proceeding with the response plots, the process and methods used in solving the algebraic equations for the steady state amplitudes

and obtaining the frequency response are discussed. The response plots for each of the four cases follows.

5.1 ANALYSIS METHODS

As stated, the frequency response of the system for each of the four cases is found by solving the reduced equations with the derivatives set to zero for an appropriate range of σ_1. Thus the problem of establishing the frequency response is reduced to that of repeatedly solving six nonlinear algebraic equations. For example, the algebraic equations governing the steady state amplitudes for case 1 are given by equations (5.1a)-(5.1f), i.e., equations (3.21) with the time derivatives set to zero.

$$\begin{aligned}&\frac{u_2}{2}(\sigma_1-\sigma_3)-\mu_1 u_1-\frac{\alpha_1}{4\omega_1}(u_3u_6-u_4u_5)-\frac{\alpha_2}{4\omega_1}(u_1u_6-u_2u_5)\\&\quad-\frac{3\alpha_3}{8\omega_1}(u_3^2u_4+u_4^3)-\frac{\alpha_4}{8\omega_1}(u_2u_3^2+3u_2u_4^2+2u_1u_3u_4)\\&\quad-\frac{3\alpha_5}{8\omega_1}(u_1^2u_2+u_2^3)-\frac{\alpha_6}{4\omega_1}(u_2u_5^2+u_2u_6^2)=0\end{aligned}\tag{5.1a}$$

$$\begin{aligned}&-\frac{u_1}{2}(\sigma_1-\sigma_3)-\mu_1 u_2+\frac{\alpha_1}{4\omega_1}(u_3u_5+u_4u_6)+\frac{\alpha_2}{4\omega_1}(u_1u_5+u_2u_6)\\&\quad+\frac{3\alpha_3}{8\omega_1}(u_3^3+u_3u_4^2)+\frac{\alpha_4}{8\omega_1}(3u_1u_3^2+u_1u_4^2+2u_2u_3u_4)\\&\quad+\frac{3\alpha_5}{8\omega_1}(u_1^3+u_1u_2^2)+\frac{\alpha_6}{4\omega_1}(u_1u_5^2+u_1u_6^2)=0\end{aligned}\tag{5.1b}$$

$$\begin{aligned}&\frac{u_4}{2}(\sigma_1+2\sigma_2-\sigma_3)-\mu_2 u_3-\frac{\alpha_7}{4\omega_2}(u_1u_6-u_2u_5)-\frac{3\alpha_8}{8\omega_2}(u_3^2u_4+u_4^3)\\&\quad-\frac{\alpha_9}{8\omega_2}(u_2u_3^2+3u_2u_4^2+2u_1u_3u_4)-\frac{\alpha_{10}}{8\omega_2}(u_1^2u_4+3u_2^2u_4+2u_1u_2u_3)\\&\quad-\frac{\alpha_{11}}{4\omega_2}(u_4u_5^2+u_4u_6^2)=0\end{aligned}\tag{5.1c}$$

$$-\frac{u_3}{2}(\sigma_1+2\sigma_2-\sigma_3)-\mu_2 u_4+\frac{\alpha_7}{4\omega_2}(u_1u_5+u_2u_6)+\frac{3\alpha_8}{8\omega_2}(u_3^3+u_3u_4^2)$$
$$+\frac{\alpha_9}{8\omega_2}(3u_1u_3^2+u_1u_4^2+2u_2u_3u_4)+\frac{\alpha_{10}}{8\omega_2}(3u_1^2u_3+u_2^2u_3+2u_1u_2u_4) \quad (5.1d)$$
$$-\frac{\alpha_{11}}{4\omega_2}(u_3u_5^2+u_3u_6^2)=0$$

$$u_6\sigma_1-\mu_3u_5-\frac{\alpha_{12}}{2\omega_3}u_1u_2-\frac{\alpha_{13}}{4\omega_3}(u_1u_4+u_2u_3)-\frac{\alpha_{14}}{4\omega_3}(u_3^2u_6+u_4^2u_6)$$
$$-\frac{\alpha_{15}}{4\omega_3}(u_1^2u_6+u_2^2u_6)-\frac{3\alpha_{16}}{8\omega_3}(u_5^2u_6+u_6^3)=0 \quad (5.1e)$$

$$-u_5\sigma_1-\mu_3u_6+\frac{\alpha_{12}}{4\omega_3}(u_1^2-u_2^2)+\frac{\alpha_{13}}{4\omega_3}(u_1u_3-u_2u_4)+\frac{\alpha_{14}}{4\omega_3}(u_3^2u_5+u_4^2u_5)$$
$$+\frac{\alpha_{15}}{4\omega_3}(u_1^2u_5+u_2^2u_5)+\frac{3\alpha_{16}}{8\omega_3}(u_5^3+u_5u_6^2)-\frac{f_3'}{2\omega_3}=0 \quad (5.1f)$$

Obtaining a response plot from the six algebraic equations consists of two phases. In the first phase, solutions to the equations are found for several values of σ_1. Typical values of σ_1 are: $\sigma_1 = 0$ (i.e., $\Omega_3 = \omega_3$) and $\sigma_1 = \pm 300$ (i.e., $\Omega_3 = 40\pi \pm 3$ rad/s). These solutions are found using a FORTRAN program based on the IMSL routine DNEQNJ (IMSL, 1980). This routine produces the solution of a set of nonlinear algebraic equations using the Levenberg-Marquardt optimization algorithm.

After the various solutions are found at the selected values of σ_1, they are used as seeds in a program which traces the solution paths, i.e. the frequency response, by iterating on the values of σ_1. The solution for the previous value of σ_1 is used as the seed in the solution algorithm for the next step. This program is also based on the IMSL routine DNEQNJ, but has the added feature that it loops on a parameter. In all cases examined herein this parameter is σ_1. The stability of each of the solutions is established by evaluating the eigenvalues of the Jacobian matrix of the

nonlinear algebraic equations. This procedure was found to be an efficient and convenient method for finding the solutions to these algebraic equations, establishing the associated stability, and thereby determining the system response.

The six solution components found for a given value of σ_1 form the three pairs of the real and imaginary components of the three coordinate variables X_1, X_2, and X_3, i.e., corresponding to the coordinates x, α, and y, which are the horizontal, angular and vertical displacements, respectively. The collective magnitudes and the corresponding stability information for an appropriate range of σ_1 values form the response plots for the system. It is these response plots for each of the four cases which are presented next.

5.2 CASE 1 (VERTICAL FORCING)

The algebraic equations to be solved for the steady state amplitudes for case 1 are given by equations (5.1a)-(5.1f). Following the procedure outlined in the previous section, frequency response plots for the magnitudes of the coordinates X_1, X_2, and X_3 are given. For this case, two response plots for each of X_1, X_2, and X_3 are presented. The first set of response plots, Figures 5.1, 5.2, and 5.3, include several of the unstable solutions with comparatively large magnitudes. These large values of response represent solutions which are not physically realizable and are only a mathematical curiosity. (The dimensions associated with X_1 and X_3 are given in meters in the response plots and in radians for X_2.) Response plots with a larger ordinate range are not shown for any of the subsequent cases and are shown here for completeness.

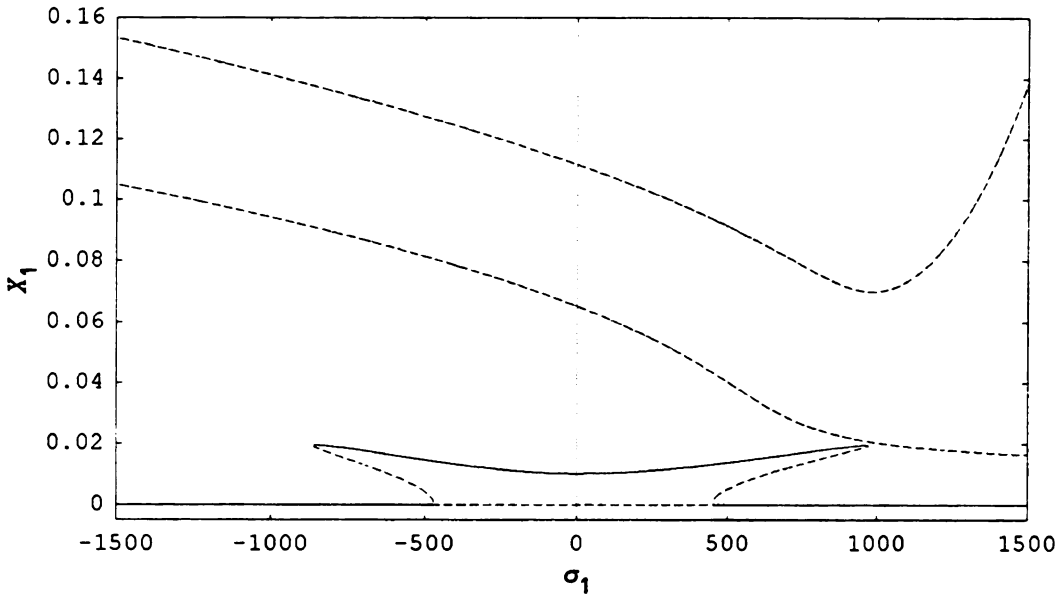

Figure 5.1 – Frequency response for X_1, case 1, horizontal response
—— stable solution, ---- unstable solution

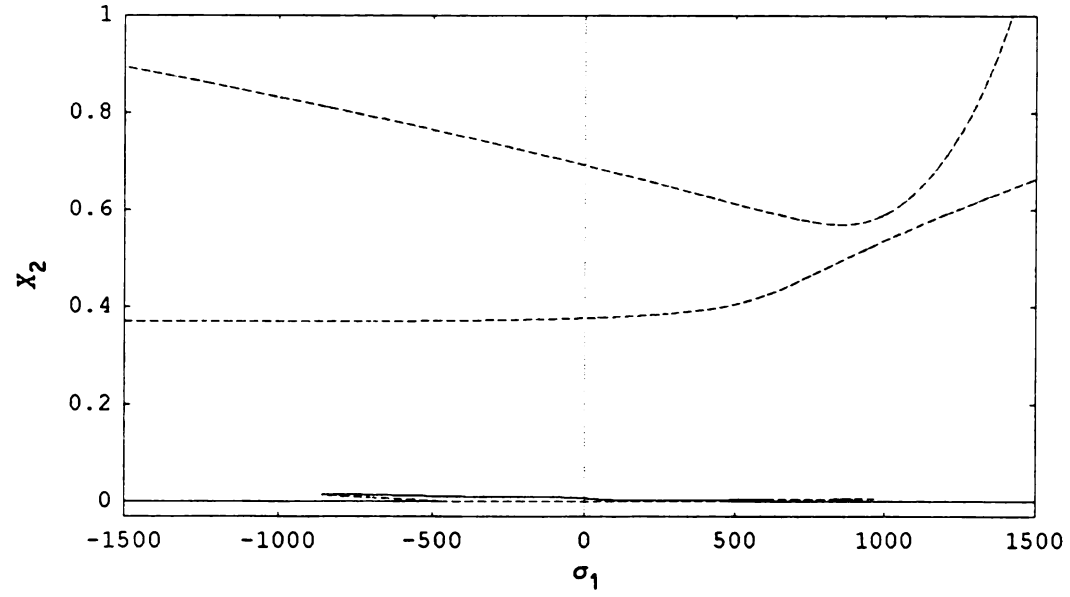

Figure 5.2 – Frequency response for X_2, case 1, rotational response
—— stable solution, ---- unstable solution

Before discussing some of the important features of these figures, the actual interpretation of the response curves is addressed. Recall equations (3.23):

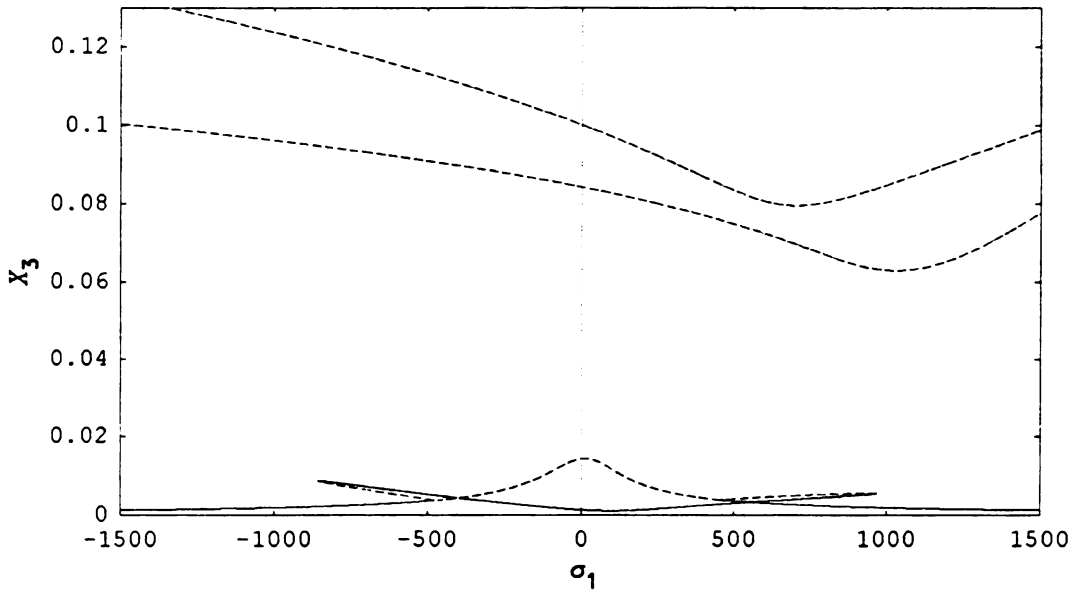

Figure 5.3 – Frequency response for X_3, case 1, vertical response
—— stable solution, ---- unstable solution

$$X_1 \approx x_{10} = \sqrt{u_1^2 + u_2^2}\cos\left[\frac{\Omega_3}{2}t + \gamma_1\right] \quad \text{where} \quad \gamma_1 = \tan^{-1}\left[\frac{u_2}{u_1}\right] \tag{5.2}$$

$$X_2 \approx x_{20} = \sqrt{u_3^2 + u_4^2}\cos\left[\frac{\Omega_3}{2}t + \gamma_2\right] \quad \text{where} \quad \gamma_2 = \tan^{-1}\left[\frac{u_4}{u_3}\right] \tag{5.3}$$

$$X_3 \approx x_{30} = \sqrt{u_5^2 + u_6^2}\cos\left[\Omega_3 t + \gamma_3\right] \quad \text{where} \quad \gamma_3 = \tan^{-1}\left[\frac{u_6}{u_5}\right] \tag{5.4}$$

and equation (3.13a):

$$\Omega_3 = \omega_3 + \epsilon\sigma_1$$

From equations (5.2) and (5.3), it can be seen that instead of oscillating at the forcing frequency Ω_3, X_1 and X_2, which are the magnitudes of the response in the horizontal and rotational directions, respectively oscillate at one half this value. Figures 5.4 and 5.5, depict

the response curves for X_1 and X_2, respectively. Therefore, these plots are unlike the usual "linear" response curves where the frequency of the response is always the same as the forcing frequency. Finally, it is noted that for all cases investigated, a 1 Hz change in the forcing frequency corresponds to a σ_1 value of 628.32. We are now in a position to discuss the features of the response curves shown in Figures 5.4-5.15.

The second set of response plots, shown in Figures 5.4, 5.5, and 5.6, have a reduced range of response amplitude to show more explicitly the transitions between the linear and nonlinear solutions. It is seen that away from the external resonance, i.e. $\sigma_1 \neq 0$, the motion of the system follows that of the linear system. For this case, the linearized system is a set of three uncoupled linear oscillators. Therefore, as the forcing acts only on coordinate X_3, the linear solution for the X_1 and X_2 coordinates is, to this level of approximation, the trivial solution for all σ_1. Slowly increasing the frequency of the forcing starting from far below this resonance leads to unstable linear response for the X_1 and X_2 coordinates which occurs at $\sigma_1 \approx -470$. At this value of the detuning, the X_1 and X_2 coordinates abruptly shift from the trivial solution up to a nonzero steady state response. The linear solution for the X_3 coordinate also becomes unstable at this value of σ_1 and the steady state response jumps up to a different stable solution. These non-trivial steady state solutions continue until $\sigma_1 \approx 971$ where all of the coordinates experience downward jumps back to their respective linear solutions.

When starting far above the resonances and decreasing the frequency of the forcing, transition from the linear solutions to the nonlinear solutions occurs at $\sigma_1 \approx 450$. These solutions continue until a large downward jump back to the linear solutions is experienced at $\sigma_1 \approx -860$.

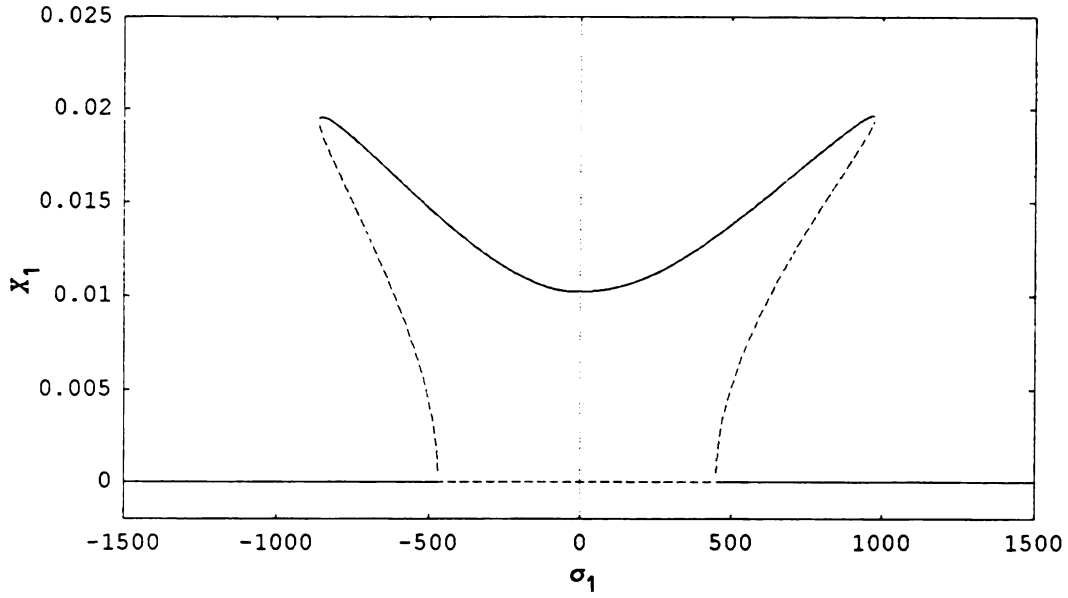

Figure 5.4 — Frequency response for X_1, case 1, horizontal response
—— stable solution, ---- unstable solution

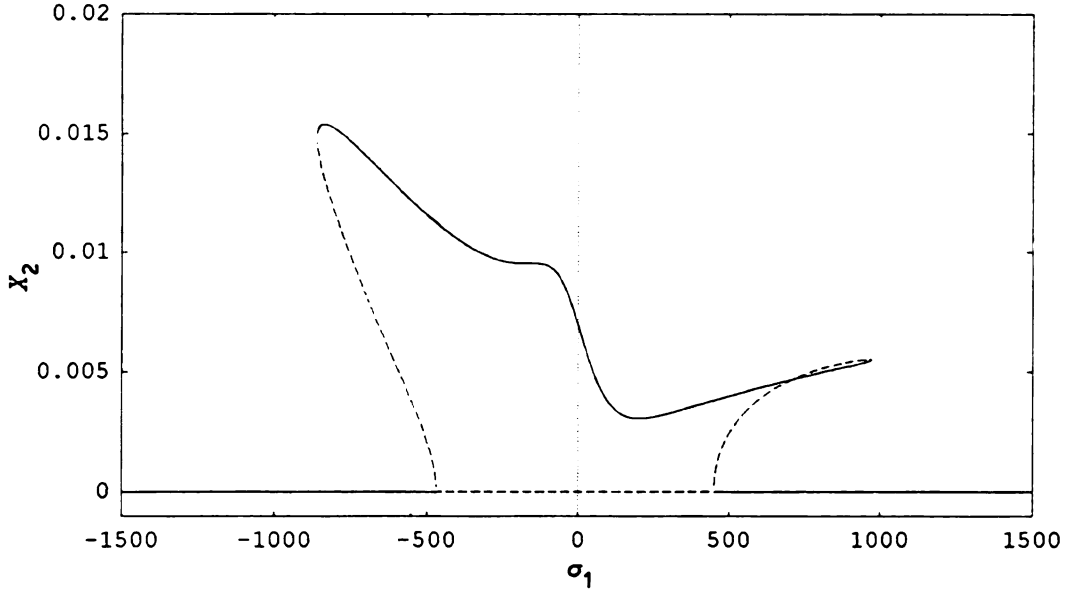

Figure 5.5 — Frequency response for X_2, case 1, rotational response
—— stable solution, ---- unstable solution

Response similar to the response described here has been demonstrated analytically for two degree of freedom systems (Nayfeh and

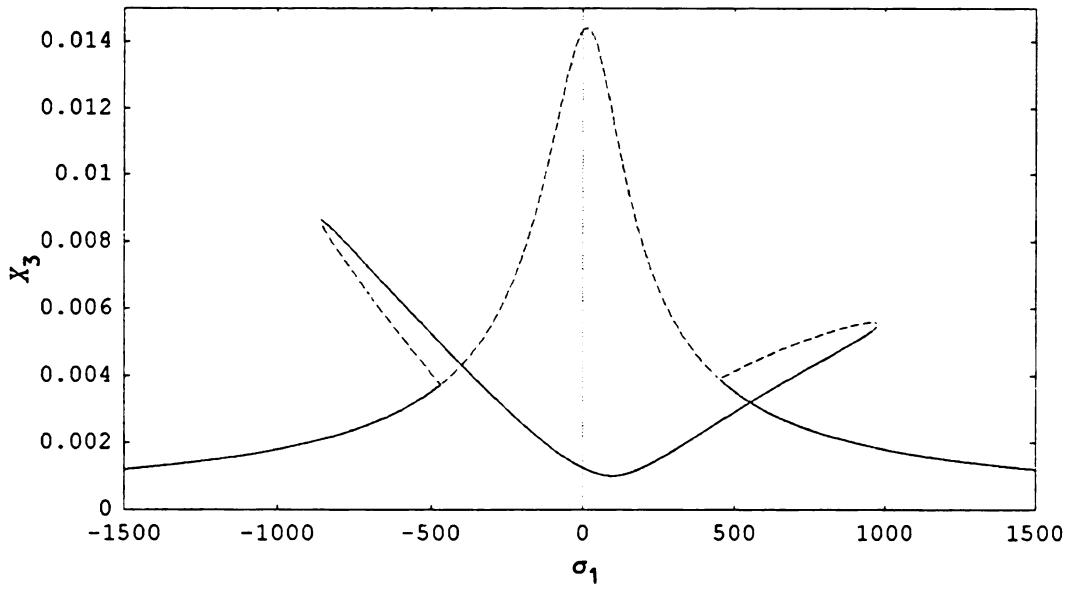

Figure 5.6 – Frequency response for X_3, case 1, vertical response
—— stable solution, ---- unstable solution

Mook, 1979; Haddow, et. al., 1984; and Perkins, 1992). Additionally, in Haddow, et. al. (1984), this response was also verified experimentally. The system investigated here exhibits some of the same features shown in these references. In particular, these systems display the saturation phenomenon. This is the situation whereby increased forcing magnitude is not accompanied with an increase in the magnitude of the response variable in the direction of the forcing. Thus the mode is "saturated". This phenomena occurs over the region of nonlinear solutions and need not be associated with large displacements. In contrast, the case where only an external resonance is present (Nayfeh and Balachandran, 1989), the additional parametric resonance (actually and autoparametric resonance, see Nayfeh and Mook, (1979)) makes the response plot asymmetric about the $\sigma_1 = 0$ axis. This agrees with the results shown in Perkins (1992) where asymmetry is also shown.

This system response shows some interesting implications from the vibration isolation point of view. The response of X_3 (vertical), shown in Figure 5.6, shows that over the range $-400 \leq \sigma_1 \leq 550$, the nonlinear system shows drastically reduced response amplitudes than for the corresponding linear case. This however comes with two trade-offs. The first is that the response amplitudes for X_1 (horizontal) and X_2 (rotational), are nonzero. This is in contrast with the linear solution where the response of both of these would be zero for the entire range of σ_1. The second is that over the ranges $-860 \leq \sigma_1 \leq -400$ and $550 \leq \sigma_1 \leq 971$ the nonlinear response is greater than the linear response. However, the peak nonlinear response is still much less than the peak linear response. In particular, where the linear response reaches a maximum, the nonlinear response reaches a local minimum which is approximately seven times less than the linear solution.

Hence, it is seen that the energy has been distributed among the various coordinates rather than being concentrated in the coordinate response associated with the direction of the forcing. This type of response could be utilized effectively in circumstances where response of a system near a particular frequency, and in a coordinate direction different from the one being excited, is more tolerable than response in the direction of the forcing. For example, this might occur if a supporting structure for a system has different stiffness values in different coordinate directions.

5.3 CASE 2 (TORSIONAL FORCING)

The six algebraic equations governing the steady state amplitudes for case 2 are given by equations (3.31a)-(3.31f) with the terms containing the time derivatives, i.e., the left hand side of these

equations, set equal to zero. Following the analysis procedure outlined in Section 5.1, the frequency response plots for the coordinates X_1, X_2, and X_3 are generated.

For this case, the linearized system is again described by three uncoupled linear oscillators. Since the forcing appears in the equation for the X_2 coordinate (see equations (3.3) with $\hat{f}_3 = 0$), the linear response for the X_1 and X_3 coordinates is the trivial solution. Figures 5.7 and 5.9 show that the nonlinear response of these two coordinates does occur. In Figure 5.8, the linear solution for the X_2 coordinate is plotted in addition to the nonlinear solution. As can be seen in this figure, the amplitude of these two solutions match very closely except in the region $-100 \leq \sigma_1 \leq 100$.

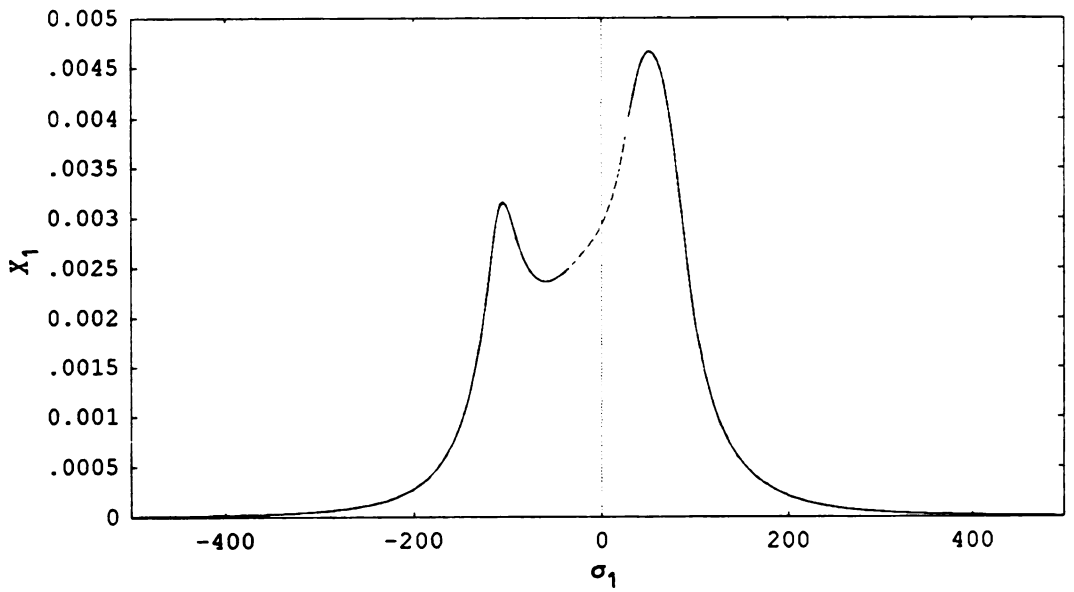

Figure 5.7 – Frequency response for X_1, case 2, horizontal response
—— stable solution, ---- unstable solution

In contrast to the response plots for case 1, the response for this case does not contain any sudden jumps from the linear to the nonlinear

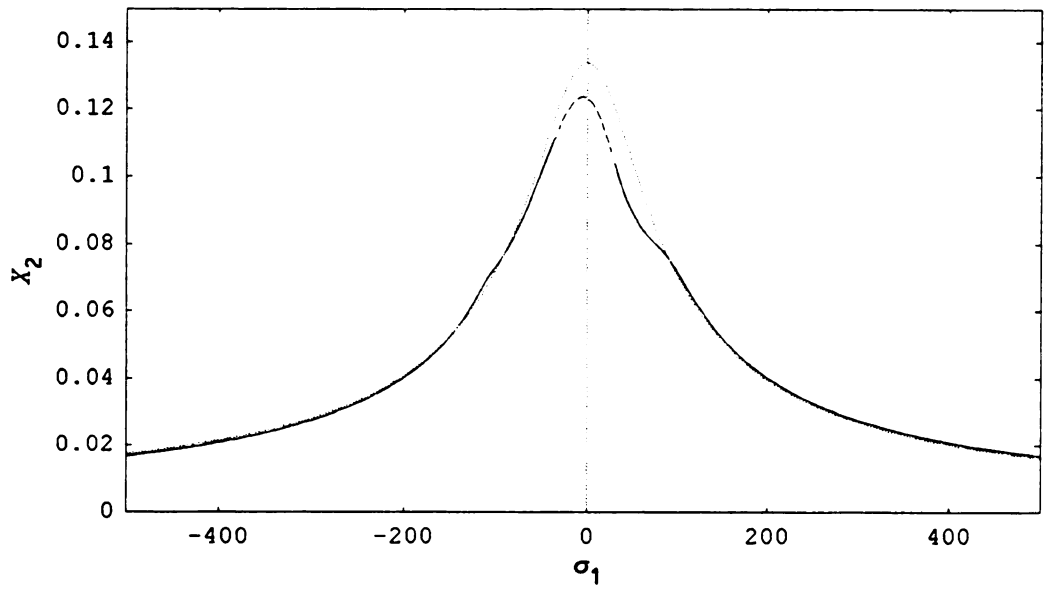

Figure 5.8 – Frequency response for X_2, case 2, rotational response
—— stable solution, --- unstable solution, ··· linear solution

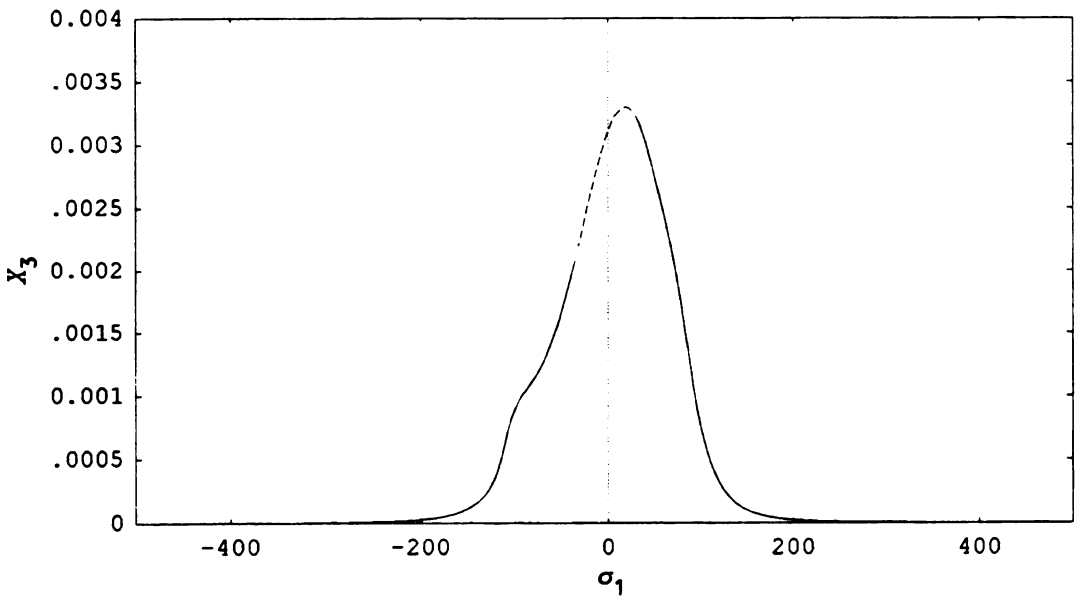

Figure 5.9 – Frequency response for X_3, case 2, vertical response
—— stable solution, ---- unstable solution

solutions. All three of the response plots have smooth transition for this range of σ_1.

As seen in Figures 5.7, 5.8, and 5.9, for $-36 \leq \sigma_1 \leq 31$, no stable steady state solutions exists. As such, the response is never expected to reach a steady state (a condition where the modal amplitudes are constant). Figure 4.6 shows the envelope of the time response for this system obtained from numerical integration of the reduced equations for $\sigma_1 = 0$ $\sigma_1 = 0$. This time response illustrates the lack of a steady state solution with constant modal amplitudes.

5.4 CASE 3 (TORSIONAL AND VERTICAL FORCING)

The six algebraic equations governing the steady state amplitudes for case 3 are given by equations (3.41) with the terms containing the time derivatives set equal to zero. Once again, we follow the procedure outlined in Section 5.1 to obtain the frequency response plots.

In this case, forcing in the equations for the X_2 and X_3 coordinates is present (see equations (3.3)). The forcing frequencies are such that for the condition investigated, external resonances are present for both of these coordinates. This is the case as the forcing frequency on the X_3 coordinate, Ω_3, arises from a second order type of unbalance whereas the forcing frequency on the X_2 coordinate is of first order, i.e., $\Omega_3 = 2\Omega_2$. The internal resonances $\omega_1 = \omega_2$ and $2\omega_1 = \omega_3$ are also assumed. The response plots for this system are given in Figures 5.10, 5.11, and 5.12.

Figure 5.10 shows the frequency response of the X_1 coordinate. Here it is seen that over the majority of the range $-500 \leq \sigma_1 \leq 500$, the response of this coordinate is multi-valued. In the range $-110 \leq \sigma_1 \leq 50$, the response is single valued. In the regions $-380 \leq \sigma_1 \leq -250$ and $220 \leq \sigma_1 \leq 450$ the response is triple valued. For $-450 \leq \sigma_1 \leq -380$ and $450 \leq \sigma_1 \leq 510$, the response is double valued. The responses of coordinates X_2 and

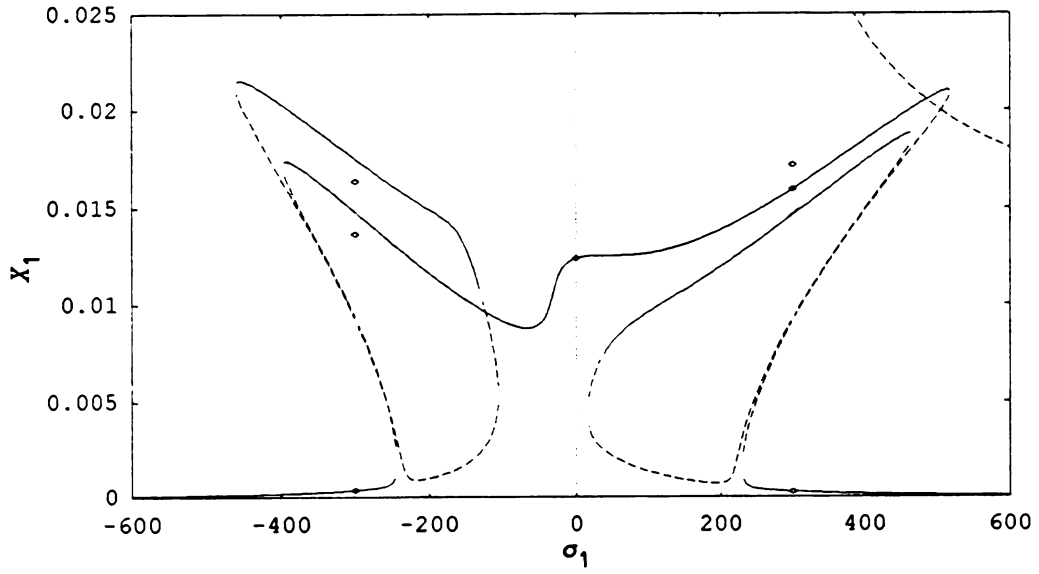

Figure 5.10 – Frequency response for X_1, case 3, horizontal response
—— stable solution, ---- unstable solution

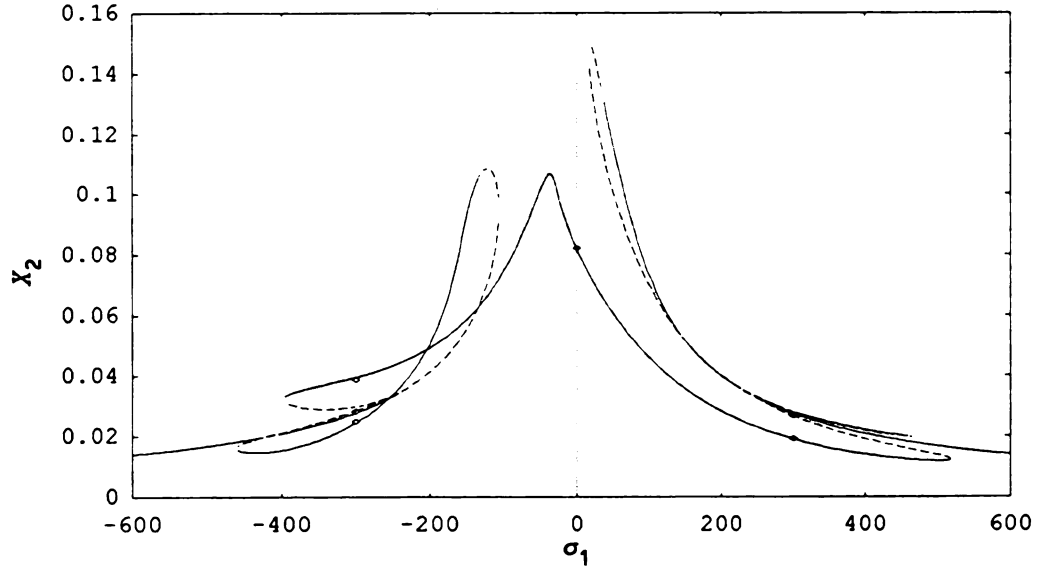

Figure 5.11 – Frequency response for X_2, case 3, rotational response
—— stable solution, ---- unstable solution

X_3, shown in Figures 5.11 and 5.12 respectively, also exhibit these same features.

For this case, verification of the response magnitudes for each of the three system coordinates was made. The verification is made through

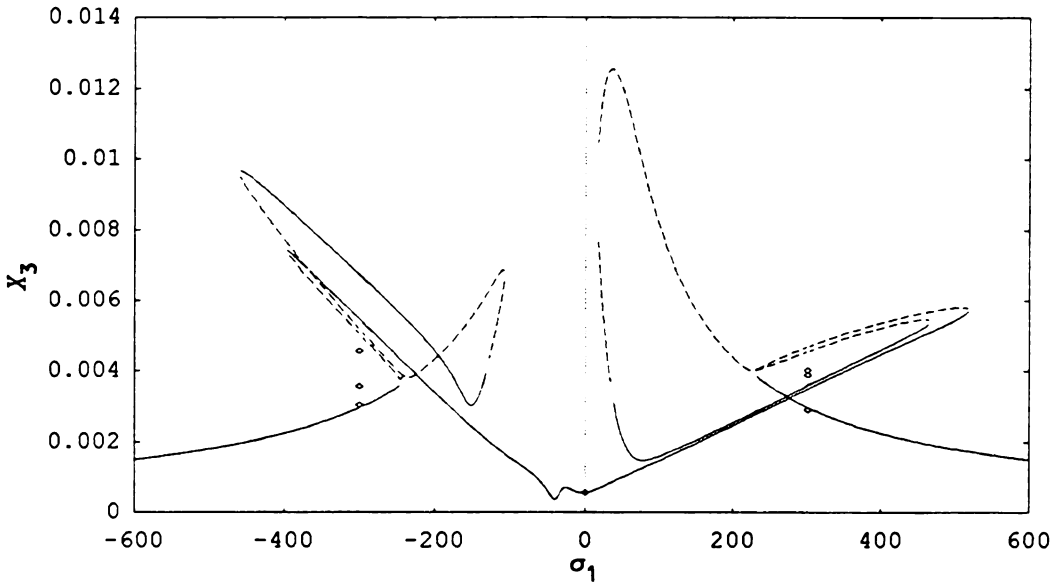

Figure 5.12 – Frequency response for X_3, case 3, vertical response
—— stable solution, ---- unstable solution

comparison with the response amplitudes predicted through numerical integration of the cubic equations to those predicted by the steady state values obtained from the reduced equations. The comparisons were made only for selected values of σ_1: $\sigma_1 = \pm 300$ and $\sigma_1 = 0$. These amplitudes are indicated in Figures 5.10, 5.11, and 5.12 by the $\diamond$. This comparison shows that for the response amplitudes predicted at $\sigma_1 = 0$, very good correlation is shown. Correlation at $\sigma_1 = \pm 300$ is also quite good. Additionally, the correlation shows good agreement between qualitative nature of the solutions.

For this case, again the linearized system for this system configuration is three uncoupled linear oscillators. Since two of the coordinates contain a forcing term, the resulting motion will contain the response from only these coordinates, but for all values of the input forcing frequencies the response would be single valued. Table 5.1 lists

a comparison of the maximum amplitudes of the linear and nonlinear responses of the system for this case.

	Linear Response	Nonlinear Response
$\|X_1\|_{max}$	0.000	0.022
$\|X_2\|_{max}$	0.135	0.125
$\|X_3\|_{max}$	0.014	0.010

Table 5.1 - Comparison of linear and nonlinear amplitudes for case 3

As in case 1, it is seen here that a large reduction in amplitude is realized in the X_3 coordinate response for the range $-200 \leq \sigma_1 \leq 200$. It is in this range that the nonlinear system produces small response compared to the linear response. This difference in amplitudes can be utilized to enhance the isolation response of the system.

5.5 CASE 4 (REDUCED AMPLITUDE TORSIONAL AND VERTICAL FORCING)

Currently, limited information is available pertaining to the magnitudes of the forcing present in an in-line four cylinder engine. The available information (Fullerton, 1984; Geck and Patton, 1984) presents data only for selected force components. In an effort to account for any uncertainty in the amplitudes, an additional load condition with smaller force magnitudes was selected and the response of the system obtained. Information from the above references was used to determine the reduction in force amplitude. The magnitudes of the forcing selected are:

F_2 = 30.000 N-m (previously 150.000 N-m)

F_3 = 500.000 N (previously 1000.000 N)

Figures 5.13, 5.14, and 5.15 show the frequency response plots for the coordinates X_1, X_2, and X_3. As shown in these response plots, the solution is still nonlinear. The comparison in the response plots with those of case 3 reveals that the onset of the nonlinear response in case 4 occurs at a smaller value of σ_1 than for case 3. This nonlinear response is also sustained for a smaller range of σ_1. This can be seen most clearly by comparing the responses of the X_3 coordinate for the two cases. In considering a sweep of the frequency parameter σ_1 from negative to positive (left to right in the figures), it can be seen that the onset of the nonlinear solution for case 3 occurs at $\sigma_1 \approx -250$, whereas for case 4 this value is $\sigma_1 \approx -160$. For increasing values of σ_1, the nonlinear solution is sustained in case 3 until $\sigma_1 \approx 510$, whereas for case 3 this value is $\sigma_1 \approx 230$.

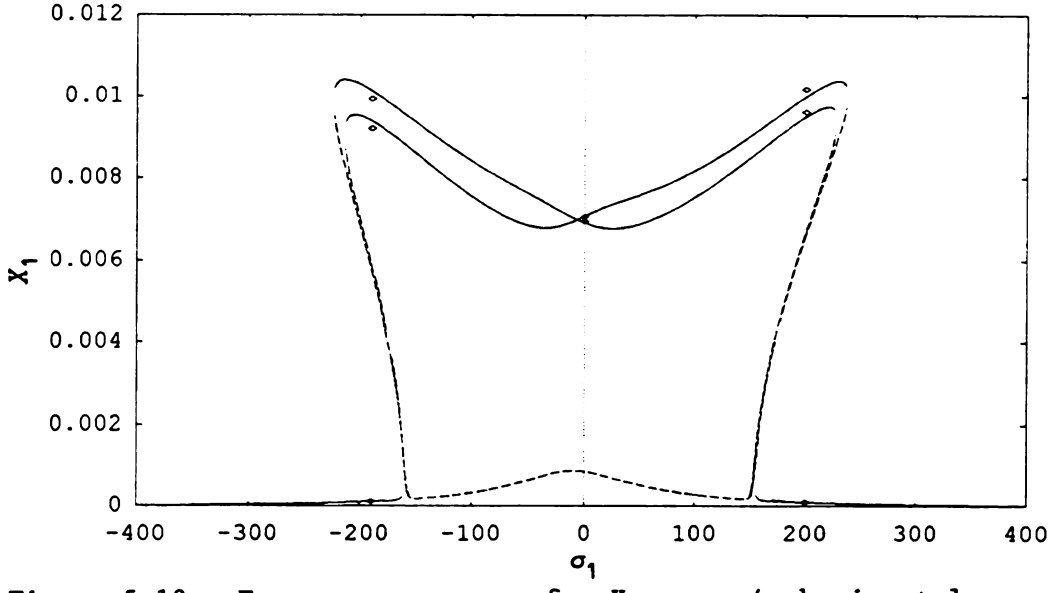

Figure 5.13 – Frequency response for X_1, case 4, horizontal response
—— stable solution, ---- unstable solution

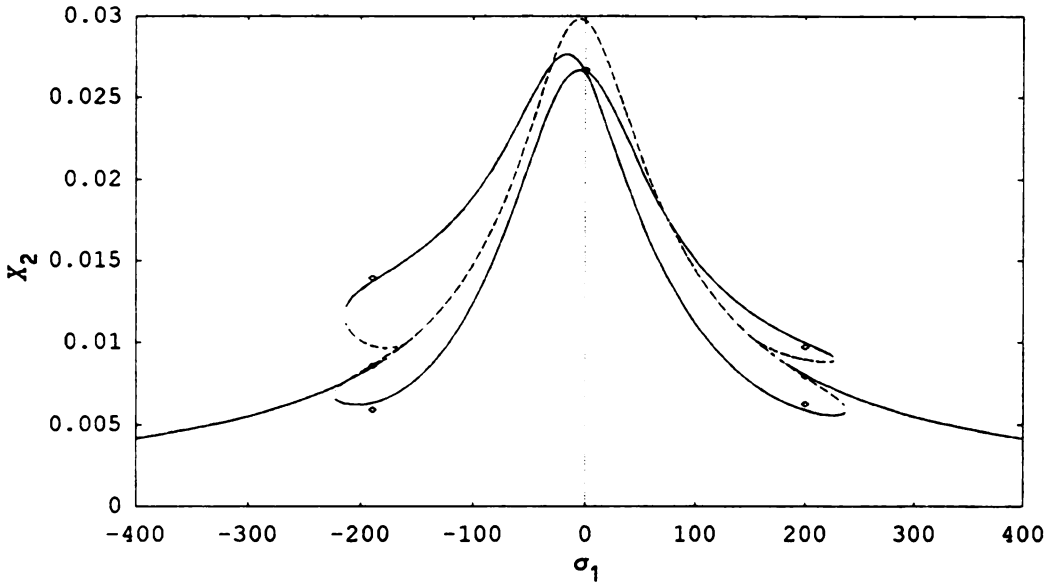

Figure 5.14 – Frequency response for X_2, case 4, rotational response
—— stable solution, ---- unstable solution

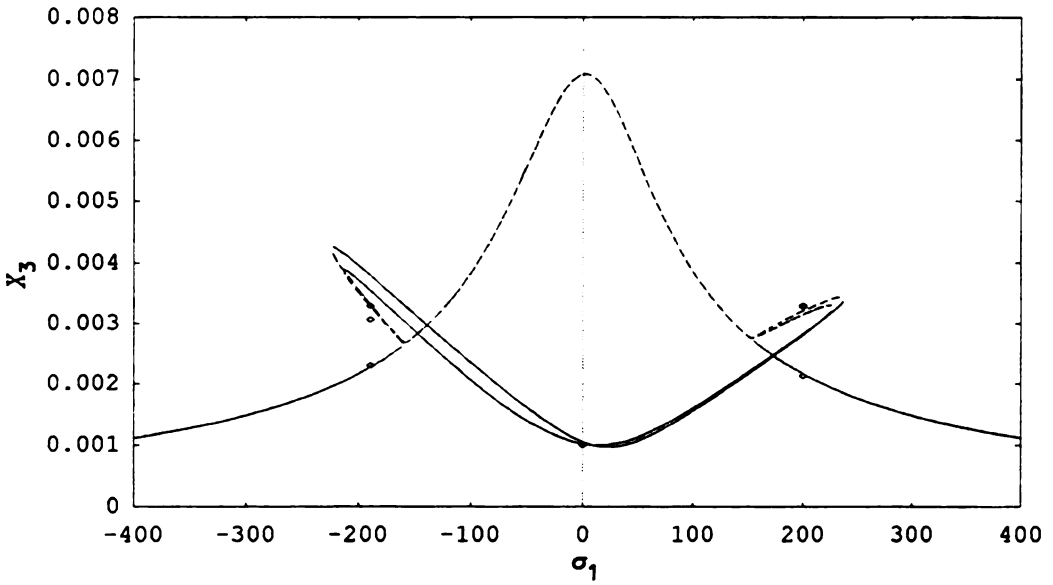

Figure 5.15 – Frequency response for X_3, case 4, vertical response
—— stable solution, ---- unstable solution

Finally, it can be seen that there is a qualitative change in the response due to the reduction in forcing amplitude. Although the response for case 3 is similar to that of case 4 in that there are corresponding regions where the solutions for the coordinates are single valued, double

valued, and triple valued, case 4 response does not exhibit the single valued response in the region containing $\sigma_1 = 0$. Close comparison shows that some interesting changes in the solutions occur as the forcing amplitudes are varied. One of the solutions which is continuous through the region given approximately by $-150 \leq \sigma_1 \leq 50$ for case 4 as shown in Figure 5.12, is discontinuous in case 3.

Aside from the differences in response due to the reduction in forcing amplitude just listed, excitation of X_1 again occurs. Therefore, even at lower forcing amplitudes, the reduction in the resonance peak associated with the X_3 coordinate can be accomplished.

5.6 MEASURES OF ISOLATOR PERFORMANCE

Having presented a collection of response plots for the displacements x, α, and y of the rigid body, it is interesting to investigate the associated forces transmitted to the foundation. This section opens with a brief discussion of isolation performance.

Various metrics have been applied to the evaluation of vibration isolation systems. Three of the measures prevalent in the literature are transmissibility, isolation effectiveness, and power transmission. Additionally, in many of the citations mentioned in this thesis, the actual force transmitted to the base (or foundation) is the measure of the performance of an isolation system. It is the purpose here to consider each of these measures and understand their use.

5.6.1 Transmissibility

The concept of transmissibility for damped, linear single degree of freedom systems is defined in many undergraduate vibrations textbooks. See for example Rao, (1986) or Thomson, (1972). For a single degree of freedom system under a harmonic force excitation applied to the mass, transmissibility is defined as $T_F = \left|\frac{F_T}{F_0}\right|$ (see Figure 5.16(a)). This quantity is also referred to as force transmissibility (Sykes, 1956; Ungar and Dietrich, 1966). Here F_0 is the force applied to the mass and F_T is the force transmitted through the spring (and damper if needed) to the foundation (see Figure 5.16(a)). It should be noted that this definition of force transmissibility is made under the assumption that the structure to which the spring and damper are attached is rigid. Transmissibility for a single mass undergoing base excitation is defined as $\left|\frac{X}{Y}\right|$ (see Figure 5.16(b)). Here Y is the amplitude of the input displacement and X is the amplitude of the displacement of the system mass.

The concept of transmissibility is defined more explicitly by Sykes, (1956) and Ungar and Dietrich, (1966), utilizing methods from modal theory (Ewins, 1986). They further qualify the concept of transmissibility with velocity transmissibility, T_V. The velocity transmissibility for an isolator positioned between a source and a receiver is defined as $T_V = \left|\frac{V_R}{V_0}\right|$, where V_R is the velocity amplitude at the receiver and V_0 is the velocity amplitude on the source side of the isolator (see Figure 5.16(b)). It can

be shown that $T_V = T_F$, at any one frequency for T_V and T_F as defined above for the single degree of freedom systems shown in Figure 5.16.

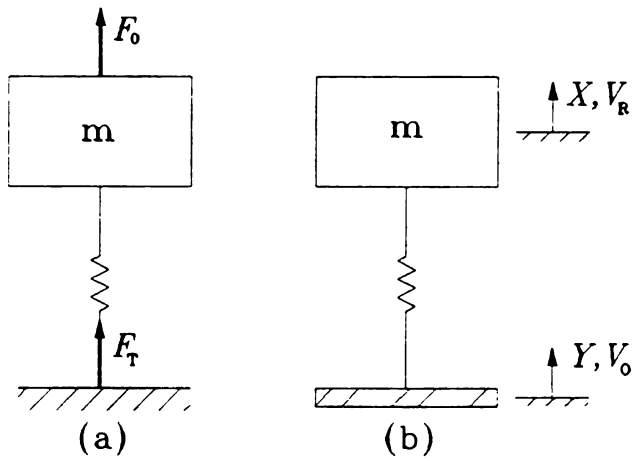

Figure 5.16 - Single degree of freedom isolation system

5.6.2 Effectiveness

These same authors also define another measure of isolator performance called effectiveness (Sykes, 1956; Ungar and Dietrich, 1966). This quantity is also referred to as isolator effectiveness, isolation effectiveness, insertion ratio and insertion loss (Rubin and Biehl, 1967). Effectiveness is the nondimensional measure of the reduction of the vibration of a system. It is the ratio of the structural vibration of the system with no isolator (the source and receiver are rigidly connected) to the structural vibration of the isolated system. If this ratio is less than unity, the isolator reduces the amplitude of the receiver velocity (acceleration or displacement). If this ratio is greater than unity, the isolator increases the amplitude of the receiver velocity (acceleration or displacement).

Recently, the notion of effectiveness has been expanded to systems that include multiple parallel isolators connecting one mass to a

foundation (Swanson, et. al.; 1994). For this system, both a velocity effectiveness and a force effectiveness are defined. For velocity effectiveness, this is done by defining a matrix, E_v, that represents the level of velocity effectiveness in the isolated mounting system:

$$v_s^h = E_v V_s^i \tag{5.2}$$

where the velocity effectiveness matrix, E_v, is given by:

$$E_v = [\, I + (Z_e + Z_s)^{-1} Z_e Z_i^{-1} Z_s \,] \tag{5.3}$$

and where v_s^h is the vector of structure velocities for the unisolated system at the mounting points to the structure, v_s^i is the vector of the structure velocities for the isolated system at the same mounting points, and Z_e, Z_s, and Z_i are the impedance matrices of the engine (rigid body), structure and isolators respectively. For the force effectiveness, this is done by defining a matrix, E_f, given by:

$$f^h = E_f f^i \tag{5.4}$$

where the force effectiveness matrix, E_f, is given by:

$$E_f = [\, I + Z_s (Z_e + Z_s)^{-1} Z_e Z_i^{-1} \,] \tag{5.5}$$

where f^h is the vector of the forces transmitted to the structure at the attachment points, f^i is the vector of the forces applied by the engine to the isolators in the isolated system, and Z_e, Z_s, and Z_i are as defined previously. The matrix equivalent of the scalar magnitude, the matrix norm, is used to extend the scalar notion of effectiveness previously developed to systems with multiple parallel isolators. Instead of

maximizing a scalar quantity as is done for a single degree of freedom system, the spectral norm of the velocity or force effectiveness matrix is used. Here the maximum and minimum singular values of the velocity effectiveness matrix or the force effectiveness matrix provide a frequency dependent measure of isolator performance.

5.6.3 Transmitted Power

Another metric for vibration isolation systems is that of power transmission, or power flow (Pinnington, 1987; Qu and Qian, 1991). In the article by Pinnington (1987), the expression for the time averaged power transmission due to a harmonic input is written for multiple input, multiple isolator system. This expression is given by:

$$\omega P = \frac{1}{2} Im([F^*]^T [A] [F]) \tag{5.6}$$

where $[F]$ is the vector of applied forces, $[A]$ is the accelerance matrix, and ω is the frequency of the applied force. The superscript T denotes the transpose and the superscript * denotes the complex conjugate. Further qualification of this expression is presented for broad band application where spectral densities are used. Correlation between the analytical method and an experimental system is presented in the cited work.

All of the metrics presented up to this point make the assumption that the system under investigation is linear. No provision is made in any of the metrics for nonlinear system response.

Moreover, except for the expanded isolation effectiveness approach utilized by Swanson, et. al. (1994), the effectiveness and transmissibility metrics assume that the chosen system response variable (force, velocity, displacement, etc.) is rectilinear in nature.

Application of these metrics to general rigid body vibration isolation problems would be inappropriate, because the system response is typically not rectilinear.

Finally, it is important to note that for the transmissibility and effectiveness metrics as applied, it is assumed that the disturbance and the response are collinear. Thus, a single isolator does not isolate in more than one direction. As such, with the use of these metrics, the vectorial aspects of the response are neglected and the actual effectiveness of the isolation system cannot be captured. Moreover, small changes in the harmonic force acting on a rigid body on resilient supports can lead to pronounced changes in the system response. This situation can affect the direction of the reaction force at the point of connection between the isolator and the foundation. Therefore, the general response of the system must be investigated in order to completely capture the system response and isolation performance.

The next section presents the results of an investigation of the vibration isolation analysis of the planar three degree of freedom rigid body. The failure of three of the metrics as applied previously and described in this section to characterize the isolation performance of the system is described. An alternative vibration isolation metric applied to the problem is established and the reasons are stated.

5.7 VIBRATION ISOLATION MEASURES FOR THE RIGID BODY SYSTEM

The application of the three metrics as presented in Section 5.6 do not fully characterize the isolation performance of the planar three

degree of freedom rigid body system. Each of these metrics will be considered here relative to the planar three degree of freedom problem.

5.7.1 Transmissibility

The theory of transmissibility was derived with two assumptions. The first is that the system response acts collinear with the forcing term and the second is that the response of the system is linear. The second of these assumptions implies that the system response consists of a single frequency. For the three degree of freedom planar rigid body system considered here, neither of these assumptions is valid. As shown in the response plots earlier in this chapter, the response of the system can occur in degrees of freedom which are not directly forced and which are not collinear with the input forcing. The response of the system is also comprised of components at more than one frequency.

One of the conveniences of force transmissibility is that it utilizes the magnitude of the applied force as a normalizing quantity in establishing the metric. For the single degree of freedom case, this is convenient as this ratio has a magnitude of unity for the static case. This serves as a reference point against which the system performance can be measured. In a like manner, independent force transmissibilities for each of the degrees of freedom could be established for the case under investigation. However, this ratio becomes meaningless for the degrees of freedom which are not forced but have nonzero response, as a division by zero will result. This is true regardless of the frequency or amplitude of the forcing.

Velocity transmissibility is not applicable to this problem due to the assumption that the system investigated here is grounded. Therefore,

the velocity at the attachment of the spring to the support has zero velocity. This results in a division by zero, regardless of the forcing frequency. Therefore, both force transmissibility and velocity transmissibility fail to completely characterize the isolation performance of this planar system.

5.7.2 Effectiveness

The notion of effectiveness is derived using the assumptions that the system response is linear and collinear with the input forcing. Therefore, response in unforced degrees of freedom not collinear with the input and response at frequencies other than the forcing frequency will not be included in the system evaluation. Additionally, the notion of effectiveness as defined by Swanson, et. al., (1994) which expands the notion of effectiveness to multi-degree of freedom systems, makes the two assumptions that the isolators act in parallel and that the system response is linear. Therefore, although this system does allow for response in more than one degree of freedom, it is inadequate in characterizing the performance of the isolation system for the planar three degree of freedom system investigated in this thesis.

5.7.3 Power Transmission

The use of power transmission was developed under the assumption that the system response is linear. In the article by Pinnington (1987), the assumption is made that the frequency of the response and the input forcing to the system are identical. Therefore, although this system does account for response in more than one degree of freedom, it does not account for system response at more than one frequency.

5.7.4 Forces Transmitted to the Foundation

The use of forces transmitted to the foundation to characterize the isolation performance of a rigid body system has been applied previously (Spiekerman, et.al., 1985; Ashrafiuon, 1993; Swanson, et. al., 1993). In each of these applications, the assumption is made that the system response is linear. Therefore, these models do not contain the complete system response performance. The nonlinear phenomena of multi-frequency response and response in unforced degrees of freedom will not be included in the system response. Hence, the resulting forces are not accounted for correctly.

5.8 ISOLATION PERFORMANCE OF THE PLANAR THREE DEGREE OF FREEDOM SYSTEM

Assessment of the isolation performance of the system in case 4 is now developed. The metric chosen for application to this system is the transmitted forces. Two modifications are required to adapt this metric to account for the nonlinear response of the system. The first modification is to develop the capability to account for the presence of more than one frequency in the system response. In this case, the system response contains two frequencies, but is periodic. Therefore, the root-mean-square (rms) of the response is used to account for multiple frequencies.

The second modification to this metric is made to account for response in all degrees of freedom. This is done by using the forces developed in each of the springs in the system. These forces are due to the response of each of the three degrees of freedom and therefore will account for the total motion of the rigid body.

Using these two modifications, the force used in the metric can be computed. First, the x and y components of the forces for each of the springs (F_{1x} and F_{1y} for k_1, F_{2x} and F_{2y} for k_2, F_{3x} and F_{3y} for k_3, and F_{4x} and F_{4y} for k_4) are computed. The total force from each pair of springs on the foundation is due to the deflection of the pairs of springs k_1 and k_2, and k_3 and k_4, given by F_{12} and F_{34} respectively. The forces are given by:

$$F_{12}(t) = \sqrt{(F_{1x}+F_{2x})^2 + (F_{1y}+F_{2y})^2} \tag{5.7}$$

$$F_{34}(t) = \sqrt{(F_{3x}+F_{4x})^2 + (F_{3y}+F_{4y})^2} \tag{5.8}$$

These forces are a function of time. Therefore, the rms value of each of these forces over one period is computed and then they are summed. This is given by:

$$\bar{F} = (F_{12})_{rms} + (F_{34})_{rms} \tag{5.9}$$

It is this force $\bar{F}$ that is used to assess the isolation performance of the rigid body system.

Figure 5.17 shows a plot of the magnitude of the force given in equation (5.9) as a function of the detuning parameter σ_1 for case 4. This figure also contains the frequency response of the linear system. Here, the linear system response was computed using the same method after setting the coefficients of the nonlinear terms to zero.

From Figure 5.17, it can be seen that in the region between $\sigma_1 \approx \pm 125$, the force transmitted to the foundation for the nonlinear system, which can be either of two stable solutions, is reduced in comparison with the forces transmitted by the equivalent linear system. In particular, the large peak in the response for the linear system is

eliminated. This performance advantage is lost in the regions $228 > \sigma_1 > 125$ and $-125 > \sigma_1 > -228$, where the transmitted forces of the nonlinear system are greater than the forces of the corresponding linear system. For $\sigma_1 > 228$ and $\sigma_1 < -228$, the linear and nonlinear solutions are identical and no advantage is realized from the nonlinear system. In these regions, the transmitted forces are much lower than those associated with the linear resonance condition and are typically of less concern.

This analysis illustrates the need for proper system modelling. Modelling this system using linear theory leads to the incorrect system response which predicts that a large peak in the transmitted forces will result surrounding $\sigma_1 = 0$.

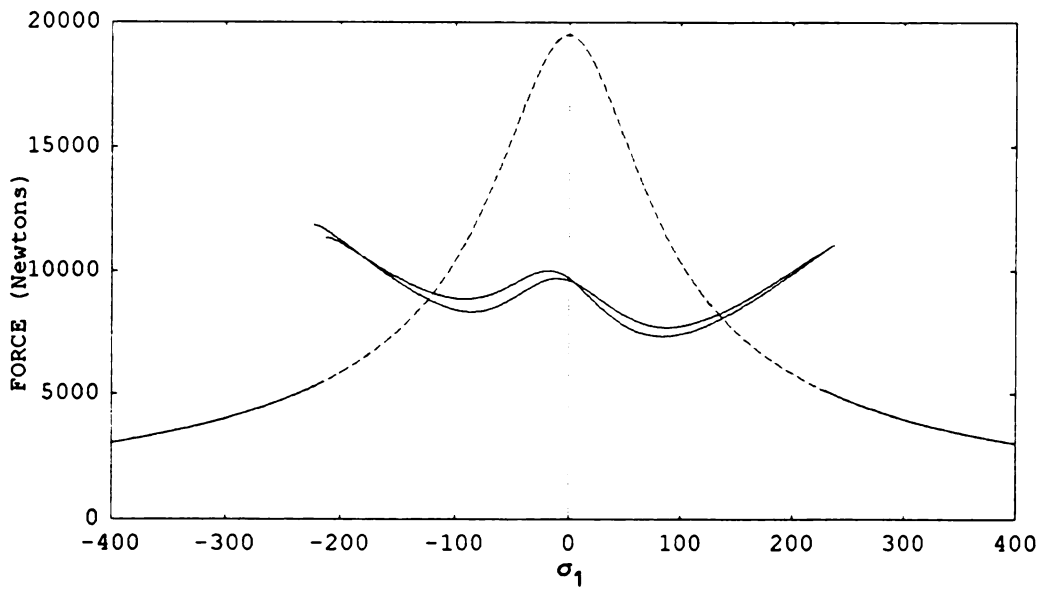

Figure 5.17 - Response plot of $\bar{F}$, the force transmitted to the foundation; —— stable solution, ---- linear solution

5.9 REMARKS

This chapter brings together the two major aspects of this investigation, that of the frequency response of a rigid body system and

the isolation performance of the same system. This chapter shows that for systems responding nonlinearly, caution must be used in assessing the isolation performance of the system. In particular, the metrics commonly used for this purpose do not adequately capture multiple frequency or multiple direction response. A modified version of the metric which monitors the forces transmitted to the base is proposed, and offers one alternative with improved effectiveness over the more commonly used measures. Using this metric, it is shown that the nonlinear response of the system can be used to eliminate the peak associated with the transmitted forces which occurs at resonance for linear systems.

The proposed metric will not likely satisfy the diverse requirements of all rigid body isolation systems. Indeed, the performance of an isolation system may require that system specific attributes be considered in formulating the measure of performance, similar to the process used in this investigation. This investigation delineates some of the difficulties which can accompany an investigation into vibration isolation of rigid bodies.

CHAPTER 6 SUMMARY AND CONCLUSIONS

This chapter first presents a summary of the major sections of this thesis. The subsequent section presents the conclusions arrived at in the investigation. Finally, recommendations for future work are offered.

6.1 SUMMARY

The thesis begins with a literature search into the topics of the harmonic response and vibration isolation of rigid bodies. This literature search establishes a foundation on which to pursue the investigation. The major topics included in the search are vibration isolation, harmonic response of multi-cylinder engines, the harmonic response of engine mounts, nonlinear vibration isolation systems, and the response of three dimensional rigid body systems.

Prior to introducing the rigid body system which is the focus of this thesis, a comprehensive review of the techniques used for isolation of automotive engines is presented. The techniques included in the review are center of percussion, natural frequency placement, torque axis, and elastic axes. This review is included to encompass the complete scope of the area of vibration isolation, particularly as it pertains to automotive engines. The following observations are made about each of these techniques.

The center of percussion technique is useful in the response of a rigid body on resilient supports to an impulsive load. This method does not address the harmonic response of the system.

Natural frequency placement, associated chiefly with optimization procedures, attempt to move the system natural frequencies away from forcing frequencies. This method is based on system response formulated from linear system theory. In light of the nonlinear response demonstrated by the system in this investigation, judgment must be used to ensure that the assumption of linear system response is valid prior to applying this technique.

The torque axis technique contends that a three dimensional rigid body under an applied torque not coincident with a principal axis will tend to oscillate about a spatial axis. Assessment of this system using the Euler equations of rigid body rotational motion as a guideline, indicates that this axis as applied in this technique does not exist.

Elastic axes theory asserts that an elastically supported rigid body responding to an applied force or torque along or about an elastic axis, will produce only a corresponding translation or rotation. It has been shown in previous work (Kim, 1991) that a physical set of axes which result in decoupled motion in all six degrees of freedom of a three dimensional rigid body does not exist. Furthermore, this notion is based on linear system theory and the response of the system demonstrated in this thesis indicates that the response a rigid body system on resilient supports can be nonlinear.

With this foundation established, the specific system investigated in this thesis is introduced. The system is planar, three degree of freedom rigid body supported by resilient elements which are attached to a rigid base. The system parameters of the rigid body used in the analysis were chosen to model the planar equivalent of an in-line four cylinder automotive engine. The equations of motion of the system are derived using

Lagrange's equations. A Taylor series expansion of the potential energy is used. The acceptance criteria which establishes the necessary number of terms required in the series was found to be important. It was found that acceptance of a Taylor series based only on a comparison between the approximate potential energy and the actual potential energy could fail to predict correct system dynamics. The acceptance criteria used in this investigation is the correlation between the predicted system response of the actual equations of motion and the equations of motion obtained using the Taylor series approximation.

Three cases of increasing complexity are investigated using the equations of motion previously derived for the rigid body system. These cases are distinguished by the type of forcing present. The forcing conditions utilized are: vertical forcing, torsional forcing, and combined vertical and torsional forcing. The method of multiple scales is used to produce the reduced equations which govern the envelopes of the response. These equations are then used to establish the steady state frequency response of the system. Repetitive solution of these equations for a varying frequency parameter is then used to establish the frequency response of the system for each of the three cases.

The frequency response of three cases investigated shows the nonlinear behavior of the system. In particular, a region was found in case 2 where a constant amplitude steady state does not exist. Cases 1 and 3 showed that a reduction in amplitude can be realized in the coordinate being forced over the linear response of the system. This reduction in amplitude is accomplished by excitation of the other modes.

Prior to the investigation of the isolation performance of the system, an overview of established isolation metrics relative to the

response characteristics of the three degree of freedom rigid body system investigated in this thesis is presented. The metrics assessed are transmissibility, isolation effectiveness, transmitted power, and forces transmitted to the foundation of the system. The assumptions made in the development of these metrics are discussed and the inability of these metrics to characterize the isolation performance of the three degree of freedom rigid body system investigated in this thesis is discussed. The metric of monitoring the forces transmitted to the base is modified to produce a measure of isolator performance which can account for nonlinear system behavior. These modifications account for multi-frequency and multi-directional system response. The application of this metric to the rigid body system shows that the resonance peak of the transmitted forces associated with the linear response of the system can be eliminated.

6.2 CONCLUSIONS

There are three conclusions resulting from this investigation. The first conclusion is the recognition that the response for a three degree of freedom rigid body can be nonlinear even if the assumption is made that the force-deflection characteristics of the supports are linear. Moreover, this nonlinear behavior does not require large response amplitudes.

The second conclusion of this investigation is that the traditional approaches to isolation performance using the measures of effectiveness, transmissibility, transmitted forces, and transmitted power, have shortcomings when applied to nonlinear systems. Specifically, these metrics do not account for the multi-frequency response of nonlinear systems. In addition, effectiveness and transmissibility, do not account for system response in coordinate directions different from the direction

of the input force. However, these two aspects of nonlinear system response have been incorporated into the metric of assessing the forces transmitted to the foundation. This alternative metric has been applied to the rigid body system.

The third conclusion is that the standard analytical methods used to determine automotive engine mount placement and orientation, i.e., natural frequency placement, torque axis, and elastic axes, may be ineffective when considering the general motion of the engine on it mounts. This ineffectiveness is due to the fact that these methods do not account for nonlinear system behavior.

6.3 RECOMMENDATIONS

Two groups of recommendations are proposed. The first two recommendations expand the analysis contained herein without requiring changes in the scope of the problem. Specifically:

i. The present analysis does not investigate the influence of the mistuning of the natural frequencies of the system. An analysis of this type will provide insight into the practical application of this theory where exact tuning of the system linear natural frequencies typically does not occur.

ii. This analysis does not investigate the affect of the variation of the underlying geometry of the system. Studies of the influence of the physical parameters on the response of the system will lead to broader understanding of the system response. This in turn can lead to optimization of the isolation performance of the system.

The second group of recommendations would result in an increase in the scope and complexity of the investigation. Four recommendations are made. They are:

i. The analysis should be expanded to analyze a three dimensional rigid body system. This system would have six degrees of freedom instead of the three degrees of freedom investigated in this thesis. This analysis should allow for arbitrary number, location, and orientation of the resilient supports. This would be a significant step toward the application of this analysis to an automotive engine.

ii. The three degree of freedom system should be investigated experimentally and the results of the analysis presented in this thesis should be correlated to the experimental results. Successful correlation would be the first step in establishing this analysis as a useful tool for the study of rigid body isolation systems.

iii. This investigation looks only at forces acting on the rigid body. Expansion of the analysis to include base excitation would have practical significance. The combination of forcing applied to the rigid body and from the base would facilitate the analysis of an engine on mounts where the engine is subjected to both road forces and forces due to engine unbalance.

iv. It is assumed in this investigation that the base to which the resilient supports are attached is rigid. This may be a reasonable assumption for some rigid body systems. However, for other systems, automotive engines in particular, this

assumption is not valid. Therefore, this analysis should be expanded to incorporate a non-rigid base.

APPENDICES

APPENDIX A

APPENDIX A

CENTER OF PERCUSSION[4]

Consider a rigid body in a horizontal plane, fixed at one point, and moving under applied loads as shown in Figure A.1(a). This system is referred to as a compound pendulum (Greenwood, 1988). The free body diagram for this rigid body is shown in Figure A.1(b) which includes the reaction force at O and applied loads. The external force system can be replaced by the resultants $m\mathbf{a}$ and $I\alpha$. The vector quantity $\mathbf{ma}$ can be broken down into its components $r\omega^2$ and $r\alpha$ which act through the center of mass in the normal and tangential directions, respectively, as shown in Figure A.1(c). Another resultant force diagram can be obtained by moving the force $mr\alpha$ to point Q along the line OG (actually beyond point G) such that the resulting moment created about O equals $I_G\alpha$. $I_G\alpha$ can then be removed from the resultant force diagram as shown in Figure A.1(d).

This condition can be written as:

$$I_G\alpha + mr^2\alpha = mr\alpha\ell \tag{A.1}$$

Replacing I_G by $k_G^2 m$ where k_G is the radius of gyration of the rigid body about G:

$$k_G^2 m\alpha + mr^2\alpha = mr\alpha\ell \tag{A.2}$$

which results in

---

[4]The topic of the center of percussion is covered in various forms in many books on dynamics and vibrations. The material presented here most closely follows that presented in Meriam (1978) and Greenwood (1988).

$$k_G^2 + r^2 = r\ell \tag{A.3}$$

Solving this for ℓ:

$$\ell = \frac{k_G^2 + r^2}{r} = \frac{k_O^2}{r} \tag{A.4}$$

where k_O is the radius of gyration of the rigid body about O. The point Q defined by this procedure is called the center of percussion of a body of fixed point O. Note that $\Sigma M_O = 0$.

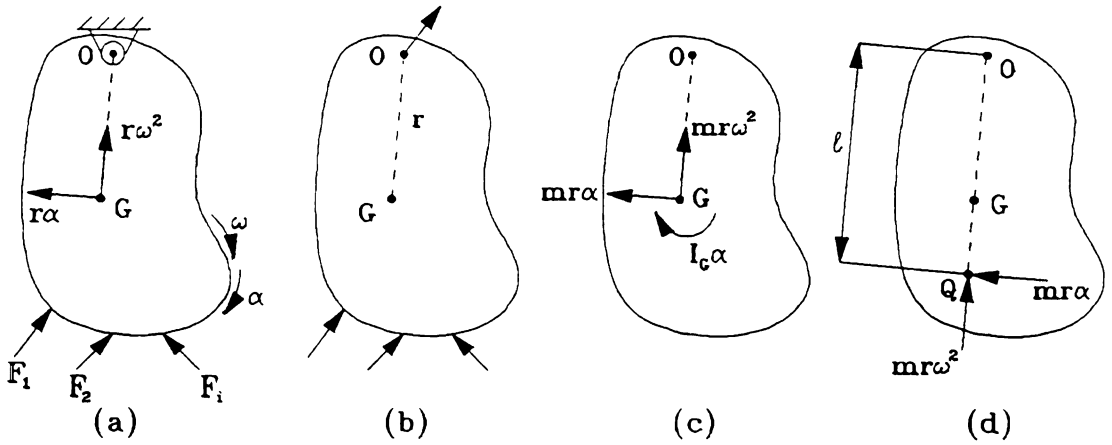

Figure A.1

The center of percussion has two interesting properties as shown by the following analysis. The first property involves the response of the rigid body to an impulsive load and the second shows a property about the natural frequency of a compound pendulum.

Consider the same compound pendulum as shown in Figure A.1(a), initially at rest, impacted by an impulse $\hat{F} \perp OG$, as shown in Figure A.2. Since by definition, the impulse is equal to the change in momentum:

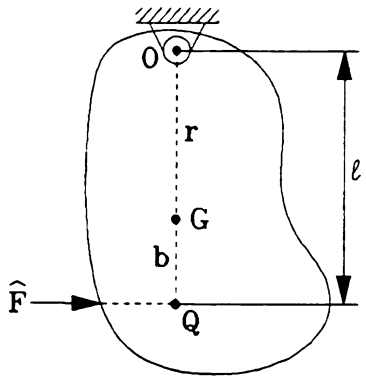

Figure A.2

$$\hat{F} = p_2 - p_1 = m(v_{G_2} - v_{G_1}) \tag{A.5}$$

Since $v_{G_1} = 0$, let $v_{G_2} = v_G = \frac{\hat{F}}{m} = r\theta$ where θ is the angular velocity of the line OG. By definition, the angular impulse of $\hat{F}$ about G, $\hat{M}$, is:

$$\hat{M} = b\hat{F} \tag{A.6}$$

Also,

$$\hat{M} = H_2 - H_1 = I_G\theta \tag{A.7}$$

Using the two previous results along with the fact that $H_1 = 0$ and $H_2 = H_G = I_G\theta$, θ can be solved for:

$$\theta = \frac{b\hat{F}}{I_G} \tag{A.8}$$

Using this relationship and that $\frac{\hat{F}}{m} = r\theta$ it can be shown that $\frac{I_G}{m} = k_G^2 = rb$.

With $b = \ell - r$, the same relationship for the location of Q is obtained as before:

$$\ell = \frac{r^2 + k_G^2}{r} \tag{A.9}$$

This demonstrates that no impulsive reaction occurs at the point O for the applied impulse $\hat{F}$. Note that an impulsive reaction at O will occur if $\hat{F}$ is applied in any direction other than perpendicular to OC.

Now consider the natural frequency for small motion of the compound pendulum:

$$\omega_h = \sqrt{\frac{mgr}{I_O}} \tag{A.10}$$

Consider the natural frequencies of the compound pendulum for motion about points O and Q. Using the previous result, the following relationships are obtained:

$$\begin{aligned} (\omega_h)_O &= \sqrt{\frac{mgr}{I_O}} \\ (\omega_h)_Q &= \sqrt{\frac{mgb}{I_Q}} \end{aligned} \tag{A.11}$$

Using the fact that $I_O = k_G^2 + r^2$, $I_Q = k_G^2 + b^2$, and that $k_G^2 = rb$, it can be shown that $(\omega_h)_O = (\omega_h)_Q$. This relationship illustrates the second property of the center of percussion which is that point O is the center of percussion for the body when Q is the center of oscillation and vice versa. Points O and Q are then referred to as reciprocal centers of percussion.

APPENDIX B

APPENDIX B

DERIVATION OF THE POTENTIAL ENERGY OF THE RIGID BODY SYSTEM

The general formulation of the equations of motion for this system, shown in Figure B.1, requires that the potential energy for the system be written in terms of the rigid body displacements (x,y,α). For this formulation, no assumptions are made regarding small motions and the full, general motion of the system is considered. To this end, each of the four springs in the system is analyzed separately.

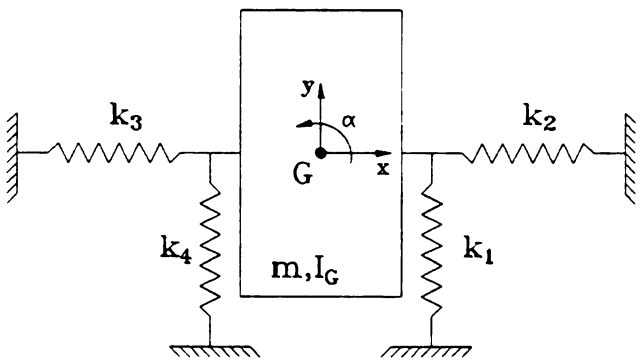

Figure B.1
Geometry of the rigid body system

To simplify the geometry of the analysis, Figures B.2 and B.3 do not explicitly show the spring element. The lengths and displacements are shown using only lines. It is the change in length of each of the springs which is required. The center of mass of the rigid body, G, is shown, but the outside dimensions of the rigid body are not shown. The distance between the center of mass and the attachment point of the springs, denoted A, is indicated in both figures as the radius of a circle.

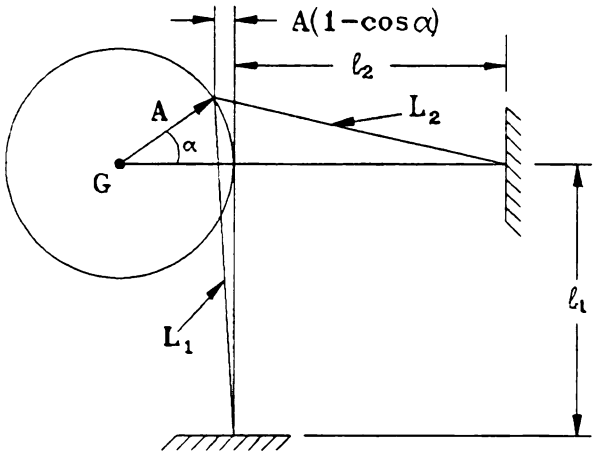

Figure B.2
Geometry associated with springs k_1 and k_2

Consider the geometry associated with springs k_1 and k_2 with free lengths ℓ_1 and ℓ_2 respectively, as shown in Figure B.2. Using the dimensions indicated, the expressions for the new lengths of spring k_1 and spring k_2, denoted L_1 and L_2, respectively, can be written:

$$L_1 = \sqrt{[\ell_1 + A\sin\alpha + y]^2 + [A(1-\cos\alpha) - x]^2} \tag{B.1}$$

$$L_2 = \sqrt{[\ell_2 + A(1-\cos\alpha) - x]^2 + [A\sin\alpha + y]^2} \tag{B.2}$$

Consider the geometry associated with springs k_3 and k_4 with free lengths ℓ_3 and ℓ_4 respectively, as shown in Figure B.3. Using the dimensions indicated, the expressions for the new lengths of spring k_3 and spring k_4, denoted L_3 and L_4, respectively, can be written:

$$L_3 = \sqrt{[\ell_3 + A(1-\cos\alpha) + x]^2 + [A\sin\alpha - y]^2} \tag{B.3}$$

$$L_4 = \sqrt{[\ell_4 - A\sin\alpha + y]^2 + [A(1-\cos\alpha) + x]^2} \tag{B.4}$$

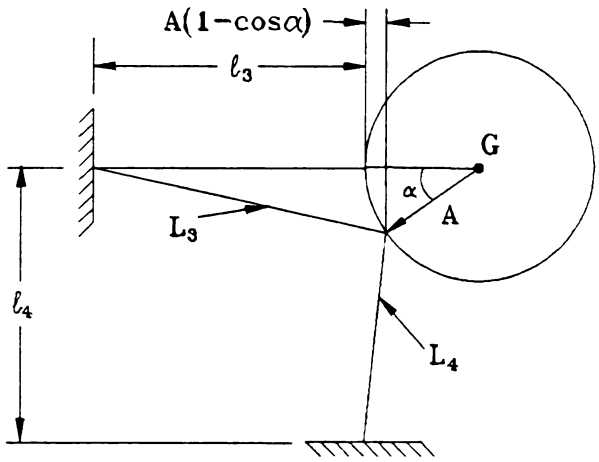

Figure B.3
Geometry associated with springs k_3 and k_4

The expression for the potential energy of the system, V can now be written:

$$V = \frac{1}{2}k_1(L_1-\ell_1)^2 + \frac{1}{2}k_2(L_2-\ell_2)^2 + \frac{1}{2}k_3(L_3-\ell_3)^2 + \frac{1}{2}k_4(L_4-\ell_4)^2 \qquad (B.5)$$

where all of the parameters have been defined previously.

APPENDIX C

APPENDIX C

MATHEMATICA PROGRAM USED FOR DERIVING THE EQUATIONS OF MOTION

The following is the source code used in the Mathematica (Wolfram, S., 1991) program to derive the equations of motion for the systems investigated in this thesis. The notation used below is consistent with that shown in the figures of Chapter 2 and Appendix B.

```
Ig = 14.155;
m = 219.4;
k1 = 1732312.8;
k2 = 433078.2;
k3 = 433078.2;
k4 = 1732312.8;
x0 = 0.0;
y0 = 0.0;
alpha0 = 0.0;
l1 = 0.102;
l2 = 0.102;
l3 = 0.102;
l4 = 0.102;
A = 0.127;

T = (1/2)*m*xdot^2 + (1/2)*m*ydot^2 + (1/2)*Ig*alphadot^2;

L1 = Sqrt[(l1 + A*(Sin[alpha]) + y)^2 +
          (x - A*(1 - Cos[alpha]))^2];
L2 = Sqrt[(l2 - (x - A*(1 - Cos[alpha])))^2 +
          (A*(Sin[alpha]) + y)^2];
L3 = Sqrt[(l3 + A*(1 - Cos[alpha]) + x)^2 +
          (y - A*(Sin[alpha]))^2];
L4 = Sqrt[(l4 + y - A*(Sin[alpha]))^2 +
           (x + A*(1 - Cos[alpha]))^2];

Va1 = (1/2)*k1*(L1-l1)^2;
Va2 = (1/2)*k2*(L2-l2)^2;
Vb1 = (1/2)*k3*(L3-l3)^2;
Vb2 = (1/2)*k4*(L4-l4)^2;

V1 = Va1 + Va2 + Vb1 + Vb2;
```

```
(* Expand the potential energy in a Taylor Series
     about equilibrium point *)

E1 = D[V1,{x,2}] /. {x->x0,y->y0,alpha->alpha0};
E2 = D[V1,{y,2}] /. {x->x0,y->y0,alpha->alpha0};
E3 = D[V1,{alpha,2}] /. {x->x0,y->y0,alpha->alpha0};
E4 = D[V1,x,y] /. {x->x0,y->y0,alpha->alpha0};
E5 = D[V1,x,alpha] /. {x->x0,y->y0,alpha->alpha0};
E6 = D[V1,y,alpha] /. {x->x0,y->y0,alpha->alpha0};
E7 = D[V1,{x,3}] /. {x->x0,y->y0,alpha->alpha0};
E8 = D[V1,{y,3}] /. {x->x0,y->y0,alpha->alpha0};
E9 = D[V1,{alpha,3}] /. {x->x0,y->y0,alpha->alpha0};
E10 = D[V1,x,x,y] /. {x->x0,y->y0,alpha->alpha0};
E11 = D[V1,x,x,alpha] /. {x->x0,y->y0,alpha->alpha0};
E12 = D[V1,x,y,y] /. {x->x0,y->y0,alpha->alpha0};
E13 = D[V1,alpha,y,y] /. {x->x0,y->y0,alpha->alpha0};
E14 = D[V1,x,alpha,alpha] /. {x->x0,y->y0,alpha->alpha0};
E15 = D[V1,y,alpha,alpha] /. {x->x0,y->y0,alpha->alpha0};
E16 = D[V1,x,y,alpha] /. {x->x0,y->y0,alpha->alpha0};
E17 = D[V1,{x,4}] /. {x->x0,y->y0,alpha->alpha0};
E18 = D[V1,{y,4}] /. {x->x0,y->y0,alpha->alpha0};
E19 = D[V1,{alpha,4}] /. {x->x0,y->y0,alpha->alpha0};
E20 = D[V1,x,x,x,y] /. {x->x0,y->y0,alpha->alpha0};
E21 = D[V1,x,x,x,alpha] /. {x->x0,y->y0,alpha->alpha0};
E22 = D[V1,x,y,y,y] /. {x->x0,y->y0,alpha->alpha0};
E23 = D[V1,y,y,y,alpha] /. {x->x0,y->y0,alpha->alpha0};
E24 = D[V1,alpha,alpha,alpha,x] /. {x->x0,y->y0,alpha->alpha0};
E25 = D[V1,alpha,alpha,alpha,y] /. {x->x0,y->y0,alpha->alpha0};
E26 = D[V1,x,x,y,y] /. {x->x0,y->y0,alpha->alpha0};
E27 = D[V1,x,x,alpha,alpha] /. {x->x0,y->y0,alpha->alpha0};
E28 = D[V1,y,y,alpha,alpha] /. {x->x0,y->y0,alpha->alpha0};
E29 = D[V1,x,x,y,alpha] /. {x->x0,y->y0,alpha->alpha0};
E30 = D[V1,x,y,y,alpha] /. {x->x0,y->y0,alpha->alpha0};
E31 = D[V1,x,y,alpha,alpha] /. {x->x0,y->y0,alpha->alpha0};

V = ((1/2)*(E1*x^2 + E2*y^2 + E3*alpha^2 + 2*E4*x*y + 2*E5*x*alpha +
  2*E6*y*alpha) +

  (1/6)*(E7*x^3 + E8*y^3 + E9*alpha^3 + 3*E10*x^2*y +
  3*E11*x^2*alpha + 3*E12*x*y^2 + 3*E13*y^2*alpha +3*E14*x*alpha^2 +
  3*E15*y*alpha^2 + 6*E16*x*y*alpha) +

  (1/24)*(E17*x^4 + E18*y^4 + E19*alpha^4 + 4*E20*x^3*y +
  4*E21*x^3*alpha + 4*E22*y^3*x + 4*E23*y^3*alpha + 4*E24*alpha^3*x +
  4*E25*alpha^3*y + 6*E26*x^2*y^2 + 6*E27*x^2*alpha^2 +
  6*E28*y^2*alpha^2 + 12*E29*x^2*y*alpha +
  12*E30*x*y^2*alpha + 12*E31*x*y*alpha^2));

PTx = D[D[T,xdot],t,NonConstants -> {xdot,ydot,alphadot,x,y,alpha}];
PTy = D[D[T,ydot],t,NonConstants -> {xdot,ydot,alphadot,x,y,alpha}];
PTalpha = D[D[T,alphadot],t,NonConstants ->
                        {xdot,ydot,alphadot,x,y,alpha}];
```

```
PVx = D[V,x];
PVy = D[V,y];
PValpha = D[V,alpha];

EQ1 = PTx + PVx;
EQ2 = PTy + PVy;
EQ3 = PTalpha + PValpha;

Print ["EQ1 = ", EQ1];
Print ["EQ2 = ", EQ2];
Print ["EQ3 = ", EQ3];
```

APPENDIX D

APPENDIX D

NONDIMENSIONALIZATION OF THE EQUATIONS OF MOTION[5]

The equations of motion of the system presented previously are the starting point for the nondimensionalization. These equations are listed again for convenience.

$$m\ddot{X}_1 + c_1\dot{X}_1 + (k_2+k_3)X_1 + \beta_1X_2X_3 + \beta_2X_1X_3 + \beta_3X_2^3 + \beta_4X_1X_2^2 + \beta_5X_1^3 + \beta_6X_1X_3^2 = F_1\cos\Omega t \tag{D.1a}$$

$$\frac{1}{3}m(A^2+B^2)\ddot{X}_2 + c_2\dot{X}_2 + A^2(k_1+k_4)X_2 + \beta_7X_1X_3 + \beta_8X_2^3 + \beta_9X_1X_2^2 + \beta_{10}X_1^2X_2 + \beta_{11}X_2X_3^2 = F_2\cos\Omega_2 t \tag{D.1b}$$

$$m\ddot{X}_3 + c_3\dot{X}_3 + (k_1+k_4)X_3 + \beta_{12}X_1^2 + \beta_{13}X_1X_2 + \beta_{14}X_2^2X_3 + \beta_{15}X_1^2X_3 + \beta_{16}X_3^2 = F_3\cos\Omega_3 t \tag{D.1c}$$

The first step in the nondimensionalization process is to designate the characteristic length, mass, and time. The characteristic mass is the mass of the rigid body m, and A is chosen as the characteristic length. Both of these dimensions are sound choices since if either of these were equal to zero, the problem would not make physical sense. The choice for a characteristic time is not as obvious. Three possible candidates are: $\sqrt{\frac{m}{k_1+k_4}}$, $\sqrt{\frac{m}{k_2+k_3}}$, or $\sqrt{\frac{m}{\beta_i A}}$. (To find these, terms which include time,

---

[5]The method used here to nondimensionalize the equations of motion is presented in Murdock (1991).

such as k_1, k_2, k_3, k_4 and any of the β_i's should be determined. Mass and length can be eliminated from these by multiplying or dividing by the already designated characteristic mass and length.) The third candidate is not a naturally appearing expression in the problem as are the first two expressions, therefore it can be eliminated. Either of the first two expressions will be a suitable characteristic time, therefore the characteristic time for this set of equations is chosen to be $\sqrt{\frac{m}{k_2+k_3}}$.

Having made these choices, the coordinates and parameters of the problem can be nondimensionalized by multiplying and dividing by these quantities raised to appropriate powers. The following are obtained:

$$x_1 := X_1/A$$

$x_2 := X_2$ has units of radians which are already dimensionless

$$x_3 := X_3/A$$

$$\omega_1^2 := (k_2+k_3)\cdot\frac{m}{k_2+k_3}\cdot\frac{1}{m} = 1$$

$$k' := A^2(k_1+k_4)\cdot\frac{m}{k_2+k_3}\cdot\frac{1}{m}\cdot\frac{1}{A^2} = \frac{k_1+k_4}{k_2+k_3}$$

$$\omega_3^2 := (k_1+k_4)\cdot\frac{m}{k_2+k_3}\cdot\frac{1}{m} = \frac{k_1+k_4}{k_2+k_3}$$

$$m' := \frac{m}{m} = 1$$

(Mass does not appear explicitly in the nondimensionalized equations.)

$$I_G := \frac{1}{3} m (A_2 + B^2) \cdot \frac{1}{m} \cdot \frac{1}{A^2} = \frac{1}{3} \left(1 + \frac{B^2}{A^2}\right) = \frac{1}{3} (1 + \nu^2) \quad (\text{where } \nu = \frac{B}{A})$$

$$t := T \cdot \sqrt{\frac{k_2 + k_3}{m}}$$

$$\hat{f}_i := F_i \cdot \frac{1}{m} \cdot \frac{1}{A} \cdot \frac{m}{k_2 + k_3}$$

$$c_1 \left[\frac{kg}{s}\right] \rightarrow 2\hat{\mu}_1 := c_1 \cdot \frac{1}{m} \cdot \sqrt{\frac{m}{k_2 + k_3}}$$

$$c_2 \left[\frac{kg \cdot m^2}{s}\right] \rightarrow 2\hat{\mu}_2 := c_2 \cdot \frac{1}{m} \cdot \sqrt{\frac{m}{k_2 + k_3}} \cdot \frac{1}{A^2}$$

$$c_3 \left[\frac{kg}{s}\right] \rightarrow 2\hat{\mu}_3 := c_3 \cdot \frac{1}{m} \cdot \sqrt{\frac{m}{k_2 + k_3}}$$

The nondimensionalization of the coefficients of the nonlinear terms, the β_i's, can be accomplished in a manner similar to that of the c_i's shown above. This can be accomplished by determining the units of each individual term required to keep the units of the equations consistent. The nondimensionalized version of these values are shown as $\hat{\alpha}_i$'s in the nondimensionalized form of the equations. The nondimensionalized form of the equations is:

$$\ddot{x}_1 + 2\hat{\mu}_1 \dot{x}_1 + \omega_1^2 x_1 + \hat{\alpha}_1 x_2 x_3 + \hat{\alpha}_2 x_1 x_3 + \hat{\alpha}_3 x_2^3 + \hat{\alpha}_4 x_1 x_2^2 + \hat{\alpha}_5 x_1^3 + \hat{\alpha}_6 x_1 x_3^2 = \hat{f}_1 \cos\Omega_1 t \qquad \text{(D.2a)}$$

$$\frac{1}{3}(1 + \nu^2)\ddot{x}_2 + 2\hat{\mu}_2 \dot{x}_2 + k' x_2 + \hat{\alpha}_7 x_1 x_3 + \hat{\alpha}_8 x_2^3 + \hat{\alpha}_9 x_1 x_2^2 + \hat{\alpha}_{10} x_1^2 x_2 + \hat{\alpha}_{11} x_2 x_3^2 = \hat{f}_2 \cos\Omega_2 t \qquad \text{(D.2b)}$$

$$\ddot{x}_3 + 2\hat{\mu}_3\dot{x}_3 + \omega_3^2 x_3 + \hat{\alpha}_{12}x_1^2 + \hat{\alpha}_{13}x_1x_2 + \hat{\alpha}_{14}x_2^2x_3 + \hat{\alpha}_{15}x_1^2x_3 + \hat{\alpha}_{16}x_3^3 = \hat{f}_3\cos\Omega_3 t \qquad \text{(D.2c)}$$

LIST OF REFERENCES

LIST OF REFERENCES

Andrews, G. J., (1960). Vibration Isolation of a Rigid Body on Resilient Supports. *The Journal of the Acoustical Society of America*, v 32, n 8: 995-1001.

Ashrafiuon, H., (1993). Design Optimization of Aircraft Engine-Mount Systems. *Journal of Vibrations and Acoustics*, v 115: 463-467.

Bachrach, Ben I., (1995). Personal communication at the Ford Motor Company, April 25, 1995.

Bernard, James E. and Starkey, John M., (1983). Engine Mount Optimization. SAE Paper 830257, Warrendale , PA.

Bolton-Knight, B. L., (1971). Engine Mounts: Analytical Methods to Reduce Noise and Vibration. *Instn. Mech. Engrs.*, C98/71.

Brach, R. Matthew and Haddow, A. G., (1993). On the Dynamic Response of Hydraulic Engine Mounts. SAE Paper 931321, SAE, Warrendale, PA.

Butsuen, T., Ookuma, M., and Nagamatsu, A., (1986). Application of Direct System Identification Method for Engine Rigid Body Mount System, SAE Paper 860551, SAE, Warrendale, PA.

Crede, Charles E., (1951). *Vibration and Shock Isolation*. John Wiley & Sons, New York, New York.

Den Hartog, J. P., (1984). *Mechanical Vibrations*, Dover Publications, Inc., New York.

Derby, Thomas F., (1973). Decoupling the Three Translational Modes from the Three Rotational Modes of a Rigid Body Supported by Four Corner-located Isolators. *Shock and Vibration Bulletin*, Bulletin 43, Part 4: 91-108.

Ewins, D. J., (1986). *Modal Testing: Theory and Practice*. Research Studies Press, Ltd., Letchworth, Hertfordshire, England.

Efstathiades, G. J. and Williams, C. J. H., (1967). Vibration Isolation Using Nonlinear Springs. *J. Mech. Sci.*, Pergamon Press, Ltd., v 9: 27-44.

Ford, D. M., (1985). An Analysis and Application of a Decoupled Engine Mount System for Idle Isolation. SAE Paper 850976, SAE, Warrendale, PA.

Fullerton, Raymond R., editor, (1984). *Front Wheel Powertrain Mounts: Design Guide*. Ford Motor Company.

Furubayashi, M., Soma, N., Nakada, T., and Iwahara, M., (1991). Estimation of the Engine Exciting Force and the Rigid Body Vibration Mode of the Powerplant, 1991 Small Engine Technology Conference Proceedings, Published by Society of Automotive Engineers of Japan, Tokyo, Japan,

Geck, Paul E. and Patton, R. D., (1984). Front Wheel Engine Mount Optimization. SAE Paper 840736, Warrendale, PA.

Gennesseoux, A., (1993). Research for New Vibration Isolation Techniques: From Hydro-Mounts to Active Mounts. SAE Paper 931324, SAE, Warrendale, PA.

Greenwood, D. T., (1988). *Principles of Dynamics*. Prentice-Hall, Englewood Cliffs, New Jersey.

Grootenhuis, P. and Ewins, D. J., (1965). Vibration of a Spring Supported Body. *Journal Mechanical Engineering Science*, v 7, n 2: 185-192.

Haddow, A. G., Barr, A. D. S., and Mook, D. T., (1984). Theoretical and Experimental Study of Modal Interaction in a Two-degree-of-freedom Structure. *J. of Sound and Vibration*, v 97, n 3: 451-473.

Hata, Hideyuki, (1992). Body Vibration Analysis Using a System Model Approach. JSAE, v 46, n 6.

Henry, R. F. and Tobias, S. A., (1959). Instability and Steady-state Coupled Motions in Vibration Isolating Suspensions. *Journal Mechanical Engineering Science*, v 1, n 1: 19-29.

Hildebrand, F. B., (1976). *Advanced Calculus for Applications*. Prentice-Hall, Englewood Cliffs, New Jersey.

Himelblau, H. Jr. and Rubin, S., (1961). Vibration of a Resiliently Supported Rigid Body. Shock and Vibration Handbook, Harris and Crede Editors, Volume 1, Chapter 3, McGraw-Hill, New York, New York.

International Mathematics and Statistical Library, Inc., (1980). Reference Manual. Houston, Texas.

John, R. A. and Straneva, E. J., (1966). A New Generation of General Aircraft Engine Mountings, SAE Paper 660222, SAE, Warrendale, PA.

Johnson, Stephen R. and Subhedar, Jay W., (1979). Computer Optimization of Engine Mount Systems. SAE Paper 790974, SAE, Warrendale, PA.

Kahn, P. B., (1990). *Mathematical Methods for Scientists and Engineers*. Wiley-Interscience, John Wiley & Sons, New York, New York.

Kim, B. J., (1991). *Three Dimensional Vibration Isolation Using Elastic Axes*. M. S. Thesis, Michigan State University, East Lansing, MI.

Kim, G. and Singh, R., (1993). Nonlinear Analysis of Automotive Hydraulic Engine Mount. *Journal of Dynamic Systems, Measurements, and Control*, v 115: 482-487.

Lee, J. M., Yim, H. J., and Kim, J., (1995). Flexible Chassis Effects on Dynamic Response of Engine Mount Systems. SAE Paper 951094, SAE, Warrendale, PA.

Matsuda, A., Hayashi, Y., and Hasegawa, J., (1987). Vibration Analysis of a Diesel Engine at Cranking and Idling Modes and Its Mounting System. SAE Paper 870964, SAE, Warrendale, PA.

Meirovitch, L., (1975). *Elements of Vibration Analysis*. McGraw-Hill, New York, New York.

Meriam, J. L., (1978). *Engineering Mechanics, Volume 2, Dynamics*. John Wiley & Sons, New York, New York.

Metwalli, S. M., (1986). Optimum Nonlinear Suspension Systems. *Journal of Mechanisms, Transmissions, and Automation in Design*, v 108, June 1986: 197-202.

Murdock, J. A., (1991). *Perturbations: Theory and Methods*. John Wiley & Sons, New York, New York.

Nayfeh, A. H. and Balachandran, B., (1989). Modal Interactions in Dynamical and Structural Systems. *Appl. Mech. Rev.*, v 42, n 11, Part 2: 175-201.

Nayfeh, A. H. and Mook, D. T., (1979). *Nonlinear Oscillations*. Wiley-Interscience, John Wiley & Sons, New York, New York.

Oh, T., Lim, J. and Lee, S. C., (1991). Engineering Practice in Optimal Design of Powertrain Mounting System for 2.0ℓ FF Engine. Proceedings for the Sixth International Pacific Conference on Automotive Engineering, Published by Korea Society of Automotive Engineers, Inc., 1638-3, Socho-dong, Seoul, South Korea: 607-616.

Perkins, N. C., (1992). Modal Interactions in the Non-linear Response of Elastic Cables Under Parametric/External Excitation. International Journal of Non-Linear Mechanics, v 27, n 2: 233-250.

Pinnington, R. J., (1987). Vibrational Power Transmission to a Seating of a Vibration Isolated Motor. *Journal of Sound and Vibration*, v 118, n 3: 515-530.

Qu, J. and Qian, B., (1991). On the Vibrational Power Flow from Engine to Elastic Structure through Single and Double Resilient Mounting Systems. SAE Paper 911057, SAE, Warrendale, PA.

Radcliffe, C. J., Picklemann, and Spiekerman, C. E., (1983). Simulation of Engine Idle Shake Vibration, SAE Paper 8302259, SAE, Warrendale, PA.

Rao, S. S., (1986). *Mechanical Vibrations*. Addison-Wesley, Reading, MA.

Rubin, S. and Biehl, F. A., (1967). Mechanical Impedance Approach to Engine Vibration Transmission Into an Aircraft Fuselage, SAE Paper 670873, SAE, Warrendale, PA.

Saitoh, S. and Igarashi, M., (1989). Optimization Study of Engine Mounting Systems, 1989 ASME 12th Biennial Conference on Mechanical Vibration and Noise, Montreal, Quebec, Canada, September 17-21.

Sakamoto, H., Yazaki, K., and Fukushima, M., (1981). Reduction of Automobile Booming Noise Using Engine Mountings That Have an Auxiliary Vibrating System, SAE Paper 810399, SAE, Warrendale, PA.

Schmitt, Regis, V. and Leingang, Charles, J., (1976). Design of Elastomeric Vibration Isolation Mounting Systems for Internal Combustion Engines, SAE Paper 760431, SAE, Warrendale, PA.

Shiomi, Kazuyuki and Mizuguchi, Hiroshi, (1991). Isolating Vibration through Use of Traveling Center of Engine Oscillation, 1991 Small Engine Technology Conference Proceedings, Published by Society of Automotive Engineers of Japan, Tokyo, Japan: 573-582.

Shoup, T. E., (1971). Shock and Vibration Isolation Using a Nonlinear Elastic Suspension. *AIAA Journal*, v 9, n 8: 1643-1645.

Shoup, T. E., (1972). Experimental Investigation of a Nonlinear Elastic Suspension, *AIAA Journal*, v 10, n 4: 559-560.

Shoup, T. E. and Simmonds, G. E., (1977). An Adjustable Spring Rate Suspension System, *AIAA Journal*, v 15, n 6: 865-866.

Singh, R., Kim, G. and Ravindra, P. V., (1992). Linear Analysis of Automotive Hydro-Mechanical Mount with Emphasis on Decoupler Characteristics. *Journal of Sound and Vibration*, v 158, n 2: 219-243.

Snowdon, John C., (1979). Vibration Isolation: Use and Characterization. *Journal of the Acoustical Society of America*, v 66, n 5: 1245-1274.

Spiekerman, C. E., Radcliffe, C. J., and Goodman, E. D., (1985). Optimal Design and Simulation of Vibration Isolation Systems. *Journal of Mechanisms, Transmission and Automation in Design*, v 107: 271-276.

Staat, L. A., (1986). Optimal Design of Vibration Isolators Based on Frequency Response. M. S. Thesis, Michigan State University, East Lansing, MI.

Swanson, D. A., Wu, H. T., and Ashrafiuon, H., (1993). Optimization of Aircraft Engine Suspension Systems. *Journal of Aircraft*, v 30, n 6: 979-984.

Swanson, D. A., Miller, L. R., and Norris, M. A., (1994). Multidimensional Mount Effectiveness for Vibration Isolation. *Journal of Aircraft*, v 31, n 1: 188-196.

Sykes, A. O., (1956). The Evaluation of Mounts Isolating Nonrigid Machines from Nonrigid Machines. *Shock and Vibration Instrumentation*, New York: ASME.

Thomson, William T., (1972). *Theory of Vibration with Applications*. Prentice-Hall, Englewood Cliffs, NJ.

Timpner, F. F., (1965). Design Considerations for Engine Mounting, (966B) SAE Paper 650093, Warrendale, PA.

Tobias, S. A., (1959). Design of Small Isolator unite for the Suppression of Low-frequency Vibration. *Journal Mechanical Engineering Science*, v 1, n 3: 280-292.

Ungar, E. E. and Dietrich, C. W., (1966). High-frequency Vibration Isolation, *Journal of Sound and Vibration*, v 4, n 2: 224-241.

Whitekus, J. D., (1994). Personal communication at the Ford Motor Company, August 3, 1994.

Wilson, William Ker, (1959). *Vibration Engineering: A Practical Treatise on the Balancing of Engines, Mechanical Vibration, and Vibration Isolation*. Charles Griffin and Company Ltd., London.

Wolfram, S., (1991). *Mathematica: A System for Doing Mathematics by Computer*. Addison-Wesley, Redwood City, CA.

Xuefeng, Jiang, (1991). A Study of Inclined Engine Mounting System Design Parameters, Proceedings for the Sixth International Pacific Conference on Automotive Engineering, Published by Korea Society of Automotive Engineers, Inc., 1638-3, Socho-dong, Seoul, South Korea: 339-345.


MICHIGAN STATE UNIV. LIBRARIES
3129301402782 9